

THE PHOTODEGRADATION OF COPOLYMERS  
OF 2,2 - CHLOROACRYLONITRILE WITH STYRENE  
AND WITH METHYL METHACRYLATE.

Submitted by:

ALAN STEWART HOLMES B.Sc. (Hons.)

in part fulfillment of the requirements for

The Degree of DOCTOR OF PHILOSOPHY.

Supervisor:

Professor Norman Grassie.

Chemistry Dept.,

University of Glasgow.

July, 1978.

ProQuest Number: 13804166

All rights reserved

INFORMATION TO ALL USERS

The quality of this reproduction is dependent upon the quality of the copy submitted.

In the unlikely event that the author did not send a complete manuscript and there are missing pages, these will be noted. Also, if material had to be removed, a note will indicate the deletion.



ProQuest 13804166

Published by ProQuest LLC (2018). Copyright of the Dissertation is held by the Author.

All rights reserved.

This work is protected against unauthorized copying under Title 17, United States Code  
Microform Edition © ProQuest LLC.

ProQuest LLC.  
789 East Eisenhower Parkway  
P.O. Box 1346  
Ann Arbor, MI 48106 – 1346

ACKNOWLEDGEMENTS

I wish to express my gratitude to the technical staff of the Chemistry Dept., in particular Mrs Frances Lawrie, for support with my research work, to the staff and students of the Polymer Group for their friendship and helpful advice, with special thanks to Mr Jim Gorman and Mr Bob Ferrie, and to my supervisor throughout the long period of this work, Professor Norman Grassie, for his constructive comments and criticisms on this thesis and his friendly guidance during the course of the work. Finally, my thanks go to my typist, a very tolerant wife.

CONTENTS.

## SUMMARY

vi

<u>CHAPTER</u>	<u>ONE</u>	INTRODUCTION	
1.1		General Aspects of Polymer Degradation.	1
1.2		Photodegradation.	2
1.3		Theoretical Considerations in Polymer Photolysis.	2
1.4		Practical Considerations in Polymer Photolysis.	9
1.5		Review of the Vacuum Photolysis of Poly(methyl methacrylate).	12
1.6		Review of the Vacuum Photolysis of Polystyrene.	14
1.7		Review of the Photolysis of Poly(2,2-chloroacrylonitrile)	17
1.8		Aim of this Work.	17
<u>CHAPTER</u>	<u>TWO</u>	EXPERIMENTAL PROCEDURE AND ANALYTICAL TECHNIQUES.	
2.1		Preparative Methods.	19
2.2		Photodegradation Techniques.	21
2.3		Analysis of Degradation Products.	30
2.4		Thermal Methods of Analysis.	36
2.5		Spectroscopic Techniques.	37
2.6		Molecular Weight Analysis	40

2.7	Microanalysis	42
<u>CHAPTER THREE</u>	POLYMER CHARACTERISATION.	
3.1	General.	43
3.2	Spectroscopic Measurements.	43
3.3	Alternative Copolymer Composition Analysis.	54
<u>CHAPTER FOUR</u>	PHOTODEGRADATION STUDIES ON COPOLYMERS OF METHYL METHACRYLATE WITH 2,2- CHLOROACRYLONITRILE.	
4.1	Introduction.	57
4.2	Molecular Weight Studies.	57
4.3	Product Analysis — Condensable Products.	68
4.4	Product Analysis — Permanent Gases.	78
4.5	Variation of Product Evolution Rate with Copolymer System.	81
4.6	Spectral Changes Occurring During Degradation.	87
4.7	Discussion.	95
<u>CHAPTER FIVE</u>	PHOTODEGRADATION OF COPOLYMERS OF STYRENE WITH 2,2-CHLOROACRYLONITRILE.	
5.1	Introduction.	105
5.2	Product Analysis.	105
5.3	Spectral Changes During Photodegradation.	119

5.4	Molecular Weight Analysis.	121
5.5	Discussion.	121
 <u>CHAPTER SIX</u>		THERMAL DEGRADATION OF PRE-IRRADIATED COPOLYMER FILMS.
6.1	Introduction.	131
6.2	Experimental Results.	132
6.3	Discussion.	149
 <u>REFERENCES</u>		159

SUMMARY.

Methyl methacrylate/2,2-chloroacrylonitrile and styrene/2,2-chloroacrylonitrile copolymers of various molar ratios have been prepared by free-radical, addition polymerisation and characterised by  $^1\text{H}$  nuclear magnetic resonance spectroscopy and microanalysis.

The photodegradation by 254nm radiation of thin copolymer films has been studied at ambient temperatures. Spectroscopic examination of the residual films, separation of degradation products by a recently developed, low-temperature, thermal volatilisation analysis technique, cumulative, quantitative product analysis and product identification by spectroscopic techniques have enabled the photodegradation processes to be studied in depth.

The results indicate that, as the proportion of 2,2-chloroacrylonitrile in the copolymer with methyl methacrylate is increased, the well-established degradative behaviour of poly(methyl methacrylate) — a rapid decrease in molecular weight and formation of products from ester decomposition — is gradually replaced by crosslinking, unsaturation, insolubility, the production of hydrogen chloride from 2,2-chloroacrylonitrile units and methyl chloride from both monomers. Around the 1 : 1 molar ratio a highly absorbing surface layer begins to be formed.

The effect of 2,2-chloroacrylonitrile units on polystyrene photodegradation is less marked. The major reaction is hydrogen

chloride formation. For the same molar ratio, the rate of formation of hydrogen chloride from 2,2-chloroacrylonitrile copolymers with styrene is considerably greater than with methyl methacrylate. This is attributed to the different absorption coefficients of radiation of the two co-monomers.

Solvent participation in photodegradation reactions is indicated by anomalous molecular weight measurements on the methyl methacrylate system and by post-irradiation absorption spectra of copolymer films of both systems.

The effect of pre-irradiation on the thermal degradative behaviour of copolymer films has been studied. The nature of the degradation products remains unchanged but the effects of crosslinking and unsaturation on the methyl methacrylate system are reflected in thermogravimetric analyses and differential condensation thermal volatilisation analyses on the system.

The initiation processes involved, the scissioning reactions, the development of unsaturation in the copolymers and the related discolouration of copolymer films are discussed in the course of the work. Comparisons are drawn with studies on similar polymer systems and various references are listed which have been found relevant to the present study.

CHAPTER ONEINTRODUCTION1.1. GENERAL ASPECTS OF POLYMER DEGRADATION.

Polymeric material can undergo various changes as a result of the conditions under which it is used or stored. Although the polymer may rapidly become unserviceable in too severe conditions, it could last indefinitely in a less arduous environment. It is thus in the interests of both the manufacturer and the consumer to be aware of the degradative effects of commonly encountered conditions such as sunlight and high temperatures.

Much research has been devoted to the causes and effects of degradation in polymers since the naissance of the plastics industry. At first progress was hindered by an imperfect understanding of the true nature and complexity of macromolecular structure and a lack of suitable analytical techniques. The expansion of the market for polymers in the late 1940's together with a more profound conception of polymer chemistry and new techniques rekindled interest in the study of degradation. In recent years this has been stimulated by the development of new applications for polymeric materials in which they must be stable to a wide variety of chemical, physical, mechanical and even biological agencies. The whole field of degradation has been encompassed

by a comprehensive review by Grassie (1).

### 1.2 PHOTODEGRADATION.

As very few polymers spend their entire existence in darkness, it is not surprising that photolytic degradative processes have received considerable attention. Detailed mechanisms began to be described in the early 1950's.

Among the first was a study by Cowley and Melville (2) of the photodegradation of poly(methyl methacrylate) at elevated temperatures under vacuum conditions. Since then, systematic studies have appeared on many polymers either in vacuo or in a gaseous atmosphere. These have been reviewed by Fox (3) and, more recently, by Ranby and Rabek (4).

Historically, prevention of degradation by the incorporation of stabilisers was the main interest of industry but, with increasing concern about the disposal of plastic waste, its attention has been focussed on the control of degradation.

### 1.3 THEORETICAL CONSIDERATIONS IN POLYMER PHOTOLYSIS.

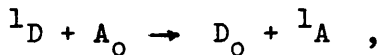
#### 1.3.1 General

Most organic molecules exist in an electronic singlet ground state. Absorption of a photon by a chromophore in a molecule results in its excitation to a state of higher energy. As the rate of internal conversion from higher excited states to the lowest excited level is extremely rapid, most photochemical reactions will occur from this state. In some cases intersystem crossing can occur from an excited singlet state to a triplet state of lower energy by a spin-forbidden transition. As both internal conversion and intersystem

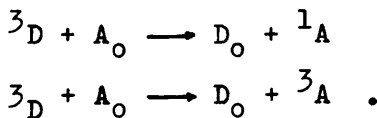
crossing are processes which occur without the absorption or emission of radiation, energy must be dissipated by other methods such as vibrational relaxation.

An excited molecule can revert to the singlet ground state from the excited singlet or triplet levels by emitting radiation. In the former transition,  $S_1 \rightarrow S_0$ , the luminescence produced is known as fluorescent radiation and in the latter,  $T_1 \rightarrow S_0$ , as phosphorescent radiation. These photophysical processes which are collectively depicted in Figure 1.1 have been described in detail by several authors (5,6).

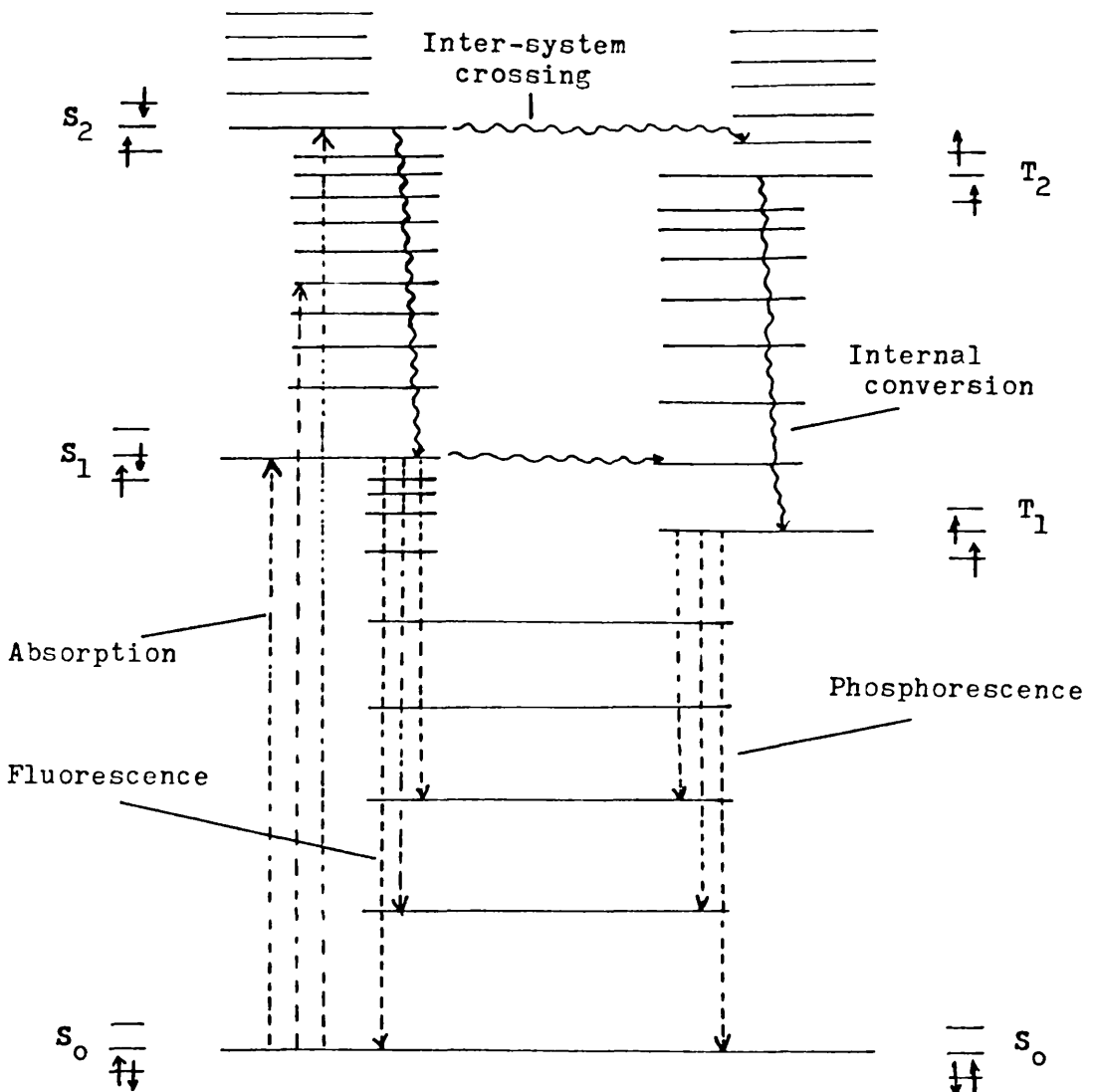
With regard to polymers the situation is complicated by chain entanglement, interchain reactions and the close proximity of adjacent chromophores on the same molecule. Other processes may occur in addition to those previously mentioned, involving the migration of energy in the polymer sample. One process, known as intermolecular energy transfer, occurs between a polymer molecule acting as donor (D) and an acceptor molecule (A) with the result that the donor molecule is quenched from its excited singlet state;



or from its excited triplet state;



This process may occur in reverse with energy transfer from an excited sensitizer molecule as donor to the ground state



Dashed lines = Radiative transitions

Wavy lines = Radiationless processes.

**FIGURE 1.1** Electronic transitions and photophysical processes in an organic molecule.

polymer molecule. These intermolecular reactions are associated with both collisional transfer, by which contact is established between the two participating molecules, and resonance transfer by which energy is exchanged over distances greater than the collision diameters. A wide variety of mechanisms and excited state intermediates are thought to be involved in both cases.

Another process which must be considered in the photochemistry of polymers is intramolecular energy transfer between chromophores along the polymer chain. The mechanism involves excited intermediates known as excimers which can form either between adjacent conjugated chromophores or unconjugated chromophores on the polymer chain. Several workers (7,8,9) have observed excimer fluorescence in studies of aromatic systems such as polystyrene and poly(vinyl naphthalene).

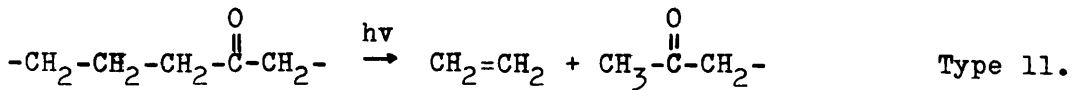
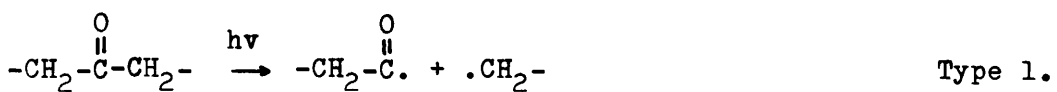
In view of the possibilities for energy transfer within a polymer system, the site of initial bond break may be distant from that of the absorbing chromophore. Dissociation of the bond may occur from an excited singlet or triplet state and results when sufficient energy accumulates at the fracture point. The energy of radiation is dependent on the wavelength of the resonance line employed eg. the mercury resonance line at 254nm is equivalent to  $471\text{kJ mol}^{-1}$ . As most organic polymers contain only carbon - carbon, carbon - hydrogen, carbon - nitrogen, carbon - oxygen and carbon - halogen bonds, the magnitude of energy required for bond scission, based on

the bond dissociation energies (10) is such that single bonds in a polymer molecule should be susceptible to cleavage when exposed to ultra-violet radiation. In practice a chromophore is required in order to first absorb energy before scissioning can occur. Further, the process may be subject to kinetic restraints, or energy dissipation processes may outweigh scissioning processes.

### 1.3.2 Chromophoric Groups.

The chromophores which might be responsible for photodegradation of polymers are the chromophoric groups in the polymer structure, oxidation products such as hydroperoxides and carbonyls, metal impurities from catalyst residues, oxygen and other impurities such as aromatic molecules.

Hydroperoxides and carbonyl groups which can form by the thermal oxidation of the polymer during fabrication, processing or storage absorb in the ultra-violet range. The action of light decomposes the hydroperoxides to yield hydroxy and alkoxy radicals. The former can abstract hydrogen leaving centres for crosslinking, the latter are capable of undergoing isomerisation and fragmentation reactions as has been discovered in studies on polypropylene (11,12). The aliphatic aldehydes and ketones are no less harmful. By a forbidden transition ultra-violet light is absorbed and a variety of cleavage reactions becomes possible. Their major photochemical reactions are known as Norrish Type I and Type II reactions:



The importance of carbonyl groups as irregular bonds in the photodegradation of polymers such as polyethylene was first suggested by Burgess (13) and has been confirmed by many workers. Metal impurities are more recent discoveries and are of particular importance in photo-oxidation studies. Transition metal ions have been used recently in the development of photodegradable polymers (14).

Oxygen in molecular form exists in the ground state as the triplet  ${}^3\text{O}_2$  ( ${}^3\Sigma_g^-$ ) and as singlet oxygen,  ${}^1\text{O}_2$  ( ${}^1\Delta_g$  or  $\Sigma_g^+$ ) in the excited state. Singlet oxygen can react with vinyl groups to form hydroperoxides. Decomposition of these may lead to disproportionation and further degradation (4). Under vacuum conditions the risk of oxygen being trapped in the film as an impurity is minimised.

### 1.3.3 Classification of Degradation Reaction Types.

Degradation processes have been broadly classified as chain scission, crosslinking and functional group reactions. These processes have been discussed at length in many authoritative texts (15,16,17,18).

Chain scission is characterised by the breakdown of the polymer backbone into chain fragments. After the initial cleavage step which may occur at random along the length of

the chain or at specific sites such as unsaturated chain ends, two extremes of behaviour may be observed. In one case, a rapid decrease in molecular weight occurs without evolution of monomer. Volatiles other than monomer may be observed resulting from functional group cleavage. This type of behaviour is common in photodegradation reactions at ambient temperatures. Alternatively, degradation may proceed by an unzipping process resulting in the evolution of large quantities of monomer. In this case the molecular weight may remain essentially constant during the early stages of reaction. The thermal degradation of poly(methyl methacrylate) is thought to occur in this fashion.

The process of crosslinking results ultimately in a three - dimensional network of polymer which renders it insoluble. Crosslinking and scissioning reactions can occur consecutively in the same polymer system eg. poly(methyl acrylate). Crosslinking induced by ultra - violet radiation results from cleavage of functional groups leaving radicals on the main chain. In polystyrene these radicals are produced by cleavage of the tertiary hydrogen atom. These radical centres can migrate (4) and combine with other radicals on adjacent chains or may add to unsaturated sites on the chains. The build - up of these crosslinks quickly leads to insolubility.

Side group reactions or functional group reactions involve alteration to the polymer structure but may include chain scission or crosslinking as a secondary step. Examples

of these are the elimination of HCl from irradiated PVC (19) and the formation of conjugated carbon-nitrogen sequences during thermal degradation of nitrile polymers (20,21,22,23,24).

#### 1.4 PRACTICAL CONSIDERATIONS IN POLYMER PHOTOLYSIS.

##### 1.4.1 Analytical Techniques.

The investigation of polymer photodegradation requires the application of complicated and highly sensitive analytical methods. The cost involved places severe limitations on the average laboratory and, consequently, most workers tend to concentrate on particular aspects of the degradation process. Many techniques have provided valuable information. Amongst those commonly employed are:

viscometry	{	analysis of molecular mass and distribution of polymers
osmometry		
ultracentrifuge		
gel permeation chromatography		
infrared, visible and ultra-violet spectroscopy	{	structural changes and product analysis
nuclear magnetic resonance (N.M.R.)		
spectroscopy		
electron microscopy		
X-ray analysis	{	
electron spin resonance (E.S.R.)		analysis of short-lived intermediates
spectroscopy		
flash photolysis		
gas chromatography	{	product analysis
mass spectrometry		

A brief description of these techniques and the instruments involved may be obtained in many polymer text books (4,25).

Thermal methods of analysis have been employed by several workers in this field to elucidate the residual structure of the irradiated polymer and to examine the effects of radiation on its thermal properties. This is particularly important where the material is exposed to both radiation and high temperatures. Leeming (26) employed thermal volatilisation analysis and differential condensation thermal volatilisation analysis in studies of polypropylene degradation. These techniques are discussed in detail in Chapter Two.

#### 1.4.2 Radiation Sources.

A variety of sources are listed in the literature which will produce emission spectra ranging from single resonance lines to continua of wavelengths. The preferential selection of wavelengths by the interposition of filters is discussed in Calvert and Pitts (10). Low pressure mercury discharge lamps are usually employed where monochromatic ultra-violet light is required. In weathering studies the sun's emission spectrum has been simulated in the laboratory by a xenon discharge lamp with appropriate filters.

Irrespective of the nature of the source, it is essential that the apparatus constructed for photolysis studies should transmit at the required wavelength. For this reason when the ultra-violet region of the spectrum is being studied all the material must be made from silica.

In order that quantitative comparisons may be made among

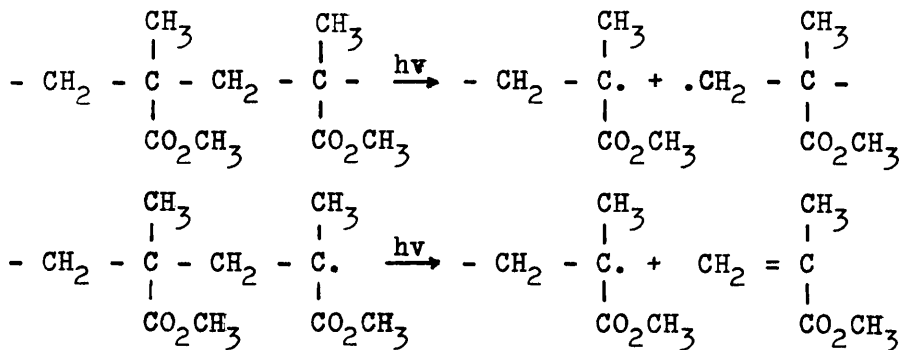
different workers, the intensity of the incident radiation is measured. This is conventionally determined by the application of chemical actinometers. The most common liquid phase actinometers are the uranyl oxalate actinometer (27,28,10) or the more rapid potassium ferrioxalate method (29) for the range 250nm to 580nm and Reinecke's salt actinometer (30) for the 350nm to 750nm range.

### 1.5 REVIEW OF THE VACUUM PHOTOLYSIS OF PMMA.

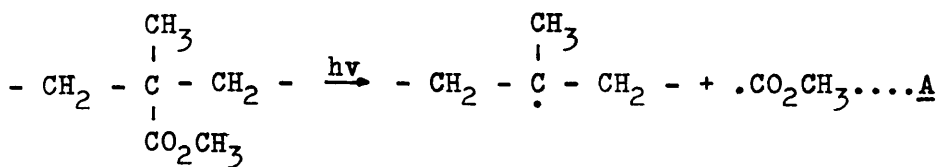
Since most of its applications are in the solid state, the photodegradation of poly (methyl methacrylate) has usually been studied in film form either cast from solution or polymerised *in situ*. The polymer has a low absorption coefficient at 254nm and no skin effects would be expected to occur. The absence of a tertiary hydrogen in the structure reduces the probability of crosslinking reactions in contrast to poly (methyl acrylate) which readily undergoes crosslinking (31).

The mechanism of photodegradation depends markedly on the reaction temperature. At higher temperatures, greater than 403K, work by Cowley and Melville (2) has shown that the polymer, when exposed to ultra-violet radiation, depolymerises in a reaction analogous to that of thermal degradation. On exposure at 433K the rate of production of monomer was found to be greater than that produced by thermal action alone at 493K and the degradation appeared to be initiated at the chain ends. MacCallum and Schoff (32), investigating the system under similar conditions, contended that the reaction

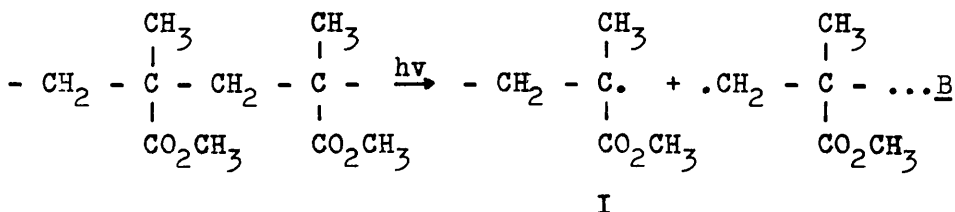
mechanism was random scission of the main chain, followed by depolymerisation to monomer:



At ambient temperatures the characteristics of the degradation are more complex. A rapid decrease in molecular weight is observed together with the production of a complex mixture of gaseous products. Fox and co-workers (33) degraded films, cast from dichloromethane solution, at 298K and identified the gaseous products as methanol, methyl formate, methyl methylacrylate, carbon dioxide, carbon monoxide, methane and hydrogen. Shultz (34), monitoring the coefficient of absorption, found that it changed during irradiation and that a new band, centred at 285nm, appeared in the ultra-violet absorption spectrum which he accredited to trapped volatiles. This aroused some controversy and Frolova, Nevskii and Ryabov (35) proposed that its formation was due to new aldehydic functional groups formed on the polymer itself. Using  $^{14}\text{C}$ -labelled polymers and mass spectrometric analysis of products, they suggested a mechanism which would account for the production of methyl formate in a primary process:

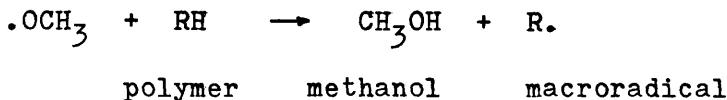
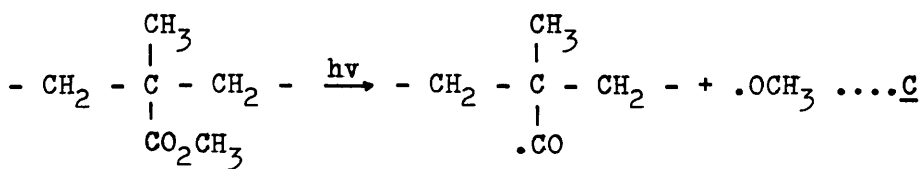


The radical then scavenged a hydrogen atom from the polymer to produce methyl formate. This process may be followed by scissioning of the main chain but comparison with quantum yields of scissioning produced by Shultz (34) suggests that a large proportion of the main chain scissioning occurs directly:

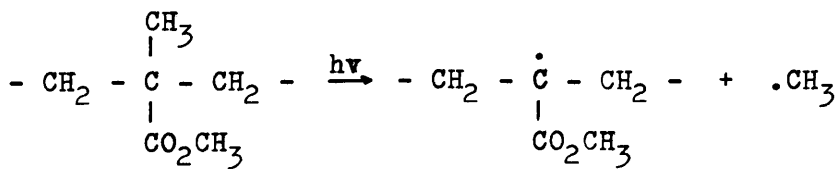


Depolymerisation of the resulting main chain radical, I, occurs over short zip lengths accounting for the production of monomer. The propagating radical, I, has been satisfactorily identified from E.S.R. spectra by Iwasaki and his co-workers (36).

The E.S.R. spectrum of irradiated polymer at 77K was identified by Kato and co-workers (37) as being due to the free radicals  $\cdot \text{CO}_2 \text{CH}_3$ ,  $\cdot \text{HCO}$  and  $\cdot \text{CH}_3$ . This lends further support to the importance of mechanism A as a primary process. The production of monomer and methyl formate have been accounted for and the remaining gaseous products reported by Fox (31) may be rationalised in terms of the breakdown of the ester side group and hydrogen abstraction from the polymer. Methanol can be produced as follows:



If this is the case, the aldehydic structures reported by Frolova et al. (35) could easily be derived from the macroradical in mechanism C by hydrogen abstraction. The observation of  $\cdot\text{HCO}$  radicals would also fit this hypothesis. These radicals may be responsible for the formation of carbon monoxide by decomposition. It is thought likely (38) that the methyl radicals are produced by photolysis of the ester side group, just as ethyl radicals are produced after irradiation of poly(ethyl methylacrylate). Ranby and Rabek (4), on the other hand, assert that the formation of methyl groups from the polymer backbone is a primary process:

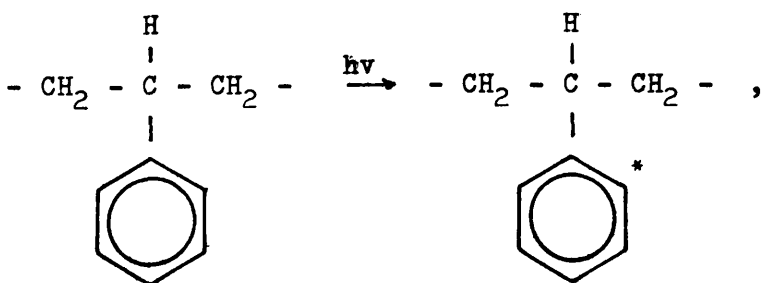


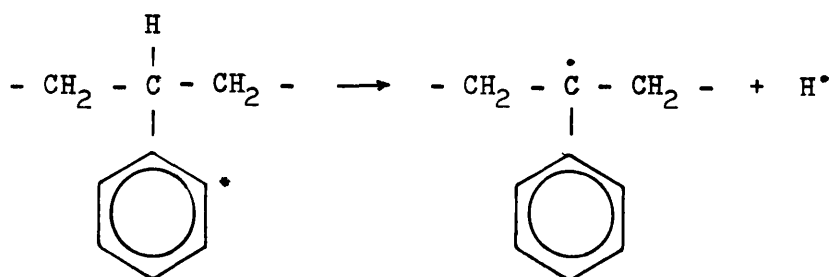
#### 1.6 REVIEW OF THE VACUUM PHOTOLYSIS OF POLYSTYRENE.

The fundamental work on this system appeared in 1965 in a series of publications by Grassie and Weir (39,40,41, 42). Since then, some controversy has arisen over the

relative importance of certain processes but the overall effects observed, viz. the evolution of gas, the development of insolubility and the discolouration of the polymer, have been firmly established.

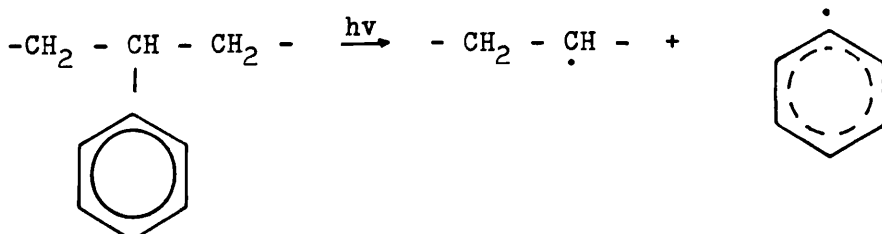
Photolysis of polystyrene occurs below 280nm where strong absorption by the polymer has been attributed (43) to the  $S_1 \leftarrow S_0$  transition in the benzene ring but the radical yield is thought to be small because of the possibilities of energy dissipation by the benzene rings (38). When Grassie and Weir investigated the irradiation of films cast from chloroform, they found that hydrogen was the only significant product. This was later substantiated by mass spectrometric studies by Fox et al. (44). The mechanism proposed by Grassie and Weir accounted for this and the strong tendency towards cross-linking. This involved absorption of energy by the benzene ring followed by energy transfer to the site of scissioning. On the basis of bond dissociation energies and conjugative effects they calculated that the most likely site was at the tertiary hydrogen on the main chain:





E.S.R. studies have established the presence of this macro-radical in the irradiated polymer (45). The production of hydrogen can then occur by the combination of hydrogen atoms or by the abstraction of hydrogen from the polymer structure. In either event two radical centres are formed on the polymer for each molecule of hydrogen evolved. Although the movements of macroradicals in the solid state are restricted, free radical centres can migrate along the polymer chain until they are trapped by impurities or by other macro-radicals forming cross-links.

Ranby and Rabek (46) reported that the triplet energy state in benzene rings was involved. This is achieved by intersystem crossing. The triplet energy of the excited benzene ring is thought to produce dissociation of the  $C_6H_5 - C$  bond:



The yellowing effect in polystyrene irradiation has aroused controversy. Grassie and Weir attributed this to

the build-up of conjugated sequences in the polymer backbone. Ranby and Rabek, however, associated the coloration with the photoisomerisation of benzene molecules present in the photodegraded polymer. This would entail the formation of structures such as fulvene and benzalvene. At present the origin of coloration remains to be firmly established.

#### 1.7 REVIEW OF THE PHOTOLYSIS OF

#### POLY(2,2-CHLOROACRYLONITRILE).

It is apparent from the literature that little interest has been shown in this polymer. Mackinnon (47) has investigated the effect of ultra-violet radiation on the thermal properties of the polymer in film form and as a powder. It was concluded that, in the powder form, radiation had no significant effect on the thermal properties of the polymer but, on films cast from dimethyl formamide solution, an increase in absorption in the visible region of the spectrum occurred and the amount of volatile products obtained from subsequent thermal degradation was markedly reduced.

#### 1.8 AIM OF THIS WORK.

In the course of his studies on thermal degradation, Grassie investigated the effect of deliberately incorporating "weak links" into polymers whose degradation patterns were well-characterised. One such "weak link" was the carbon-chlorine bond on 2,2-chloroacrylonitrile (CAN) which contained a double bond and was, therefore, suitable for addition polymerisation. In 1966 Grassie and Grant published (48) the

results of thermal degradation experiments on two copolymer systems incorporating CAN units into poly(methyl methacrylate) and polystyrene respectively.

Both copolymers were found to be very much less stable thermally than the respective homopolymers. At temperatures around 423K the CAN units acted as "weak links" in the copolymers and random scission occurred.

In view of the ecological interest in plastics which will degrade under controlled conditions, and as a natural extension of the thermal work, it was decided to investigate the effects of radiation on these two systems. In order to eliminate complicating side-effects while examining the degradation process, the work has been carried out in vacuo at ambient temperatures using essentially monochromatic radiation.

## CHAPTER TWO

### EXPERIMENTAL PROCEDURE AND ANALYTICAL TECHNIQUES.

#### 2.1 PREPARATIVE METHODS.

##### 2.1.1 Monomer Preparation.

All polymers used in this investigation were prepared in the laboratory from commercially available monomers.

Methyl methacrylate (Hopkin & Williams Ltd) and Styrene (B.P. Chemicals Ltd) were purified by washing with dilute alkali to remove indicator, then distilled water before drying over calcium chloride. Each monomer was distilled under vacuum the middle fraction being retained for polymerisation.

2,2-Chloroacrylonitrile (Aldrich Chemical Co.) was dried over Molecular Sieve Type 4A and distilled three times under vacuum discarding the two end fractions before polymerisation. This monomer was handled in stringent safety conditions because of its lachrymatory and vesicatory properties.

##### 2.1.2 Purification of Initiator.

Azo-bisisobutyronitrile (Eastman-Kodak Ltd), a free radical initiator, was recrystallised from ethanol after hot filtration to remove the insoluble polymeric material which develops from decomposition of the initiator. The melting point of the crystals obtained was found to be 103° C.

##### 2.1.3 The Copolymer Equation.

The copolymer equation provides a method of calculating the mole ratios of monomer necessary in the reaction feed

mixture to produce the desired composition of the copolymer. This equation,

$$\frac{m_1}{m_2} = \frac{M_1}{M_2} \cdot \frac{r_1 M_1 + M_2}{M_1 + r_2 M_2},$$

where  $m_1/m_2$  is the ratio of the monomers in the copolymer, and  $M_1/M_2$  is the ratio of the monomers in the feed mixture, may be used when the reactivity ratios  $r_1$  and  $r_2$  are known.

#### 2.1.4 Polymerisation Technique.

The copolymers were prepared in vacuo by free radical bulk polymerisation initiated by the thermal decomposition of azo-bisisobutyronitrile. The apparatus was constructed from Pyrex glass and evacuated by a silicone oil diffusion pump backed by a rotary oil pump and liquid nitrogen traps, capable of producing a vacuum of  $10^{-4}$  torr or better. A solution of the initiator in "Analar" grade acetone was poured into a reaction dilatometer and the solvent removed by boiling under vacuum. Precalculated volumes of degassed monomers were then distilled under vacuum from graduated reservoirs into the dilatometer. The reagents were sealed in the dilatometer, transferred to a thermostatted water bath and polymerised to the required conversion as determined by the amount of contraction in the solution (49). Copolymers with a high percentage of styrene or methyl methacrylate formed a homogeneous solution in their

monomer mixture. On completion of polymerisation the solution was slowly added, dropwise, into "Analar" methanol which precipitated the copolymer as an amorphous solid. The copolymers were reprecipitated twice from "Analar" acetone after filtering and finally dried in a vacuum oven.

Copolymers with a high percentage of 2,2-chloroacrylonitrile polymerised heterogeneously and were filtered to remove the unreacted monomer. The polymer which was soluble in acetone, was reprecipitated twice in methanol before drying. The composition of the copolymer was determined by elemental analysis.

## 2.2 PHOTODEGRADATION TECHNIQUES.

### 2.2.1 Polymer Form.

For the purpose of irradiation the polymers were cast as films from solution on to discs 30mm in diameter. The solvent was removed by heating the films in a vacuum oven at 40-50°C for 48 hours, followed by room temperature evacuation at a pressure of  $10^{-4}$  torr or better. The films were detached from discs before irradiation to prevent solvent retention at the interface. The advantage of casting a film from solution by solvent evaporation is that the technique is not accompanied by side effects such as oxidation or partial degradation of polymer which often results when standard methods such as hot pressing or moulding are employed.

### 2.2.2 Solvent Purity.

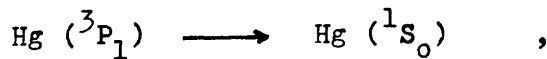
All solvents used for film casting were of "Analar" grade

or equivalent, freshly distilled and dried over Molecular Sieve Type 4A or 3A to remove impurities. In order to exclude atmospheric moisture the films were stored in a vacuum desiccator.

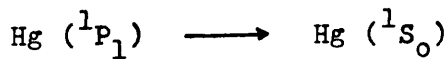
### 2.2.3 Source of Radiation.

The most widely used source of radiation in photodegradation studies is the mercury arc lamp, the spectral distribution of which is pressure dependent (4). The output at low pressure ( $10^{-3}$  torr) consists of several distinct lines of which two, at 184.9nm and 253.7nm respectively, are by far the most intense. The medium pressure lamp provides radiation in the 220-400nm range, requiring filters for isolation of the individual lines whereas the high pressure lamp with its multitude of lines produces a continuous band of radiation.

For the purpose of this work the source employed was a Hanovia Chromatolite lamp which is a low pressure mercury lamp emitting predominantly in the resonance line at 253.7nm assigned to



and to a minor extent at 184.9nm due to



as shown in Figure 2.1. The lamp was connected to a LTH Transistorised 1kVA Voltage Regulator to ensure that any variations in the mains voltage did not affect the lamp output.

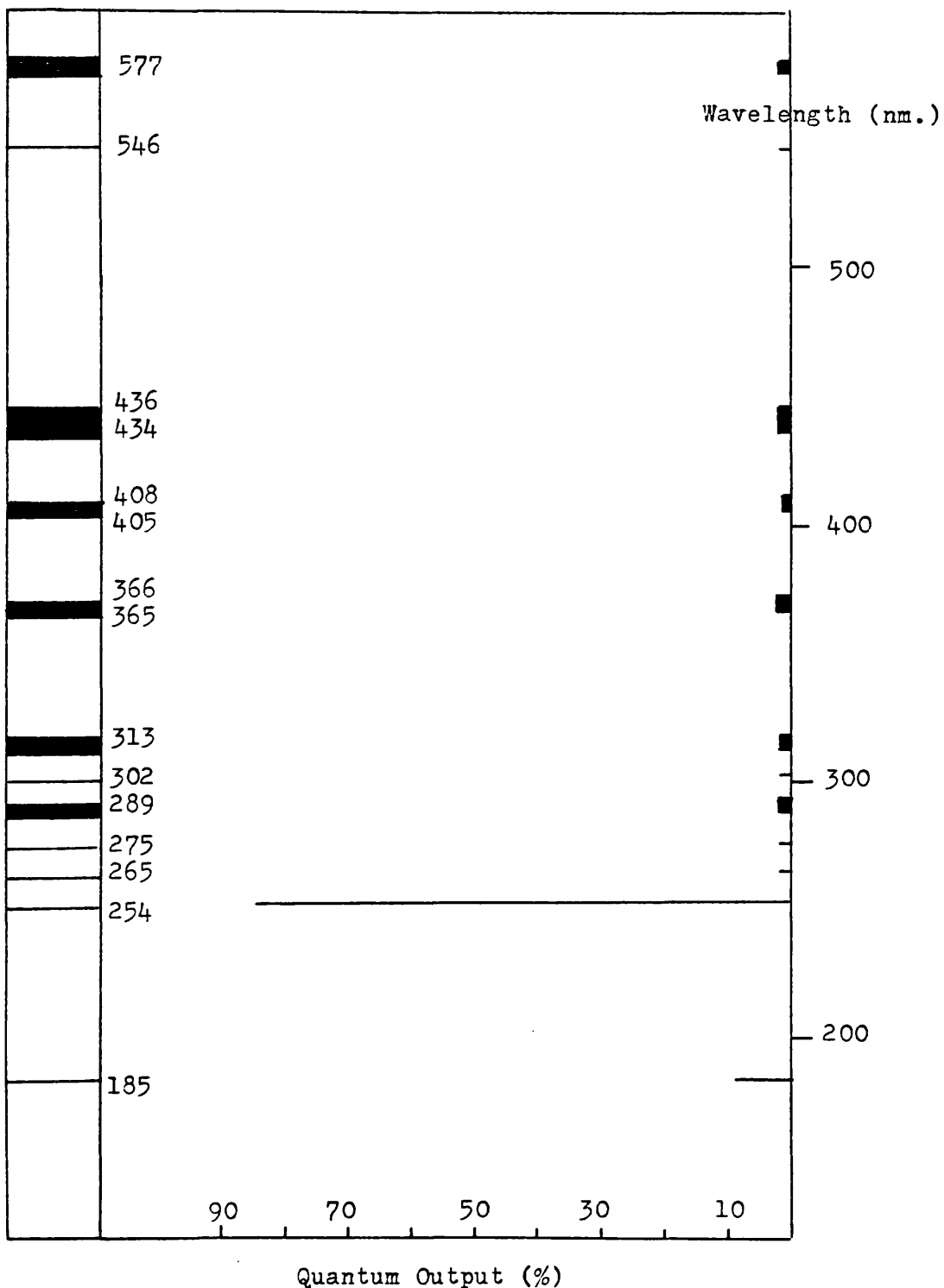


FIGURE 2.1 Emission Spectrum of Hanovia Lamp.

#### 2.2.4 Deterioration of Source.

As the life expectancy of the average lamp varied from 200 hours to 400 hours, it was necessary to monitor the output intensity to detect any sign of deterioration. A J-225 Blak-Ray ultra-violet meter consisting of a photovoltaic sensor connected to a meter was employed to register the intensity of the lamp prior to each exposure. It was found that the lamp required a fifteen minute warm-up period before reaching a constant output intensity.

#### 2.2.5 The Photolysis Cell.

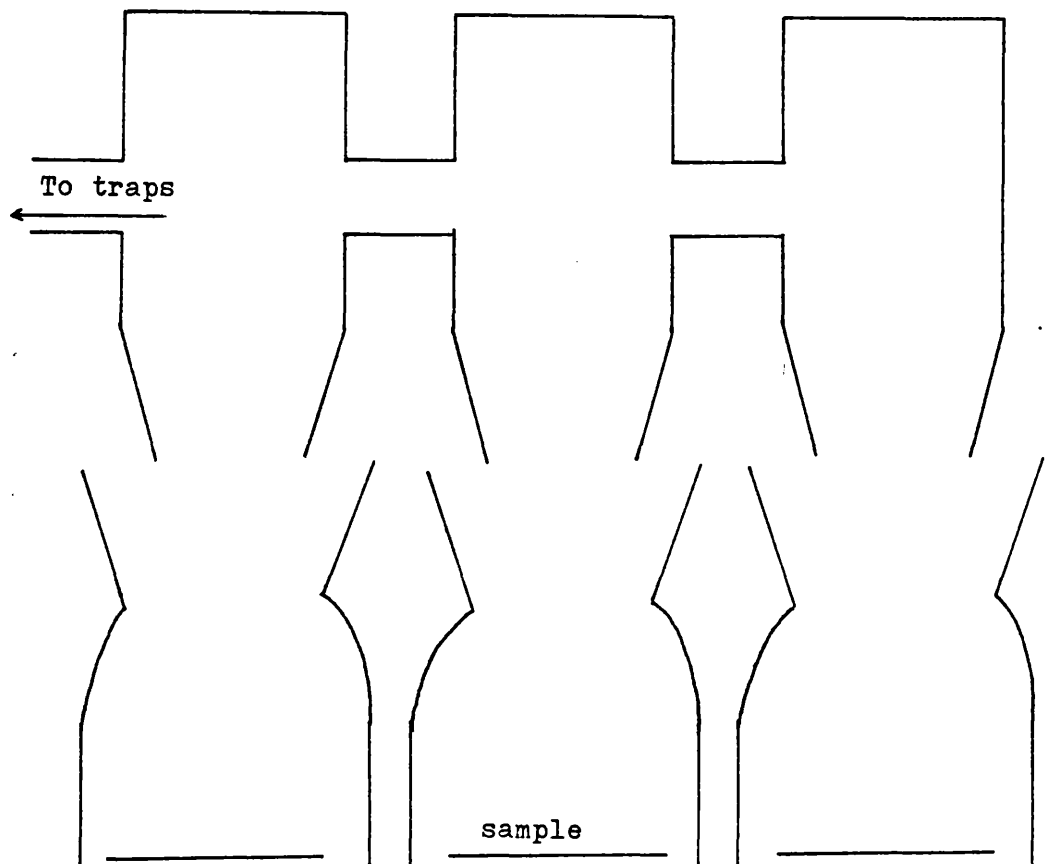
The main requirement of any photolysis cell is transparency to the wavelength of the radiation employed. For this reason the cell illustrated in Figure 2.2 was constructed. The lower half was made from silica with an optically flat, fused silica base plate and connected to the upper part by a greased, ground glass joint.

In order to increase the area of the polymer sample exposed to the radiation, three cells were linked together in parallel. The lamp was situated below the base of the cell and parallel to the plane of the base plate.

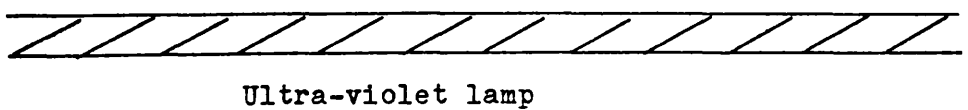
#### 2.2.6 Monochromaticity of the Source.

It has already been shown that approximately 95% of the output of the lamp is composed of resonance lines at 253.7nm and 184.9nm. Under experimental conditions the radiation encounters air and fused silica en route to the film. The main absorbing constituent of the air is oxygen which absorbs strongly in the Schumann-Runge bands from 176-195nm

Pyrex glass upper assembly



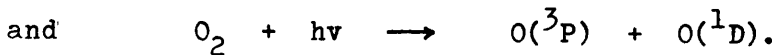
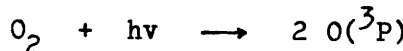
Silica pots with circular bases



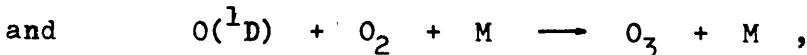
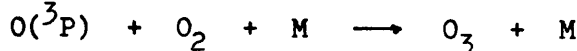
Ultra-violet lamp

FIGURE 2.2 The Photolysis Cell.

producing photodissociation (50):



Ozone is produced concurrently:



where M is a third body. Only the 184.9nm line has sufficient energy to dissociate oxygen. As a 10mm path length of air is sufficient to absorb this line completely (51), its intensity at the sample should be negligible. The 253.7nm line is not absorbed by air and is only slightly attenuated by passage through fused silica (see Figure 2.3). Since the intensities of the longer wavelengths are negligible compared to the 253.7nm line, the radiation at the polymer film may be considered to be monochromatic.

#### 2.2.7 Actinometry.

For a quantitative assessment of the effects of photo-degradation and in order that comparisons may be made between results from different systems, it is necessary to determine the intensity of monochromatic radiation within the reaction cell. A convenient method for measuring this quantity, which was adapted for the present study, involved the use of the potassium ferrioxalate liquid phase actinometer developed by Hatchard and Parker (29). The effect of radiation on a solution of potassium ferrioxalate in aqueous sulphuric acid solution is to reduce the iron from the ferric to the ferrous state involving the following

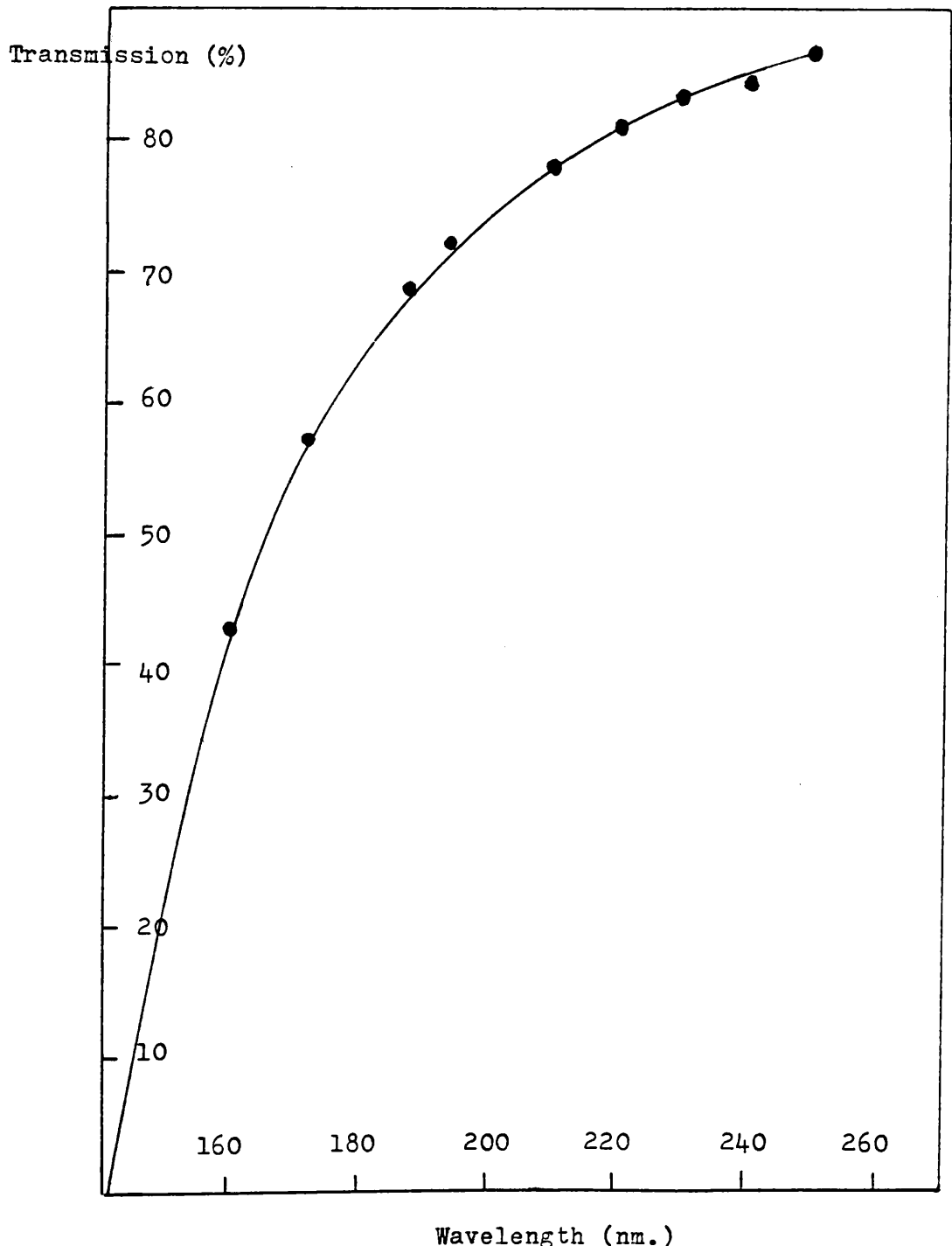
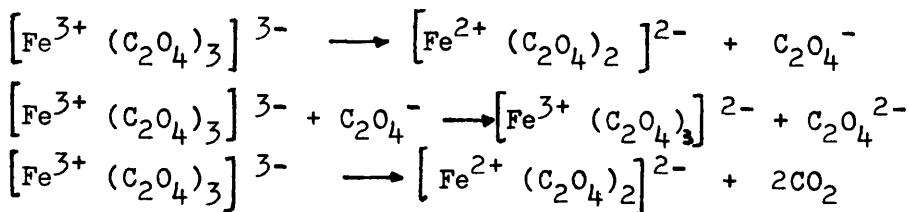


FIGURE 2.3 Transmission spectrum of fused Silica. (2mm.).

reactions (51):



After irradiation the ferrous ions can be converted into the red (1,10 phenanthroline- $\text{Fe}^{2+}$ ) complex which can be readily determined spectrophotometrically. A detailed summary of the preparation of green potassium ferrioxalate crystals is described by Hatchard and Parker (29), and Calvert and Pitts (10). The actinometer solution was prepared and handled under dark-room conditions.

A standard calibration graph for the analysis of the ferrous-phenanthroline complex was first prepared using a Hitachi-Perkin-Elmer 139 UV-Visible spectrophotometer. 15ml of a 0.006M ferrioxalate solution was added to each photolysis cell and irradiated at a fixed distance for one minute. 10ml of this solution was pipetted into a 25ml volumetric flask together with 2ml of 1,10 phenanthroline solution and 5ml of buffer solution and diluted to the 25ml mark. An identical blank solution was prepared using unirradiated potassium ferrioxalate solution. The transmission of the complex was measured at 510nm in a 10mm cell against the blank reference.

The number of ferrous ions formed during the photolysis, ( $n\text{Fe}^{2+}$ ), was calculated from the equation:

$$nFe^{2+} = \frac{6.023 \times 10^{20} V_1 V_2 \log I_0 / I}{V_2 L E}$$

where  $V_1$  is the volume of the irradiated solution,

$V_2$  is the volume of the irradiated solution extracted  
for analysis,

$V_3$  is the final volume to which the aliquot,  $V_2$ , was  
diluted,

$\log I_0 / I$  is the measured optical density of the solution at  
510nm,

L is the path length of the cell

and E is the experimental value of the molar extinction  
coefficient determined from the calibration graph.

The light intensity,  $I_0^i$ , just inside the cell window was  
calculated as follows (10):

$$I_0^i = \frac{nE}{\Phi Fe^{2+} \times t(1-10^{-E(A)L})} \quad \text{quanta per second}$$

where  $\Phi Fe^{2+}$  is the quantum yield of product  $Fe^{2+}$  (equal to  
1.25 at 254nm),

t is the exposure time

and  $(1-I_0^i/I) = 1-10^{-E(A)L}$  is the fraction of incident  
light absorbed.

## 2.3 ANALYSIS OF DEGRADATION PRODUCTS.

### 2.3.1 Introduction.

For short periods of irradiation by a low intensity lamp at ambient temperatures the quantity of volatile material produced is very small and its analysis requires sensitive techniques. Such a technique was employed by McGill and Ackerman (52) in their study of the photolysis of poly(methyl acrylate) and proved to be more sensitive than conventional gas chromatographic methods. With several modifications the McGill system was adopted for the purpose of this work. In view of the importance of the results obtained from it, the principles and procedure are outlined below.

### 2.3.2 Separation Technique.

Photodegradation products which exist as vapours under low pressure conditions can be condensed at liquid nitrogen temperature (77K) at a specific point in the system determined by the location of the liquid nitrogen cold trap. These products are readily separated from the permanent gases which are pumped through the system without condensing.

If a second liquid nitrogen trap is placed at an adjacent point in the system and the products in the first are allowed to warm up, they will transfer to the second trap in a specific sequence. Replacing the first trap and removing the second reproduces the transfer sequence. The transfer is monitored on a pressure gauge which is located between the two traps and responds to the presence of minute traces of

volatiles. When linked to a recorder, the pressure output is obtained as a trace, the profile of which depends on the rate of warming up of products, the dimensions of the system, the location of the gauge-head and the amount of material present.

In practice a G5C-2 gaugehead on a Pirani 14 thermocconductivity vacuum gauge (Edwards High Vacuum) was used to monitor pressure. The temperature at the donating trap was measured by a chromel-alumel thermocouple. Both the pressure gauge and the thermocouple were linked to a Leeds Northrup 12-channel recorder with a full scale deflection of 10mV. The system is illustrated in Figure 2.4.

The separation of components was found to improve as the rate of warming up was reduced until the optimum trace was obtained. Ideally, one product should transfer completely without the concomitant transfer of another. The rate of transfer was controlled by the introduction of an inner trap containing a liquid initially frozen to liquid nitrogen temperature by an outer trap. Removal of the latter allowed the inner trap to warm up at a rate dependent on heat transfer from surroundings. This in turn was controllable by the application of insulating jackets. Both petroleum ether (b.p. 40 - 60°C) and benzene were found by McGill to be suitable for the inner trap. The latter was employed in this study despite its carcinogenic nature.

A typical trace obtained on this system is shown in Figure 2.5. It arises from the condensable photodegradation products of poly(2,2-chloroacrylonitrile) film cast from

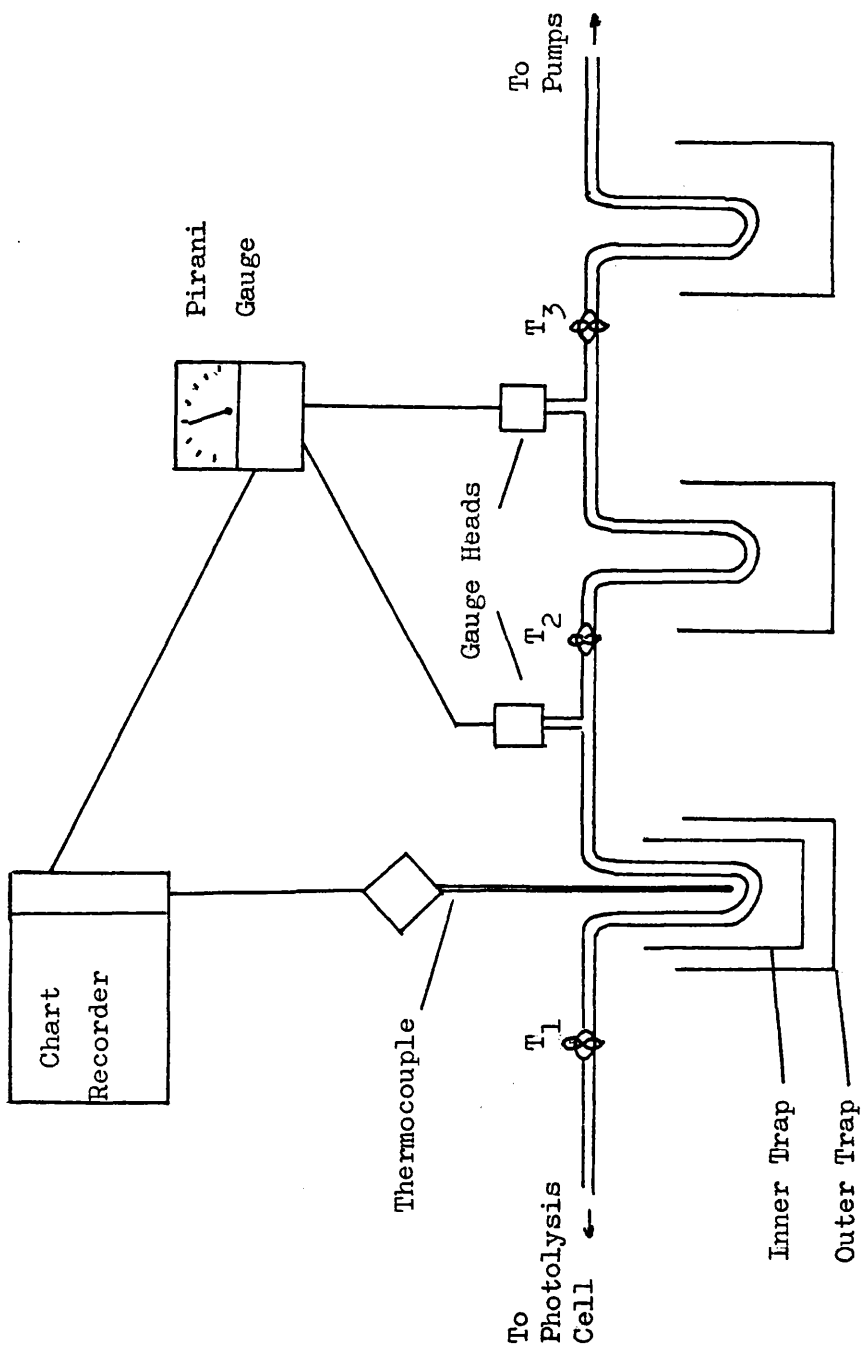


**FIGURE 2.4** Separation Unit for Qualitative Analysis.

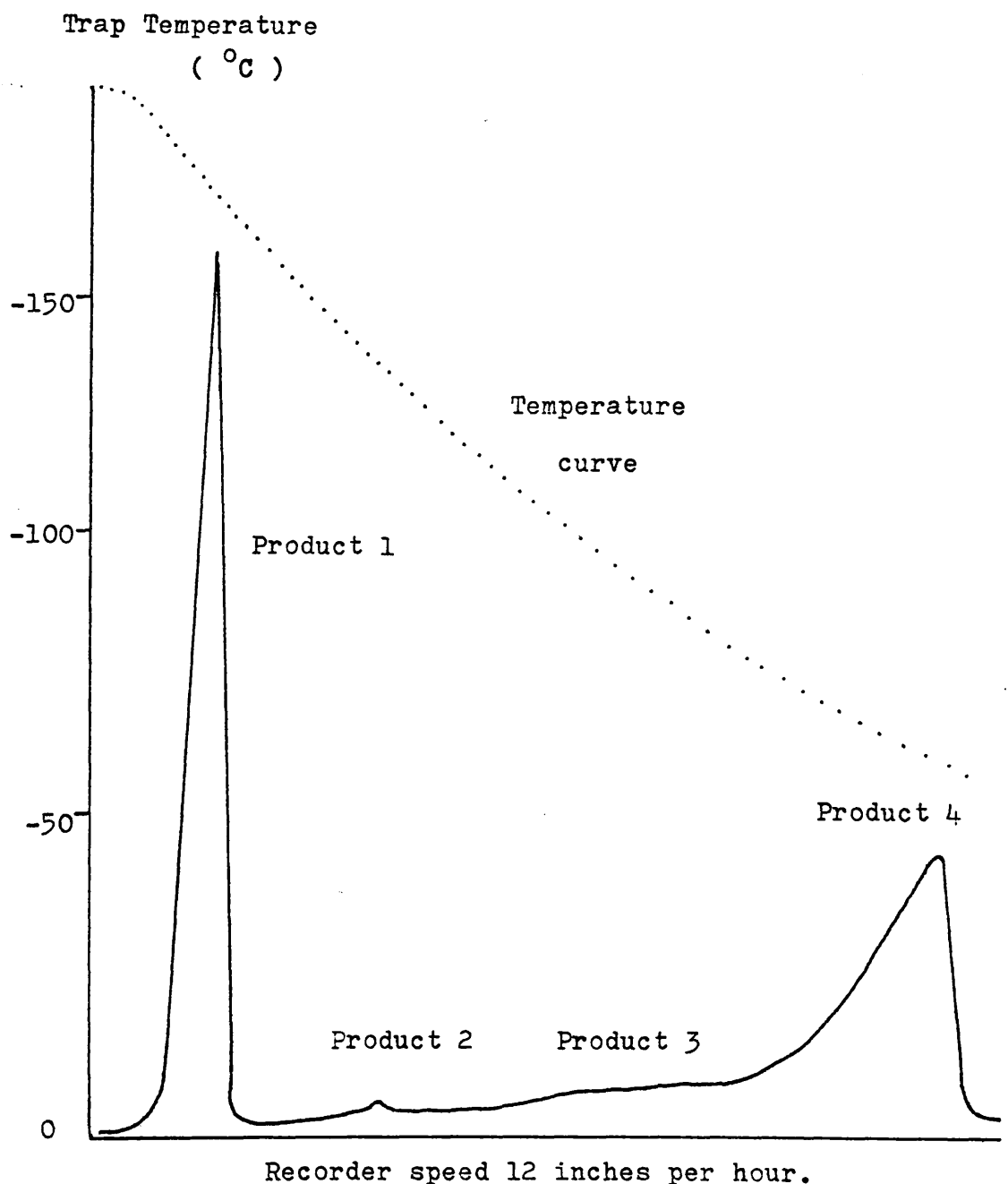


FIGURE 2.5 Typical trace from the sub-ambient distillation apparatus.  
( Photolysis products from poly(2,2-chloroacrylonitrile) ).

acetone solution. A continual temperature print-out from the donating trap accompanies the trace, but this may be replaced, for ease of comparison, by direct peak maxima temperatures.

### 2.3.3 Qualitative Analysis.

The products of degradation were condensed at A (see diagram in Figure 2.4) during photolysis by benzene at liquid nitrogen temperature in the inner trap. On completion of irradiation, pumping was continued to ensure that all volatile products had been removed from the system. With taps 1 and 3 closed a trace was obtained for transfer from A to B. The products were identified from the characteristic temperatures at which each reached its maximum pressure in transfer as recorded by the Pirani gauge. These temperatures were obtained by introducing substances expected as products to the system both in the pure state and as mixtures and recording their traces. When large quantities of the particular products were present, the pressure maxima shifted to higher temperatures (52).

Alternatively, when a sufficient quantity of each product was separated, it was transferred to a gas cell for analysis by infrared spectroscopy and mass spectrometry.

The main limitation of the technique lies in its inapplicability to products which are not condensable at 77K.

### 2.3.4 Quantitative Analysis.

Each product was separated by the technique employed in the previous section and transferred to an isolated part of the system as shown in Figure 2.6. The substance warmed up to

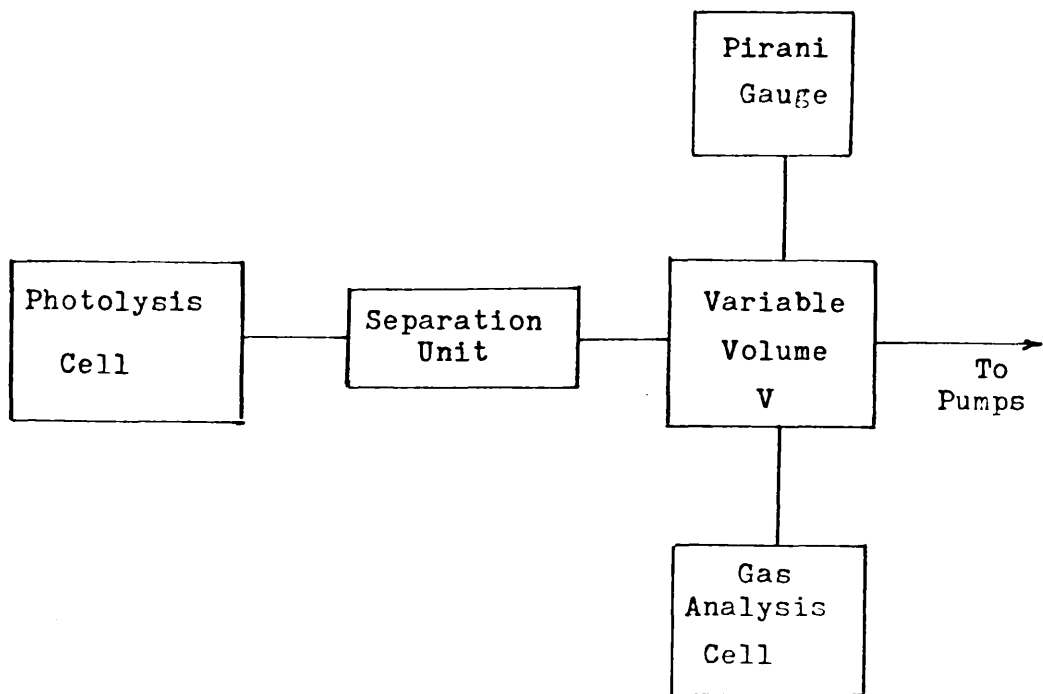


FIGURE 2.6. Schematic representation of Quantitative Analysis System.

ambient temperature and the pressure recorded on the Pirani gauge. The variable volume, V, ensured that the pressure of the gas in the system was measured on the most sensitive pressure scale of the gauge. As the Pirani gauge had been calibrated for dry nitrogen, new calibration curves were constructed when other gases were to be measured. The calibration curve for carbon dioxide was obtained from the Pirani gauge manufacturer.

The recorder output calibration graph (supplied by Edwards High Vacuum) indicated that the recorder response to pressure was non-linear. Thus the conventional techniques of measuring peak areas (as in the case of gas chromatography) were inapplicable. However, a limited use of this method was found. Providing that the same gas is being measured, peaks which are identical in all respects, in other words geometrically congruent, give identical pressure readings by the previous technique and peaks in which the maxima occur below  $2 \times 10^{-3}$  torr are comparable in terms of area which, to a first approximation, is proportional to pressure.

### 2.3.5 Calibration Curves for Pirani Gauge.

Calibration curves were constructed to correct the response of the gauge when gases having a thermal conductivity different from nitrogen were measured by the technique described in the previous section. The pressure of gas in a closed system at ambient temperature was measured on both a Pirani gauge and a McLeod Gauge (53). By varying the pressure of gas in the system by increments

from an external reservoir, the range of the gauge was completely covered. As the M<sup>C</sup>Leod Gauge gives an absolute reading of pressure, no further calibration was required.

#### 2.3.6 Non-condensable Gases.

The so-called permanent gases were readily separated from the system as described above. By introducing a Topler pump to the system, the gases were conveyed to collection flasks for mass spectrometric analysis. No attempt was made to separate the permanent gases for quantitative analysis.

### 2.4 THERMAL METHODS OF ANALYSIS.

#### 2.4.1 Thermogravimetry (TG).

Thermogravimetric analysis results were obtained on a Du Pont 950 Thermogravimetric Analyser. As the design of the instrument restricted its use to powder samples, the platinum balance pan had to be modified to accommodate film fragments. All measurements were recorded in a dynamic nitrogen atmosphere at a programmed heating rate of 10<sup>0</sup>C per minute.

#### 2.4.2 Differential Condensation Thermal Volatilisation Analysis (DCTVA).

The technique of Thermal Volatilisation Analysis, (TVA), was first described by M<sup>C</sup>Neill (54) and measures the pressure of volatile material evolved from a heated polymer sample in a continuously pumped system as it passes from the heated area to a liquid nitrogen trap. By inserting a trap at a temperature between ambient and liquid nitrogen in front of the pressure gauge, a response will only be obtained for

substances sufficiently volatile to pass through the trap. By varying the temperature of the intervening trap, a considerable amount of information may be obtained about the nature of the products. The DCTVA apparatus depicted in Figure 2.7 was later developed by M<sup>c</sup>Neill (55) in order to obtain the same information in a single experiment. Four traps at different temperatures are placed before the main trap with a Pirani gauge placed after each of the five traps in the system. The Pirani responses are fed into a multi-point recorder at the same time as a temperature versus time response from a thermocouple in contact with the sample in the degradation oven. A thermogram is obtained which is characteristic of particular polymer and gives information about stability, reaction mechanisms and the nature of the volatile products.

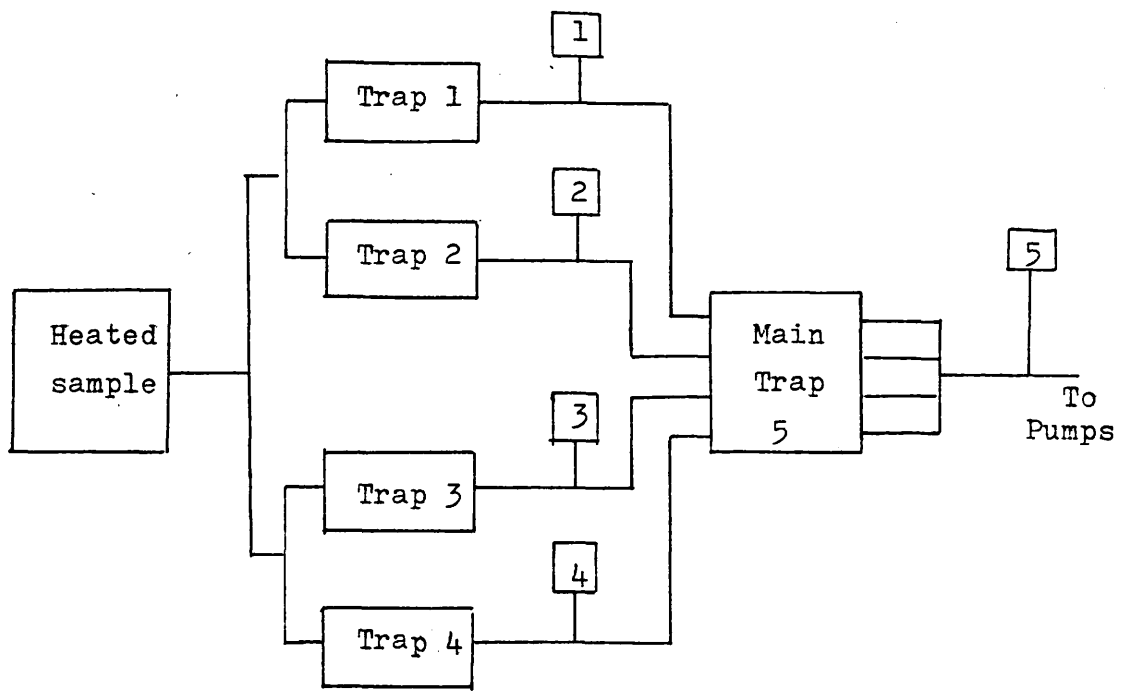
This technique was employed for examining the effects of photodegradation on the thermal stability of copolymers.

## 2.5 SPECTROSCOPIC TECHNIQUES.

### 2.5.1 Infrared Spectroscopy.

A minimum volume gas cell of 20mm path length was employed in the analysis of gaseous products. The volatiles were condensed in a capillary tube at the base of the cell which was sealed under vacuum. On warming-up the products expanded into the main chamber which was orientated to allow the infrared beam to pass through via the NaCl plates at either end.

Absorption changes in polymer films were monitored by



NORMAL WORKING TEMPERATURES :

Trap 1       $0^{\circ}\text{C}$

Trap 2       $-45^{\circ}\text{C}$

Trap 3       $-75^{\circ}\text{C}$

Trap 4       $-100^{\circ}\text{C}$

Trap 5       $-196^{\circ}\text{C}$

1,2,3,4 and 5 = Pirani Gauge Heads

FIGURE 2.7. Schematic diagram of the Four Line

Differential Condensation TVA System.

clamping them at a specific point in a magnetic holder, ensuring that the same portion of the film was measured each time.

Polymers in the powdered state were first ground up with potassium bromide and pressed into transparent discs.

All spectra were recorded on Perkin Elmer 225 or 257 Grating spectrophotometers with gas purging facilities.

#### 2.5.2 Ultra-Violet Spectroscopy.

All spectra were recorded on a Unicam SP800 spectrophotometer. Films were secured to a carrier plate by a magnet while gaseous products were treated as in the previous section.

#### 2.5.3 Mass Spectrometry.

Samples were analysed on an A.E.I. MS12 Mass Spectrometer with gold inlet system for gases and gallium inlet for liquids. The instrument was purged overnight when gaseous samples were to be analysed.

#### 2.5.4 Nuclear Magnetic Resonance Spectroscopy (NMR).

100MHz high resolution  $^1\text{H}$  NMR spectra were obtained in solution at elevated temperatures. Copolymers with methyl methacrylate were dissolved in chlorobenzene or acetone-d<sub>6</sub> with tetramethylsilane as internal standard. Copolymers with styrene were recorded in deutero-chloroform solution. Varian HA100 and Varian XLL100 NMR spectrometers provided the data.

NMR spectroscopy is an ideal method for providing the information about the stereochemical configuration of polymer molecules. Those derived from substituted polyolefins

contain a series of asymmetric carbons along the backbone. If a polymer chain derived from an  $\alpha,\alpha$ -disubstituted monomer  $\text{CH}_2 = \text{CXY}$ , is extended in planar fashion as illustrated in Figure 2.8, the resulting conformation in which all the "X" groups lie above the plane and all the "Y" groups below, or vice-versa, is said to be isotactic. The configuration in which the "X" groups lie alternately above and below the plane is termed syndiotactic, and a random sequence along the chain results in an atactic or heterotactic configuration.

By concentrating on an individual unit in a polymer and observing its orientation with regard to adjacent units, it is possible to envisage different environments for the  $\alpha$ -substituents on the central monomer units of isotactic, syndiotactic and heterotactic triads of monomer units (56). Consideration of diads, triads and longer sequences can be used to explain the experimental observations.

## 2.6 MOLECULAR WEIGHT ANALYSIS.

The number average molecular weight of polymers was obtained on a Mechrolab Model 501 High Speed Membrane Osmometer fitted with a Sylvania 300 grade cellophane membrane and employing toluene or methyl ethyl ketone as solvent. The molecular weight is determined from the thermodynamic relationship:

$$\frac{\Pi}{c} = \frac{RT}{M_n} + b c$$

where  $\Pi$  is the osmotic pressure,

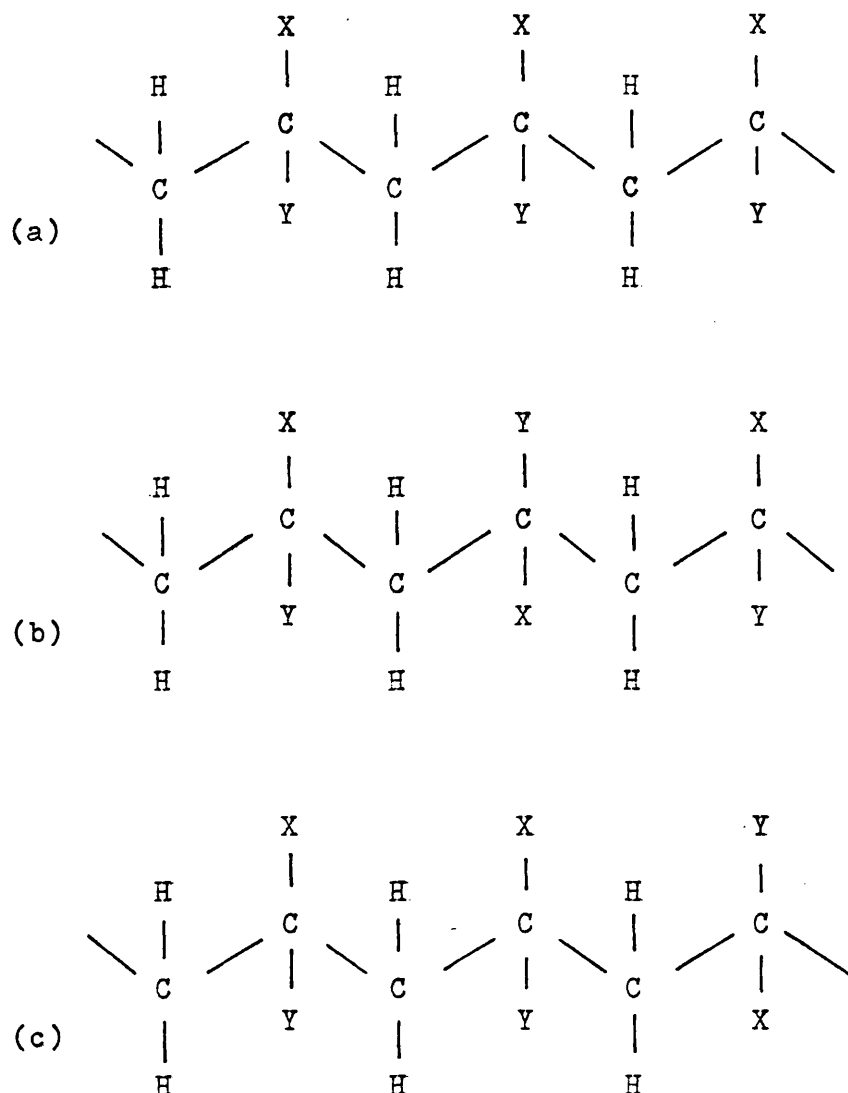


FIGURE 2.8. Segments of polymer chain derived from  $\text{CH}_2 = \text{CXY}$  monomer extended in planar fashion. The molecular configurations are termed

- (a) isotactic,
- (b) syndiotactic and
- (c) atactic or heterotactic.

C is the concentration of the polymer solution,

R is the Gas Constant,

$M_n$  is the number average molecular weight

and T is the temperature of the solution.

The osmotic pressure is recorded for various concentrations of polymer solution. By graphical methods a plot of  $\pi_C$

versus C is extrapolated to infinite dilution where

$$\frac{\pi}{C_{c \rightarrow 0}} = \frac{RT}{M_n}$$

and the molecular weight is obtained by calculation.

## 2.7 MICROANALYSIS.

The percentage of carbon, nitrogen and hydrogen in samples of polymer in powder form was determined on a Perkin Elmer 240 Elemental Analyser. A quantitative analysis of chlorine was obtained by combustion followed by titration with mercuric nitrate.

CHAPTER THREEPOLYMER CHARACTERISATION3.1 GENERAL.

The techniques of polymerisation and purification of the copolymers are broadly outlined in Chapter Two. The conditions of polymerisation are summarised in Table 3.1 and Table 3.3. The molar feed ratios were determined from the copolymer composition equation by inserting the values for the reactivity ratios obtained by Grant (57) for the polymerisation of methyl methacrylate (MMA) with 2,2-chloro-acrylonitrile (CAN), and by Yamada and Otsu (58) for the polymerisation of styrene (STY) with CAN. These are as follows;

$$\text{CAN - MMA} \quad r_1 = 0.43, r_2 = 0.17$$

$$\text{and} \quad \text{CAN - STY} \quad r_1 = 0.13, r_2 = 0.06,$$

where, in each case,  $r_1$  refers to CAN.

The composition of each copolymer was determined by microanalysis and, as shown in Table 3.2 and Table 3.4, agreed with the values calculated from the molar feed ratios.

3.2 SPECTROSCOPIC MEASUREMENTS.3.2.1 Infrared Spectroscopy.

A most extraordinary feature of infrared spectra of the copolymers was the low intensity of the nitrile peak in comparison with the corresponding absorption in copolymers of acrylonitrile with vinyl chloride. In homopolymers of CAN

MMA - CAN COPOLYMERSTABLE 3.1

Reference Number	Molar Feed Ratio (CAN/MMA)	Theoretical Composition	Composition by Microanalysis.		
		MMA	CAN	MMA	CAN
MMC 100	—	100	0	100	0
MMC 90	0.021	90	10	90	10
MMC 85	0.055	80	20	85	15
MMC 74	0.055	80	20	74	26
MMC 50	0.629	50	50	50	50
MMC 35	3.373	30	70	35	65

TABLE 3.2

Reference Number	Initiator Conc'n (% W/V)	Degree of Conversion	Purification System
		Conversion	Solvent Non-solvent
MMC 100	0.05	8	Acetone Methanol
MMC 90	0.05	2	Acetone Methanol
MMC 85	0.10	4	Acetone Methanol
MMC 74	0.05	5	Acetone Methanol
MMC 50	0.50	5	Butanone Benzene
MMC 35	0.50	5	Butanone Benzene

STY - CAN COPOLYMERSTABLE 3.3

Reference Number	Molar Feed Ratio (CAN/STY)	Theoretical Composition		Composition by Microanalysis.	
		STY	CAN	STY	CAN
STC 100	—	100	0	100	0
STC 875	0.0075	90	10	87.5	12.5
STC 75	0.0197	80	20	75	25
STC 69	0.0298	75	25	69	31

TABLE 3.4

Reference Number	Initiator Conc'n (%W/V)	(%)Degree of Conversion	Purification System
			Solvent Non-solvent
STC 100	0.1	4	Acetone Methanol
STC 875	0.50	1.8	Acetone Methanol
STC 75	0.05	5	Acetone Methanol
STC 69	0.05	5	Acetone Methanol

the nitrile peak is reported to be similarly weak as a result of the quenching effect of the chlorine atom (57). Studies by Thompson et al. (59) have shown that polar substituents can have a large impact on the apparent absorption of adjacent nitrile groups. An illustration of this effect is found by comparing the relative intensities of the nitrile absorptions of  $\text{ClCH}_2\text{CN}$  and  $\text{CH}_3\text{CH}_2\text{CN}$ . The absorption by the latter compound was greater by a factor of ten.

The spectra of copolymers with low CAN content, viz. MMC 90 and STC 875, were only marginally distinguishable from those of the respective homopolymers, poly(MMA) and poly(STY), particularly in thin film form where interference fringes tend to obscure nitrile absorption and were, therefore, considered unsuitable as a method of identification. As the proportion of CAN in the copolymer is increased, the nitrile peak grows in intensity. The peak maximum was measured as  $2241 \pm 1 \text{ cm}^{-1}$  which is  $20\text{cm}^{-1}$  lower than that reported for the homopolymer, poly(CAN). The measurement was made on a Perkin Elmer 225 Grating spectrometer which had been previously calibrated against carbon monoxide band frequencies in this region.

The remaining absorptions in the copolymer spectra corresponded to bands associated with the respective homopolymers with the exception of a peak centred at  $640\text{cm}^{-1}$  which increased in intensity as the proportion of CAN was raised. Absorptions in this region are characteristic of carbon - halogen vibrations.

### 3.2.2 N.M.R. Spectroscopy.

#### (i) MMA - CAN system.

The  $^1\text{H}$  N.M.R. spectrum of MMC 100 in chlorobenzene solution at 393K is shown in Figure 3.1A. In this solvent the  $\alpha$ - methyl resonance is markedly dependent on configuration whereas that of the methoxy group is not (60). Therefore, as three types of triad occur, namely syndiotactic, isotactic and heterotactic, the protons of the  $\alpha$ -methyl group absorb at a single frequency which depends on the stereochemical environment. By comparison with published spectra (61) for poly(MMA) the resonances associated with the spectrum of MMC 100 are assigned in Table 3.5.

The methylene resonance predicted for pure isotactic poly(MMA) is an AB quartet and that for pure syndiotactic poly(MMA) a singlet. The complicated profile of the methylene resonance of MMC 100 cannot be fully explained in terms of diads since longer configurational sequences must be taken into consideration.

The area under each peak in the  $\alpha$ -methyl triplet gives a measure of the relative amounts of each triad present. A visual examination is sufficient to determine that the polymer is predominantly syndiotactic. This is consistent with the configuration normally adopted by free radical polymerisation at moderate temperatures.

The effect of incorporating CAN into poly(MMA) is shown in Figure 3.1B. The copolymer containing 10 per cent CAN units causes important changes in the different bands. A new band

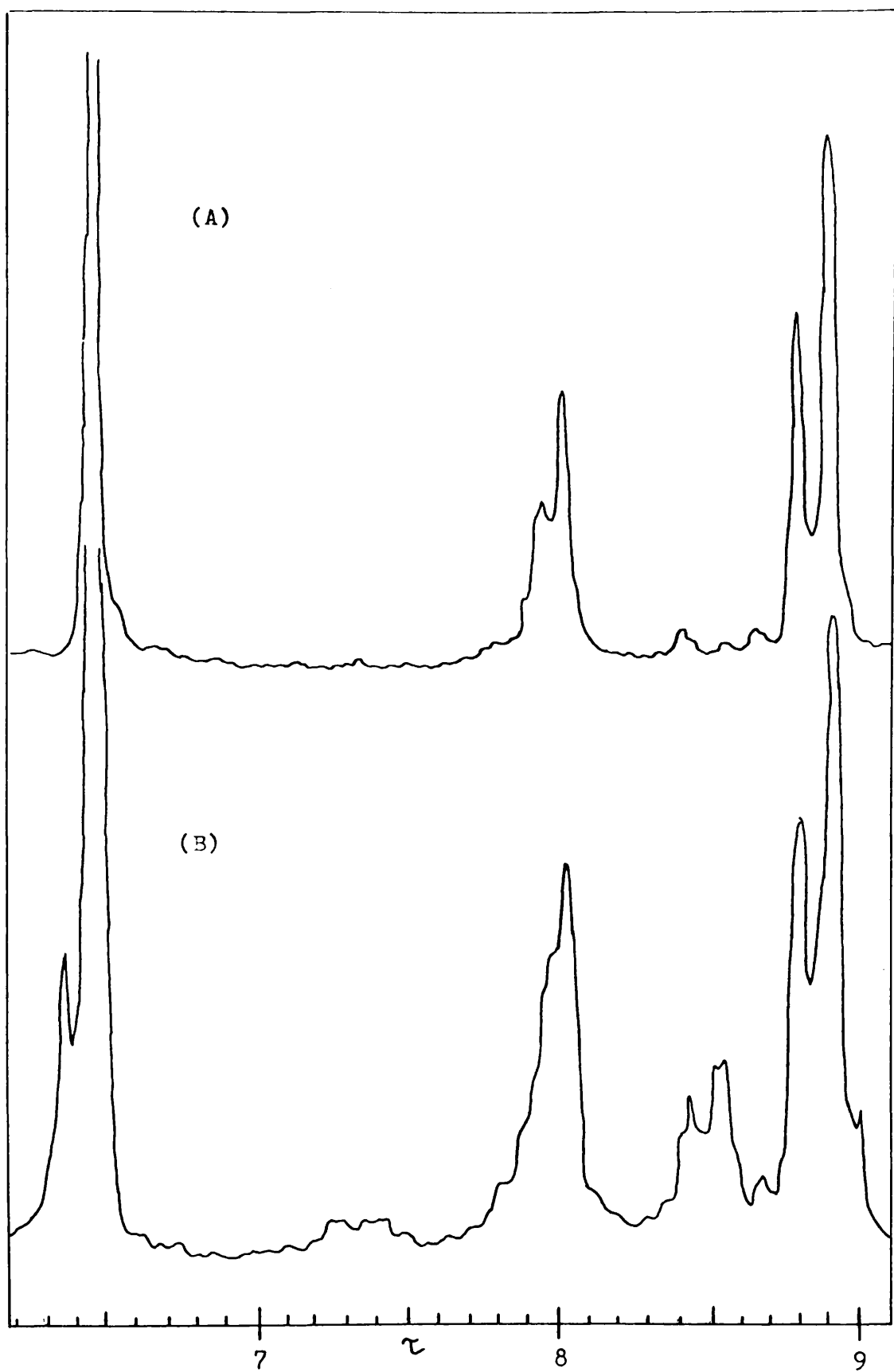


**FIGURE 3.1** 100 MHz NMR Spectra of (A) PMMA and  
(B) MMA-CAN Copolymer with molar ratio 90 : 10.

TABLE 3.5N.M.R. Assignments for Poly(Methyl Methacrylate) from Fig. 3.1A.

Resonance ( $\tau$ ) (Int. Ref. T.M.S.)	Assignment
8.84	$\alpha$ - $\text{CH}_3$ in syndiotactic triad
8.73	$\alpha$ - $\text{CH}_3$ in heterotactic triad
8.61	$\alpha$ - $\text{CH}_3$ in isotactic triad
7.97 7.89	$\beta$ - methylene protons
6.42 6.40	methoxy protons

TABLE 3.6Variation in Methoxy Resonances with Copolymer Composition.

Copolymer Composition (mole % CAN)	Methoxy Resonances ( $\tau$ ) (in order of intensity)
11	6.12 > 6.08 > 6.04
25	6.08 > 6.04 >> 6.12 > 6.00
50	6.00 > 6.04
65	6.00

appears in the methoxy region at  $6.30\tau$  which can be attributed to MMA units adjacent to CAN units. Two new peaks are visible at  $8.50\tau$  and  $8.39\tau$  respectively and an absorption in the  $7.1-7.6\tau$  region is just emerging.

By considering the strong electronegativity of the CAN unit it is reasonable to assign the peaks at  $8.50-8.39\tau$  to  $\alpha$ -methyl groups and those in the  $7.1-7.6\tau$  region to methylene groups. This was confirmed by measuring the integral of the areas under the  $\alpha$ -methyl and  $\beta$ -methylene peaks. In a copolymer with 10 per cent CAN units the proton ratio for  $-\text{CH}_3$  :  $-\text{CH}_2$  groups can be calculated as 2.7 : 2. Only by making the above assumption was this ratio obtainable. Thus the  $\beta$ -methylene absorbing downfield must be beta to both a " $-\text{CO}_2\text{CH}_3$ " and a " $-\text{CN}$ " group while the  $\alpha$ -methyl at low field must be adjacent to a CAN unit.

In order to determine the effects of increasing the CAN content in the copolymer, measurements were carried out in acetone- $d_6$  which proved to be the most suitable common solvent for the copolymers. The spectra, recorded at 333K are shown in Figure 3.2. Spectrum A is that of MMC 90 and it is obvious that the overall pattern is similar to that obtained in chlorobenzene with the exception of the apparent shifts and the peaks corresponding to impurities such as water and acetone.

Over the range of copolymers studied there are three principal areas of absorption due to the  $\alpha$ -methyl protons (ca. 9.00-7.70 $\tau$ ), the protons of the methylene groups

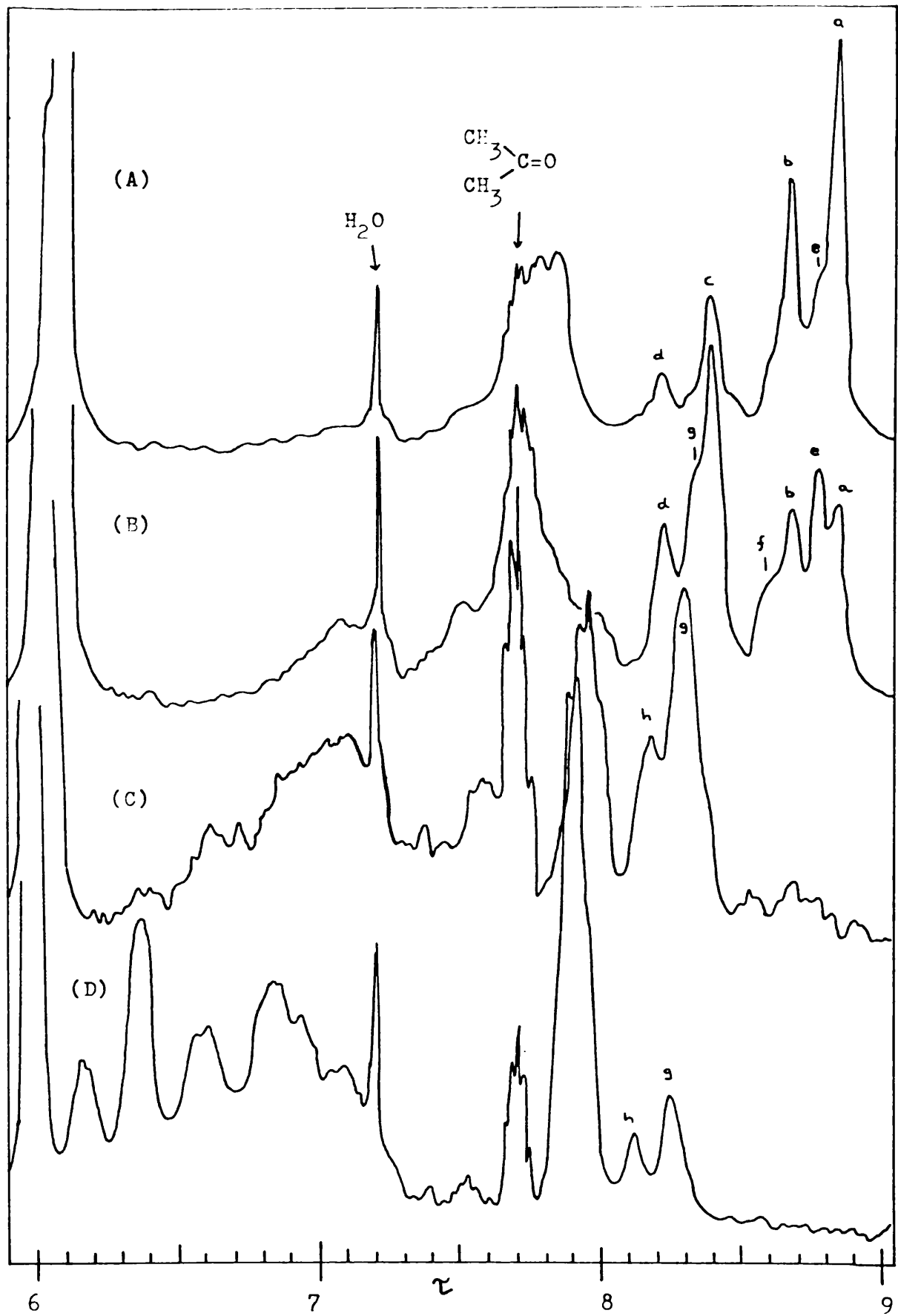


FIGURE 3.2 100 MHz NMR Spectra of MMA-CAN Copolymers.

(ca. 7.70-6.10 $\tau$ ) and the methoxy protons (ca. 6.10-5.90 $\tau$ ). It is obvious that as the CAN content increases each of the resonance peaks shifts downfield.

The  $\alpha$ -methyl protons which show a dependence on configuration in acetone are also particularly interesting. At a concentration of 10 per cent CAN units peaks "a" and "b", which correspond to triads in pure poly(MMA), predominate over absorptions at "c" and "d" which have been attributed to  $\alpha$ -methyl groups adjacent to CAN units. On increasing the CAN content to 15 per cent (spectrum B) the intensity of "c" and "d" increases at the expense of "a" and "b". New peaks at "f" and "e" (which can be recognised as a shoulder on "a" in spectrum A) begin to emerge. In this case longer configurational sequences such as pentads must be considered in which the central methyl group is affected by CAN units over a distance of at least one MMA unit.

In the 50 per cent CAN copolymer (spectrum C) peaks "a", "b", "e" and "f" have almost disappeared with the implication that few MMA triads can exist at this composition. This is consistent with the low values obtained for reactivity ratios which suggest a tendency for the monomers to polymerise in an alternating sequence. In fact, the new peak which occurs at 7.96 $\tau$  can be attributed to the central methyl of a CAN - MMA - CAN triad because of the large downfield shift. Peaks "g" and "h" which were previously only present as shoulders on "c" and "d" have superceded the latter on the downfield side suggesting that sequences such as CAN - MMA - MMA - CAN - MMA

are becoming increasingly prevalent.

The structure of the copolymer with 65 per cent CAN units based on  $\alpha$ -methyl measurements would appear to be almost completely alternating. MMA diads are still in evidence but no trace of MMA triads remains.

On examining the methylene resonances a more complex picture emerges. In terms of diads three possible structures exist visually MMA - MMA, MMA - CAN and CAN - CAN. By comparing spectrum A with spectrum D it is possible to limit MMA - MMA diads to the upper region of absorbance (ca. 7.9 - 7.4 $\tau$ ). There appears to be considerable overlap between the other types of diads but the CAN - CAN would be expected to occur at lower field adjacent to the methoxy resonance.

On the scale of Figure 3.2 the fine structure of the methoxy peak is absent but shoulders have been observed on the peaks in spectra A, B and C. In spectrum D the peak is virtually a singlet. The resonances are recorded in Table 3.6. A general trend becomes apparent in which the methoxy resonance corresponds initially to that in poly(MMA) and finally to that in an alternating copolymer.

#### (ii) STY - CAN system.

Gaylord and Patnaik (62) have investigated the N.M.R. spectra of a series of STY - CAN copolymers prepared by free radical polymerisation. By comparison with their assignments the spectra of STC 875, STC 75 and STC 69 have been characterised.

Three principal areas of absorbance can be distinguished:

2.5 - 3.5 $\tau$  ; assigned to aromatic protons,  
6.5 - 7.7 $\tau$  ; assigned to  $\alpha$ -methine protons of STY,  
7.7 - 8.5 $\tau$  ; assigned to  $\beta$ -methylene protons.

It was found that, as the CAN content of the copolymer was increased, each of the resonance peaks shifted downfield. This is consistent with the observations on the three copolymers which were studied in deutero-chloroform at 363K.

The spectrum of STC 69 is shown in Figure 3.3. The splitting of the phenyl resonance at 3.00 $\tau$  is thought to be caused by environmental groups. The methylene protons common to both CAN and STY units appear as a single peak at the highest field strength (8.10 $\tau$ ) and some overlap can occur with the methine resonance at 7.6 $\tau$ . The resonance at 6.8 $\tau$  is attributed to methine protons centred in CAN - STY - CAN triads (62). As little overall change occurred in the spectra on increasing the CAN content no distinction could be made between methylene groups centred in STY - STY diads and those in STY - CAN diads.

### 3.3 ALTERNATIVE COPOLYMER COMPOSITION ANALYSIS.

Microanalysis is not necessarily the most reliable method for measuring the relative amount of each monomer in a copolymer. If characteristic peaks can be distinguished for the two monomers in the  $^1\text{H}$  N.M.R. spectrum of the copolymer, the relative amount of each component can be calculated from the ratio of the areas under those peaks (63). The ratios are obtained from the integral curve of protons provided by the spectrometer. In the copolymers studied, however, no

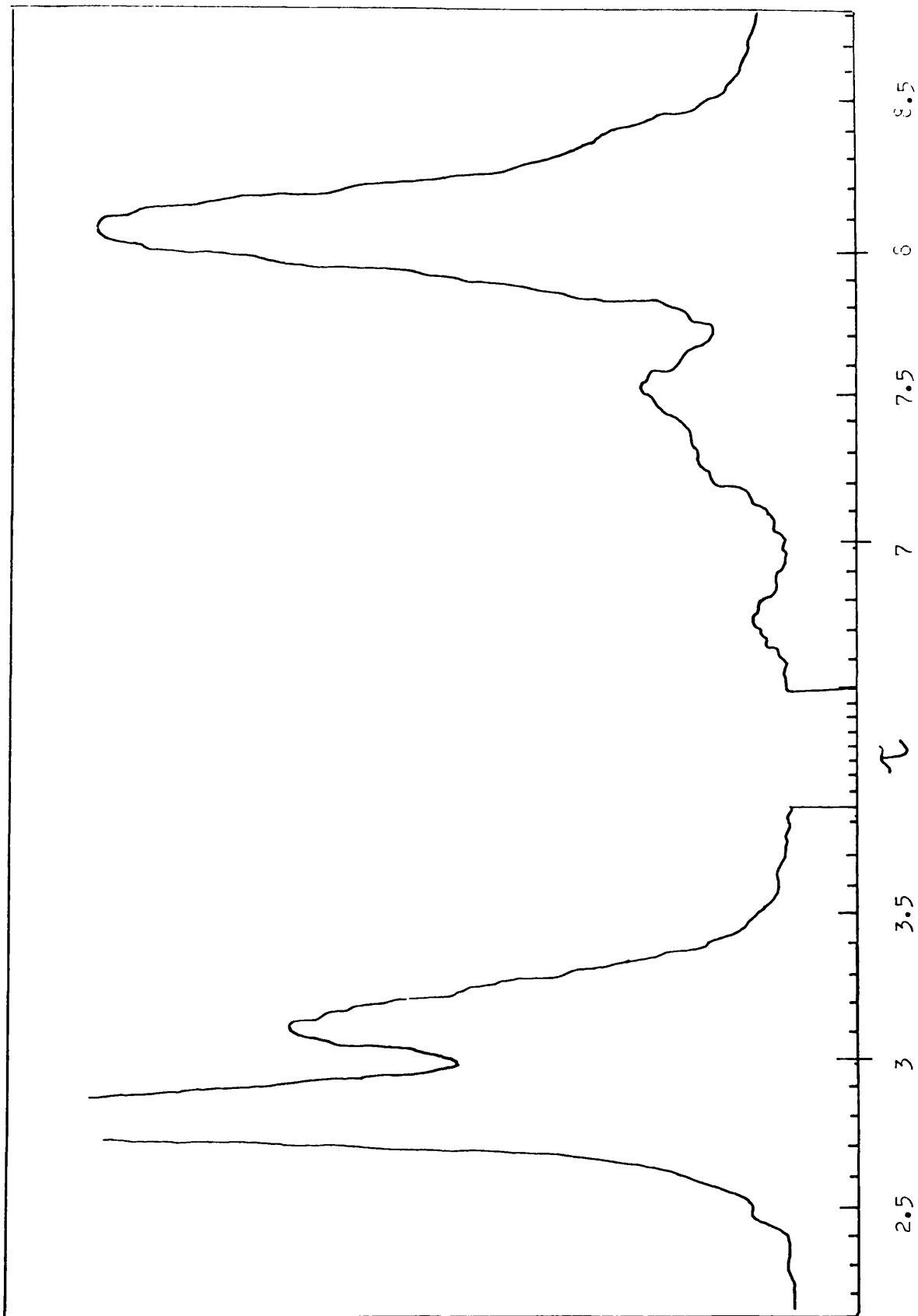


FIGURE 3.3 100 MHz NMR Spectrum of STY-CAN Copolymer  
with molar ratio 69 : 31.

characteristic peak could be resolved for the CAN unit.

An alternative method is available involving the total proton difference between the two monomers, eight from MMA, eight from STY and two from CAN. In the case of the MMA - CAN system,

where  $X$  = the molar ratio of MMA to CAN in the copolymer,

then 
$$\frac{I_{\text{total}}}{I_{-\text{CH}_2-}} = Y = \frac{(8X + 2)}{(2X + 2)}$$

in which  $I_{\text{total}}$  and  $I_{-\text{CH}_2-}$  are the integrals of the peaks associated with the whole copolymer and the methylene groups respectively.

Therefore,

$$X = \frac{(Y - 1)}{(4 - Y)}$$

In the case of a copolymer containing ten per cent CAN units the value of  $Y$  would be 3.7, and for a copolymer with twenty per cent CAN units  $Y$  becomes 3.4.

In view of the impurities in the spectra of MMA - CAN copolymers caused by acetone and water and the small difference in  $Y$  values over a 10% change in composition, the method was considered insufficiently accurate for this system. In the case of the STY - CAN copolymer system the methylene resonance could not be distinguished completely from the methine resonance and the method was inapplicable. Microanalysis was, therefore, accepted as the most reliable method of analysis of copolymer composition.

## CHAPTER FOUR

### PHOTODEGRADATION STUDIES ON COPOLYMERS OF METHYL METHACRYLATE WITH 2,2-CHLOROACRYLONITRILE.

#### 4.1 INTRODUCTION.

The investigation into the photolysis of the methyl methacrylate - 2,2-chloroacrylonitrile (CAN) copolymer system has been approached from several angles and it is hoped that by combining the information obtained from each a more complete picture can be built up of the overall degradation reaction.

The main points of interest are

- (a) the molecular weight changes in the film,
- (b) the spectroscopic changes in the film, and
- (c) the evolution of volatile products during degradation.

The sample form, sample history and degradation apparatus and conditions have been described in the appropriate sections of previous chapters.

#### 4.2 MOLECULAR WEIGHT STUDIES.

##### 4.2.1 Background.

The outstanding characteristic of the photolysis of poly(methyl methacrylate) films at ambient temperatures, as stated in Chapter One, is a rapid decrease in molecular weight. This is typical of a polymer undergoing random chain scissioning. It is important to examine the effect on the rate of scissioning of poly(methyl methacrylate) of incorporating small amounts of CAN units.

A measure of the rate of scissioning can be obtained from the relationship,

$$\frac{s}{P_0} = \frac{1}{P_t} - \frac{1}{P_0} = kt \quad \dots \dots \dots \quad (4.1)$$

in which  $s$  is the number of bonds broken per molecule of initial chain length  $P_0$  and  $P_t$  is the average chain length at the time of degradation  $t$ .  $k$  is a constant. Equation 4.1 may be applied to random scissioning processes at low conversions regardless of the cause of degradation (18).

The value of  $k$  in photodegradation, where it is assumed that only scissioning is occurring is given by Equation 4.2,

$$k = \frac{m}{N} \Phi_s I_a \quad \dots \dots \dots \quad (4.2)$$

in which  $m$  is the molecular weight of monomer,  $N$  is Avogadro's Number,  $I_a$  is the intensity of absorbed radiation per gram and  $\Phi_s$  is the quantum yield for scissioning.

By substituting average molecular weight for average chain length in Equation 4.1, the relationship becomes

$$\frac{s/MW_0}{MW_0} = \frac{1/MW_t}{MW_0} - \frac{1}{MW_0} = \frac{1}{N} \Phi_s I_a t \quad \dots \dots \quad (4.3)$$

$$= k' t. \quad \dots \dots \quad (4.4)$$

When the reciprocal of molecular weight is plotted against the time of exposure for a polymer during degradation, the slope of the graph,  $k'$ , is a measure of the rate of degradation.

In comparing the rates of scissioning of polymer samples consideration must be given to the sample histories and, particularly, to the method of preparation of the films.

As films cast from solution may contain traces of residual solvent in the matrix, the effect of this on the degradation

must be examined. Fox (3) has stated that the problem of finding a photolytically inert solvent is not likely to be solved and, indeed, many solvents have been shown to play an important part in the degradation of their polymer hosts (4). One example of this is the effect of residual tetrahydrofuran on the photolysis of poly(vinyl chloride). Gibb and MacCallum (64) observed that when the concentration of residual solvent is increased, there is a corresponding shift towards the formation of shorter polyenes in the PVC film.

In order to study possible effects of this kind on the methyl methacrylate - CAN copolymer, samples of films cast from various solvents were degraded under identical conditions. The number average molecular weights of the residual films after degradation were measured by osmometry in toluene solution. The technique and operating conditions for the osmometer are described in Chapter Two.

As intensity of light varies within a film depending on thickness, degradation throughout the sample will be non-uniform. Therefore, only average molecular weights are determined and only average quantum yields may be obtained. In practice 50mg samples of polymer film of average thickness 50 microns were irradiated at a distance of 0.18m from the ultra-violet source.

#### 4.2.2 Effect of incorporated CAN units on the rate of scissioning in poly(methyl methacrylate) films.

Samples of pure poly(methyl methacrylate), MMC 100, and the copolymer containing 10 mole per cent CAN units, MMC 90, of

similar initial number average molecular weight (ca.  $3 \times 10^5$ ) were degraded under identical conditions. The effect of the ultra-violet radiation on the molecular weight of each polymer, expressed as a percentage of the initial value, is illustrated in Figure 4.1 and Figure 4.2. The rapid decrease in molecular weight observed in both cases is typical of a polymer undergoing random scissioning of the main chain.

A graphical application of Equation 4.4 is shown in Figure 4.3 for both polymers. As the slope of the graph is a measure of the rate of scissioning occurring during degradation, it is obvious that under the experimental conditions the random incorporation of 10 mole per cent CAN units slightly depresses the scissioning rate in poly(methyl methacrylate) although it remains of the same order of magnitude.

Under the same conditions MMC 74 (26 mole % CAN) was found to be parti\_ally insoluble in both toluene and acetone after an exposure period of five minutes. Copolymers with a higher CAN content also became insoluble on irradiation. Some sol-gel analyses (65) were attempted on the residual films after extraction in a Soxhlet apparatus. These were found to be very irreproducible, presumably due to the sensitivity of the copolymer to reaction during the extraction process, and were, therefore, discontinued. Similar problems of copolymer modification were encountered in the preparation of films from copolymers with a high CAN content during which the normal method of removing solvent from the film matrix,

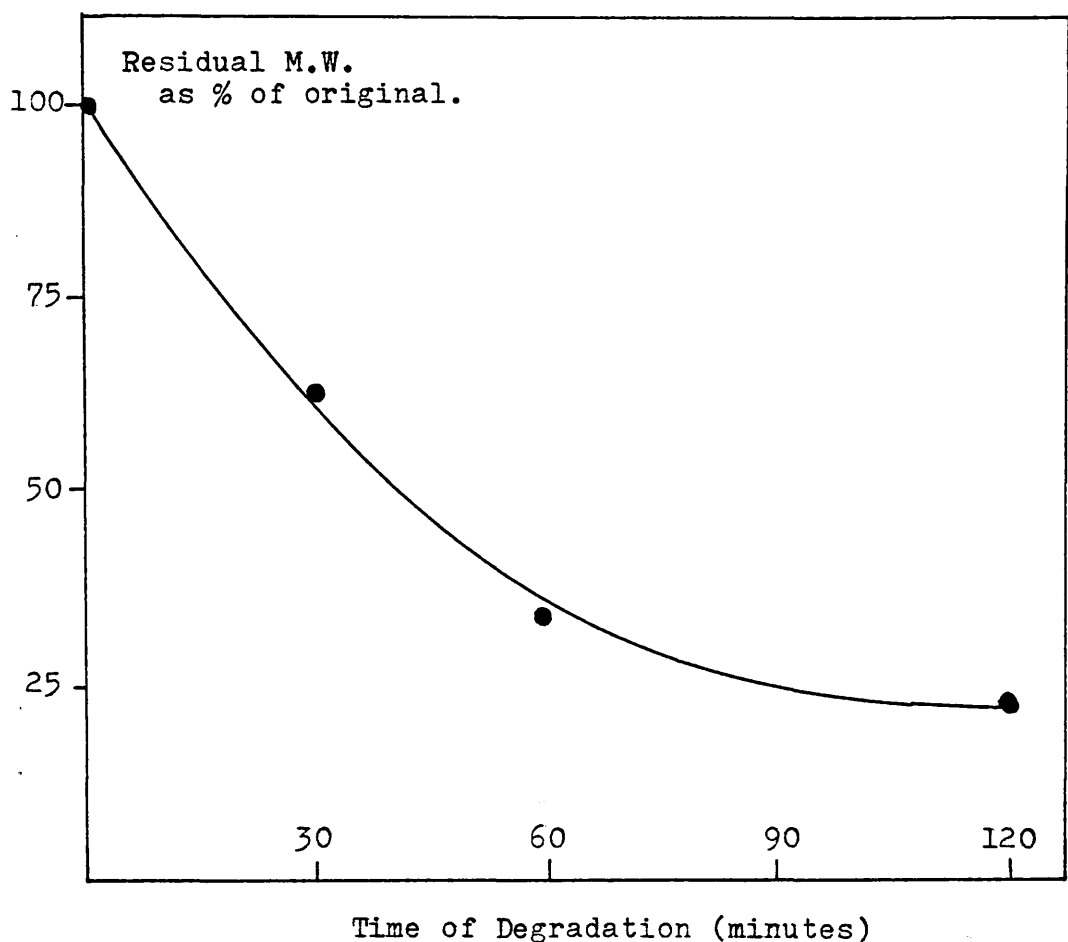


FIGURE 4.1 Effect of degradation on the molecular weight of poly(methyl methacrylate) cast from ethyl acetate solution.

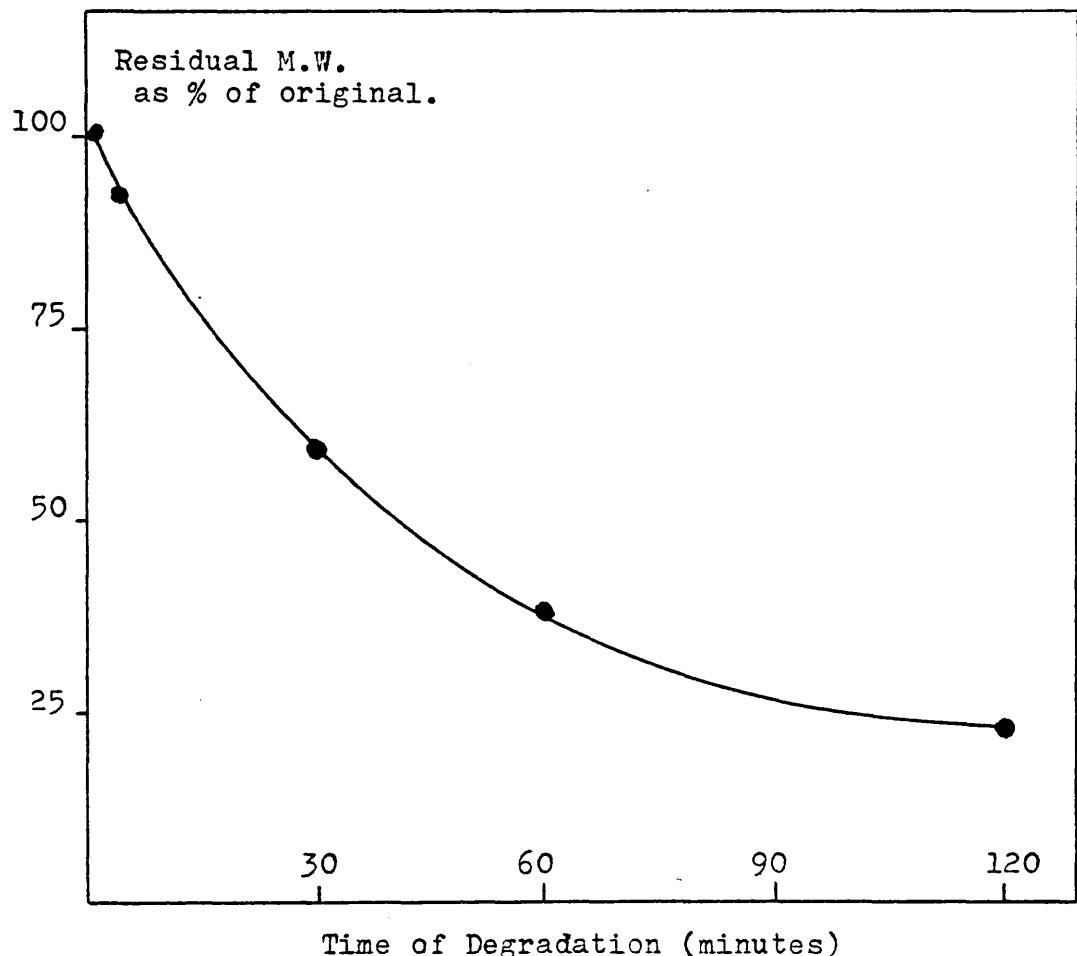


FIGURE 4.2 Effect of degradation on the molecular weight of the 90 mole % MMA copolymer cast from ethyl acetate solution.

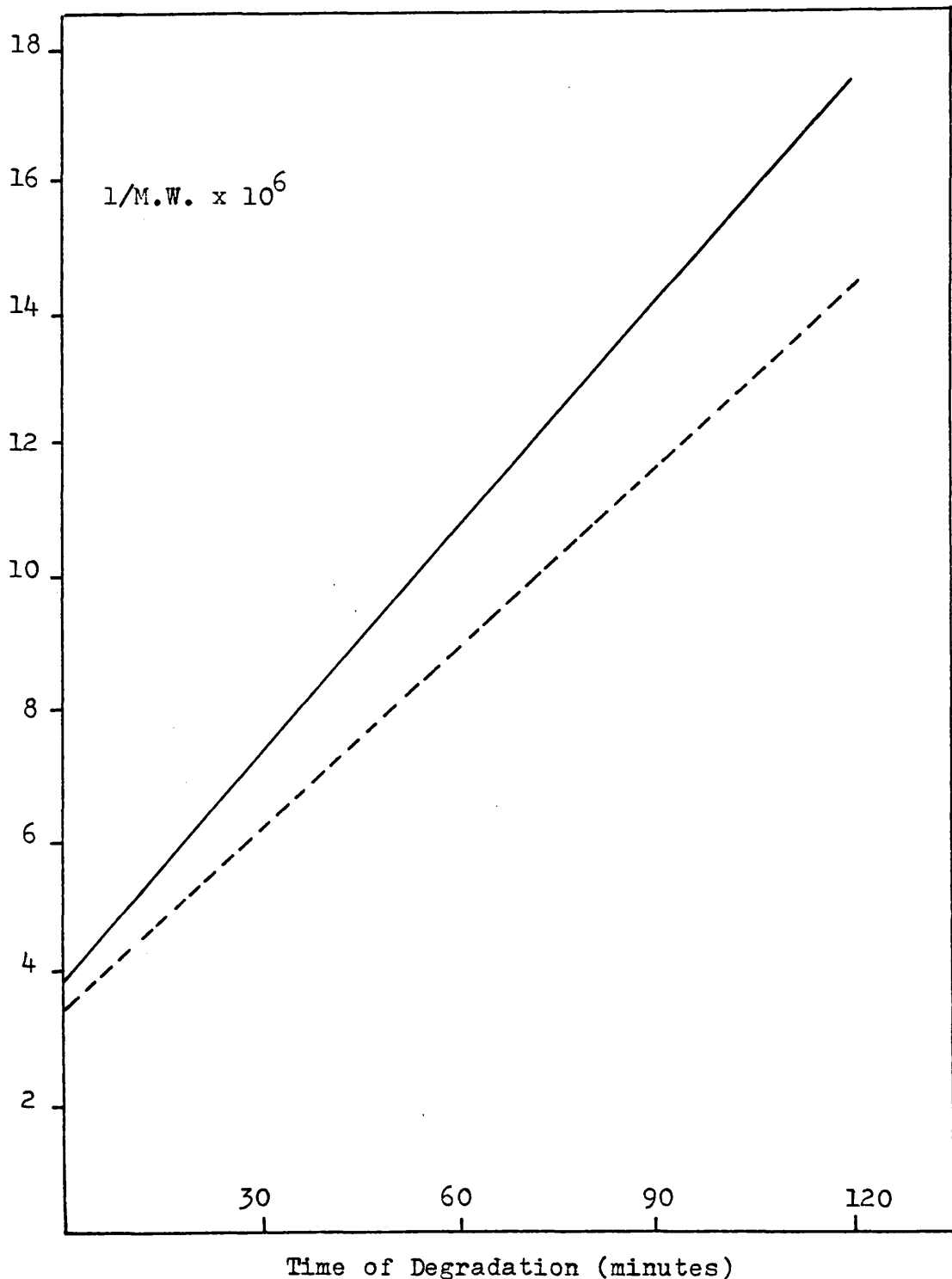


FIGURE 4.3 Dependence of reciprocal molecular weight upon time of degradation of the 90 mole % MMA copolymer (broken line) and poly(methyl methacrylate) under identical conditions.

that is by heating under vacuum conditions, is sufficient to discolour the samples.

#### 4.2.3 Effect of residual solvent on copolymer degradation.

In view of the results obtained in the previous section, it is clear that the copolymer most amenable to study is MMC 90. Separate samples from the same batch of copolymer were dissolved in acetone, chloroform and ethyl acetate respectively and cast as 50mg films. The solvent was removed at ambient temperatures in a vacuum oven for a 48 hour period.

Thermogravimetric analysis of 50mg film samples from the same batch of MMC 90 treated under identical conditions revealed that solvent constituted 4-7 per cent of the total film weight. This technique is described in Chapter Two and the significance of the result is discussed further in the final chapter.

The degradation behaviour of the three systems is shown in Figure 4.2, Figure 4.4 and Figure 4.5 respectively. When these results are converted into relative scissioning rates, as illustrated in Figure 4.6, a marked reduction in rate is observed for films prepared from chloroform solution.

#### 4.2.4 Determination of the quantum yield for scissioning.

The graphs of reciprocal molecular weight against time of exposure shown in Figure 4.6 provide a measure of the relative rates of degradation of the copolymer systems. Of somewhat more general application is the quantum yield for scissioning,  $\Phi_s$ , which is obtained from the quantity  $k'N/I_a$  defined in Equation 4.3 and Equation 4.4.

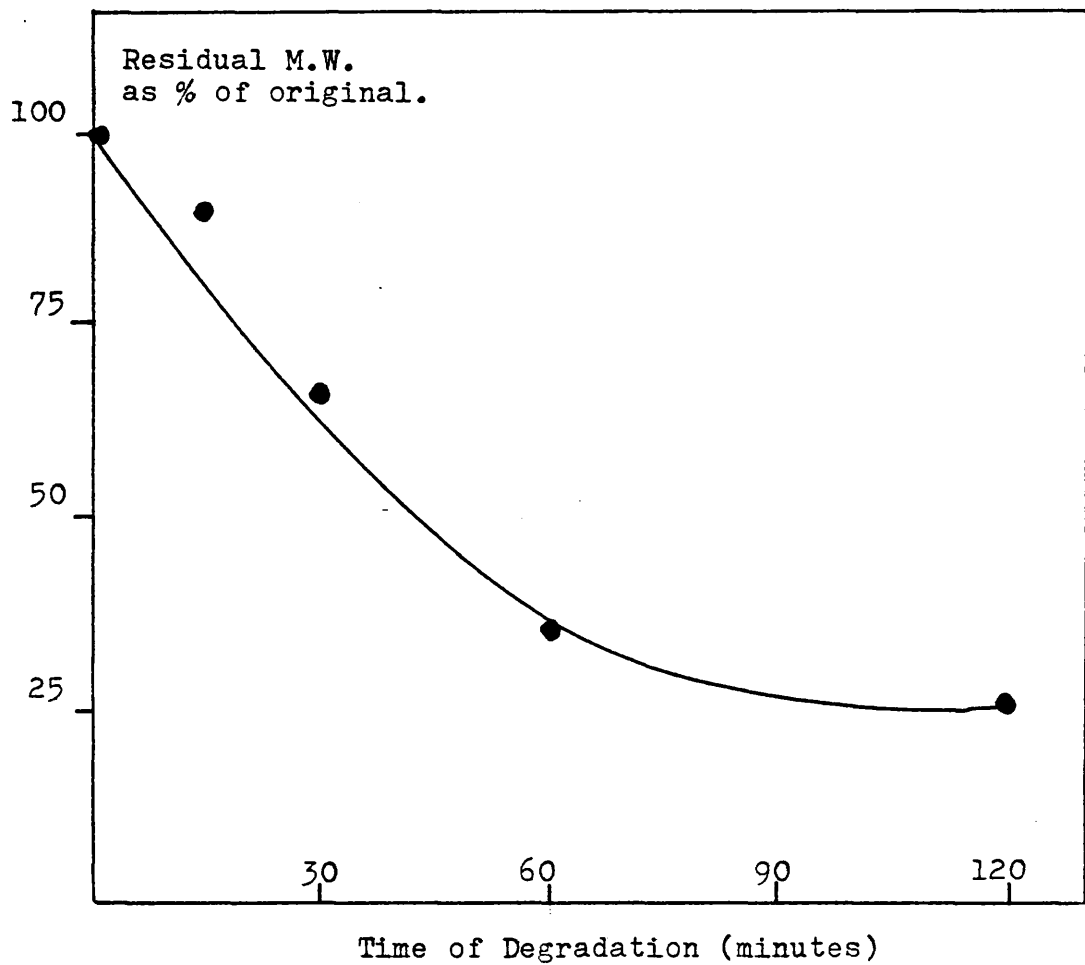


FIGURE 4.4 Effect of degradation on the molecular weight of the 90 mole % MMA copolymer cast from acetone solution.

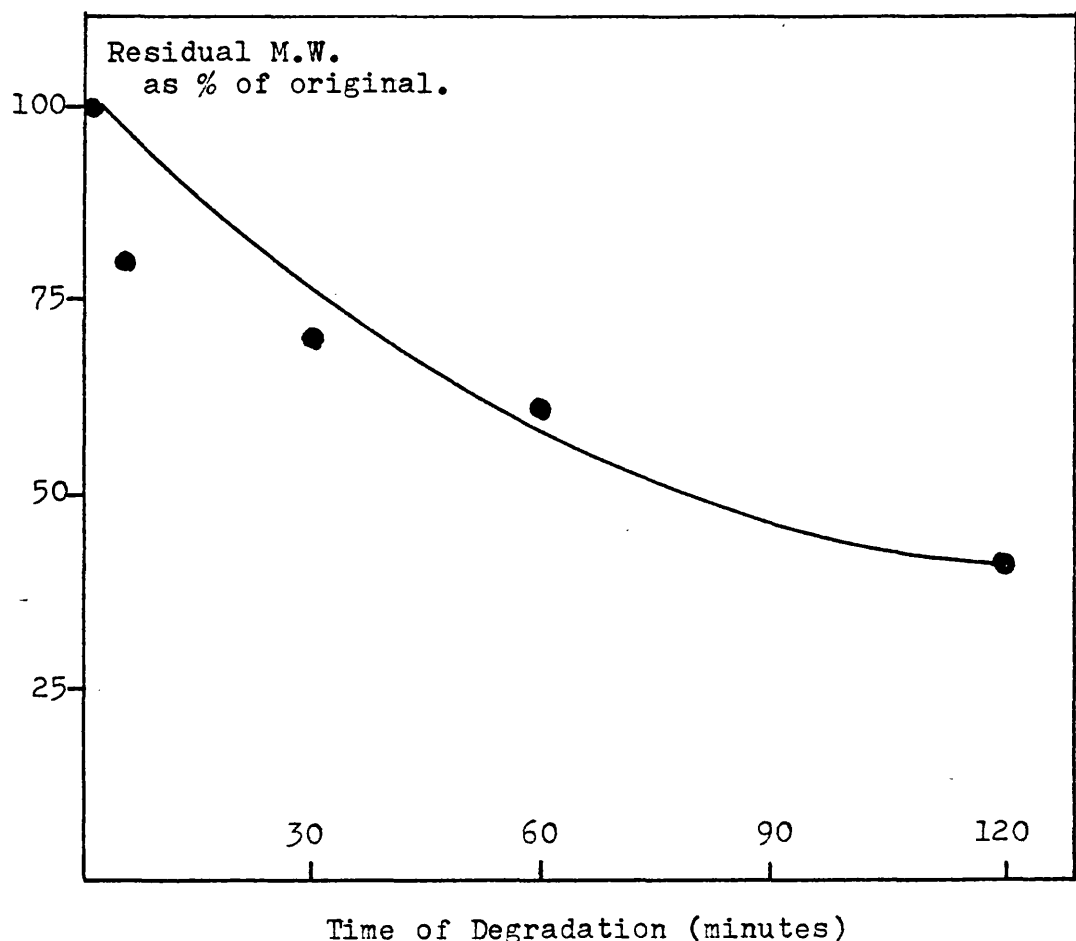


FIGURE 4.5 Effect of degradation on the molecular weight of the 90 mole % MMA copolymer cast from chloroform solution.

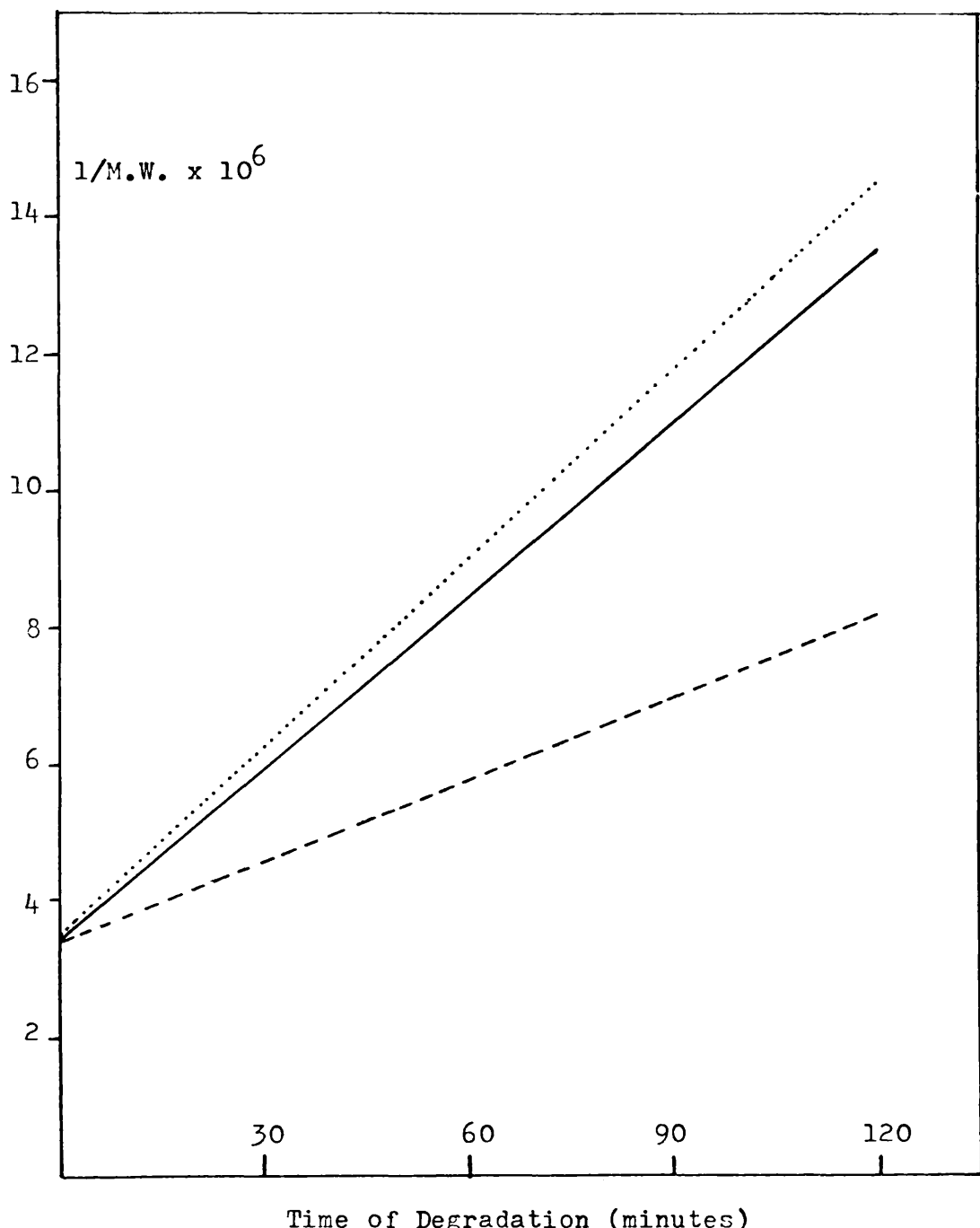


FIGURE 4.6 Dependence of reciprocal molecular weight upon time of degradation of the 90mole % MMA copolymer cast from  
 (a) ethyl acetate solution (dotted line),  
 (b) acetone solution  
 and (c) chloroform solution (dashed line).

The absorption of ultra-violet radiation by the polymer films was determined by spectrophotometry and actinometry using the potassium ferrioxalate system developed by Hatchard and Parker (29) and described in Chapter Two.

The results summarised in Table 4.1 are derived from a series of exposures. It is apparent that the values of  $\Phi_s$  for the MMC 90 copolymer, regardless of solvent, are consistently lower than in the pure poly(methyl methacrylate) film. There is, also, a significant decrease in the value of  $\Phi_s$  for MMC 90 cast from chloroform solution compared to the values for the other MMC 90 films.

#### 4.3 PRODUCT ANALYSIS.      I. CONDENSABLE PRODUCTS.

##### 4.3.1 Introduction.

During the course of studies on scissioning rates, the quantity of volatile material produced was insufficient for convenient analysis. Consequently the sample area was increased and the sample-to-source distance reduced until a suitable evolution rate was obtained ( $I_0^1$  measured as  $3.04 \times 10^{16}$  quanta  $s^{-1}$ ).

A detailed description of the degradation apparatus which consists of photolysis cell, separation unit and analytical gas cells is given in Chapter Two together with the techniques and procedures involved. The separation unit was first calibrated for gases which might reasonably be expected to be found as degradation products by recording the distillation temperature at which each gas reached its maximum pressure. It was found that, for a fixed heating

TABLE 4.1.

Determination of the Quantum Yield for Scissioning  
for MMC 100 and MMC 90.

Polymer Reference	MMC 100	MMC90	MMC 90	MMC 90
Casting Solvent	Ethyl acetate	Ethyl acetate	Acetone	Chloroform
Log $I_o/I$	0.5	0.6	0.6	0.6
$I_o$ (quanta $s^{-1}$ ) $\times 10^{-15}$	2.34	2.34	2.34	2.34
$I_a$ (quanta $s^{-1} g^{-1}$ ) $\times 10^{-16}$	3.2	3.5	3.5	3.5
$k'$ (moles $g^{-1} s^{-1}$ ) $\times 10^9$	1.83	1.55	1.42	0.68
$\Phi_s$ (scissions/quantum)	0.034	0.027	0.024	0.012

rate, as the quantity of gas is reduced, a shift in the distillation maximum to a lower temperature occurs and separation is improved. This point is illustrated in Figure 4.7.

Finally, it should be noted that, as pressure is recorded on a logarithmic scale and the pirani response, dependent on thermal conductivity, requires to be calibrated for each gas, there is no direct relationship between the areas under the different peaks in a product trace.

#### 4.3.2 Control test for the separation unit.

As the major photolysis products of poly(methyl methacrylate) are well-established (33,34), MMC 100 was first degraded as a control test for the separation unit. Samples, approximately 20 microns thick and  $7 \text{ cm}^2$  in area, cast from dimethoxymethane solution were degraded in the photolysis cell and the volatile products were trapped at liquid nitrogen temperature. Typical traces obtained from consecutive exposures of one hour and two hours respectively are illustrated in Figure 4.8. In both cases five peaks can be distinguished, corresponding to five condensed products.

There are four major photolysis products from poly(methyl methacrylate) which are condensable at liquid  $\text{N}_2$  temperature, viz. carbon dioxide, methyl formate, methanol and methyl methacrylate. In many cases residual solvent is also present.

The five peaks in the traces from MMC 100 can each be assigned to a product by consulting the data in Table 4.2.

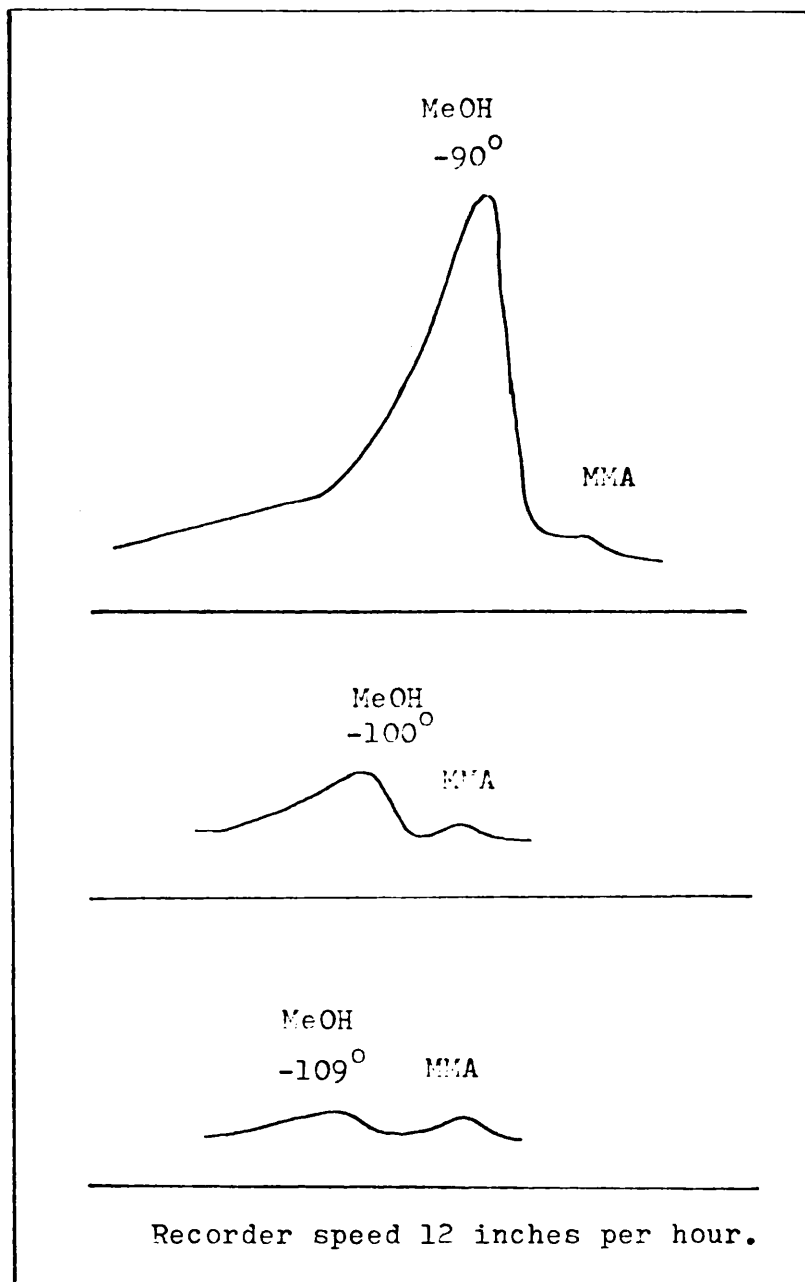
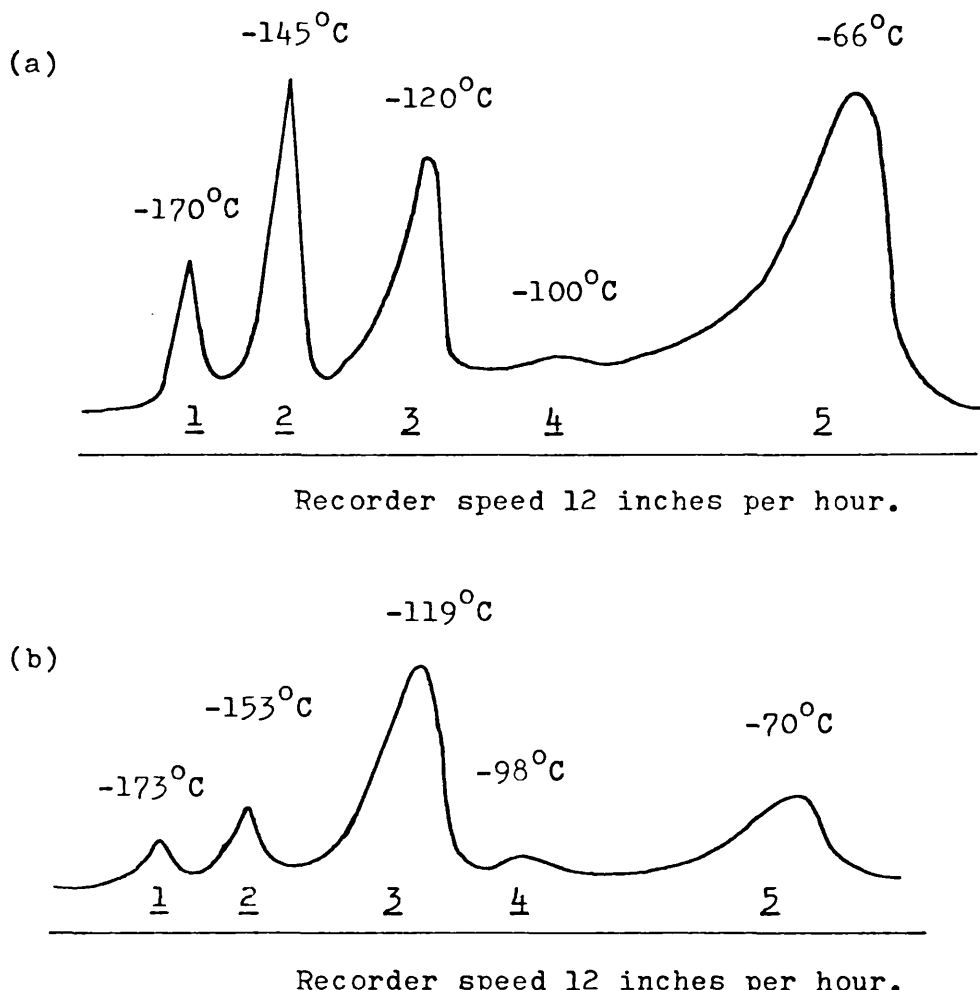


FIGURE 4.7 The two-fold effect of reducing the quantity of methanol in the product trace while the amount of methyl methacrylate is kept constant,

- (1) the distillation temperature is decreased
- (2) separation is improved.



**FIGURE 4.8.** Product trace from the photodegradation of MMC 100 film cast from dimethoxy-methane solution after

- a two-hour exposure period,
- a further one-hour exposure period.

As peaks 1,2 and 3 (carbon dioxide, dimethoxymethane and methyl formate respectively) are, clearly, not overlapping each product can be separately processed and identified. The areas under peaks 4 and 5, however, are made up of contributions from both methanol and methyl methacrylate. For complete separation of these products the pressure of one must be considerably reduced as illustrated previously in Figure 4.7.

The control test on the separation unit has shown the efficiency of the method and the traces from MMC 100 can be used as a reference for copolymers containing blocks of methyl methacrylate units.

#### 4.3.3 Photolysis products from MMC 90.

The traces obtained from the condensable degradation products from MMC 90 had between five and eight peak maxima depending on the casting solvent employed. Products were identified by conventional methods and by comparison with distillation data from the photolysis of MMC 100. A summary of the assignments is provided in Table 4.3.

Samples of MMC 90 cast from dimethoxymethane produced a six-peak trace. Five of the peaks corresponded to the trace from MMC 100, the sixth was identified from its characteristic absorption in the infrared region at  $3050 - 2600 \text{ cm}^{-1}$  as hydrogen chloride. The same result was obtained for samples cast from ethyl acetate solution, with ethyl acetate replacing dimethoxymethane in the products.

Only five peaks were apparent (Figure 4.9b) when

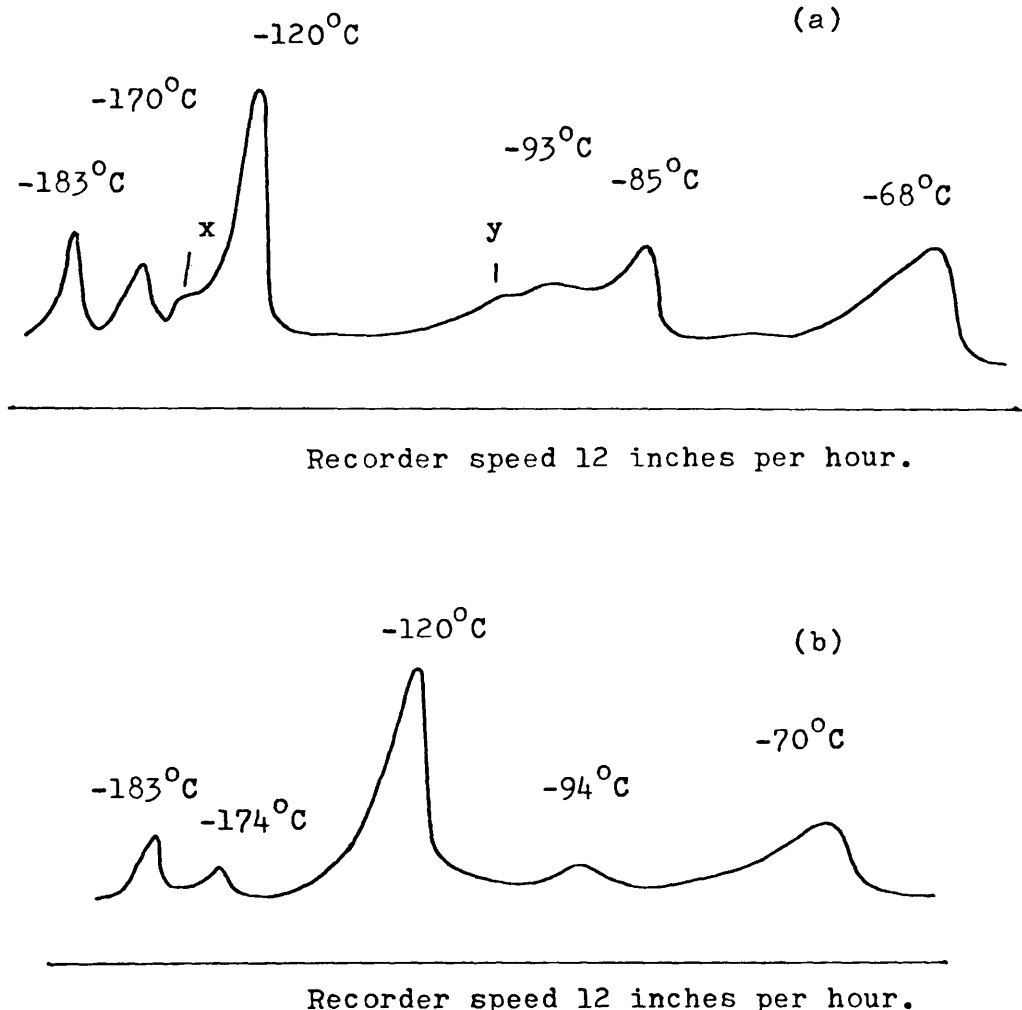


**FIGURE 4.9.** Traces obtained from the products of photodegradation of MMC 90 cast from

- (a) benzene solution,
- (b) dichloromethane solution.

TABLE 4.2.

<u>Product</u>	<u>Distillation Maxima ( <math>\pm 10^{\circ}\text{C}</math> )</u>
Hydrogen Chloride	- 185 $^{\circ}\text{C}$
Carbon Dioxide	- 172 $^{\circ}\text{C}$
Methyl Chloride	- 155 $^{\circ}\text{C}$
Methyl Formate	- 118 $^{\circ}\text{C}$
Methanol	- 96 $^{\circ}\text{C}$
Methyl Methacrylate	- 68 $^{\circ}\text{C}$
Dichloromethane	- 122 $^{\circ}\text{C}$
Dimethoxymethane	- 148 $^{\circ}\text{C}$

TABLE 4.3.Photolysis Products from MMC 90 Film.

<u>Separation Maxima</u>	<u>Infrared Analysis</u>	<u>Mass Spectrometric Analysis</u>	<u>Product</u>
-177 $^{\circ}\text{C}$	3050 - 2600 $\text{cm}^{-1}$	36/100, 38/30, 35/15, 37/5	HCl
-167 $^{\circ}\text{C}$	2320, 670 $\text{cm}^{-1}$	44/100, 16/9	$\text{CO}_2$
-120 $^{\circ}\text{C}$	see Fig. 4.10	—	Methyl Formate
-94 $^{\circ}\text{C}$	—	31/100, 32/70, 29/70	Methanol
-70 $^{\circ}\text{C}$	—	41/100, 69/60, 39/50, 100/25	Methyl Methacrylate

dichloromethane was employed as casting solvent. However, in this case, when the peak with maximum at  $-120^{\circ}\text{C}$  was separated and analysed, the infrared spectrum as shown in Figure 4.10 revealed the presence of both methyl formate and solvent.

Finally, films cast from benzene solution gave rise to seven and occasionally eight products as indicated in a typical trace in Figure 4.9a. The peaks denoted "x" and "y" correspond to the distillation temperatures associated with methyl chloride and 2,2-chloroacrylonitrile respectively. The latter peak was frequently absent.

Prolonged irradiation of MMC 90 from dichloromethane and dimethoxymethane solution respectively gave rise to a peak typical of methyl chloride but this could not be confirmed by mass spectrometry.

#### 4.3.4 Photolysis products from MMC 74.

As illustrated in Figure 4.11, a typical trace from the photolysis products of MMC 74 film contained the four peaks associated with poly(methyl methacrylate) together with hydrogen chloride and methyl chloride. The latter product was identified from the mass spectrometric values of m/e 50, 15 and 52 in the ratio 100 : 70 : 30. The casting solvent was present to a small degree, but masked by methyl formate.

#### 4.3.5 Photolysis products from MMC 50.

A trace similar to that from MMC 74 was obtained. At this mole ratio of monomers new products associated with CAN might reasonably be expected to appear in the trace. An extended irradiation period resulted in the trace in Figure 4.12. On

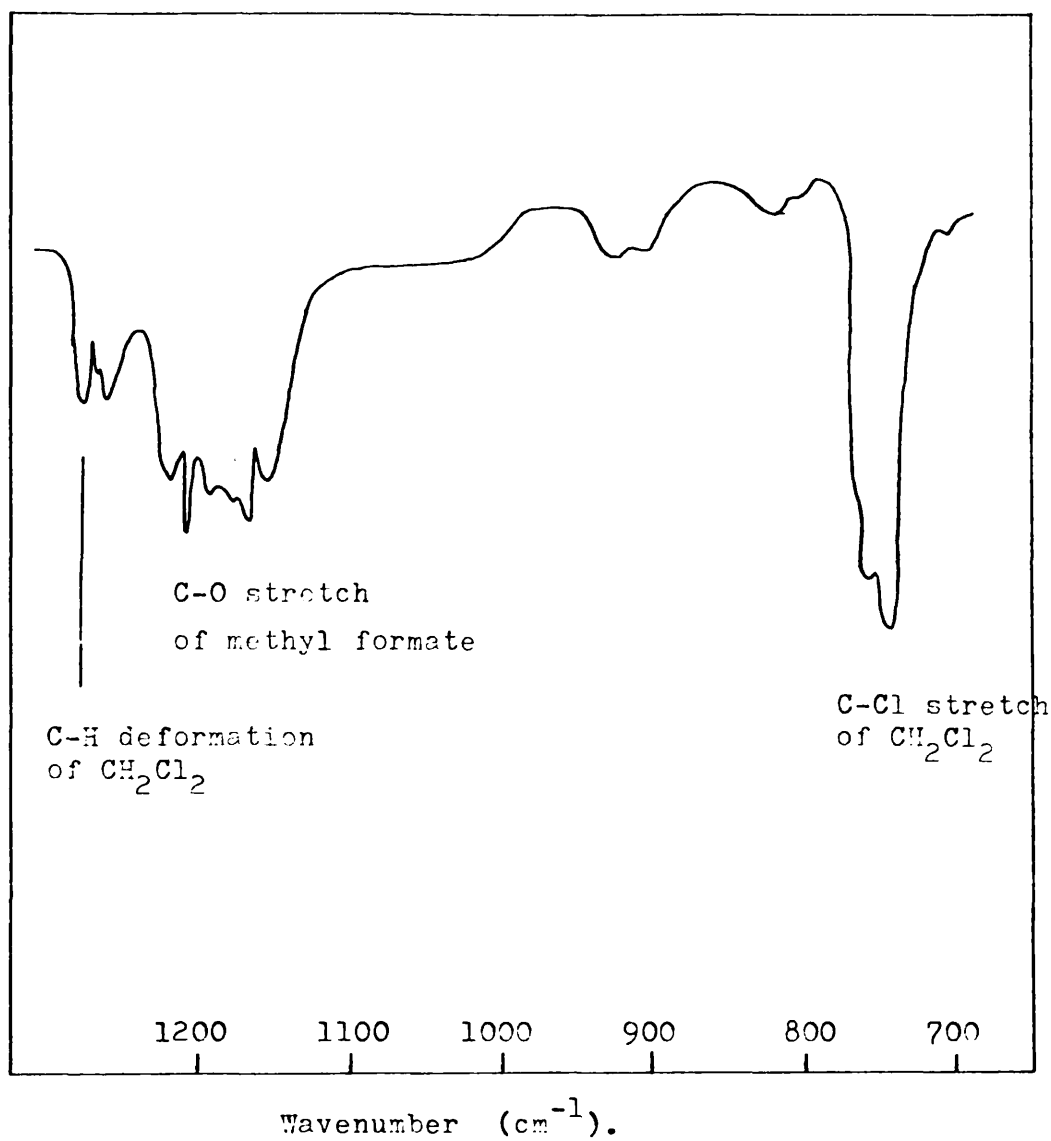


**FIGURE 4.10.** Infrared spectrum of -120° peak from product trace of MMC90 cast from  $\text{CH}_2\text{Cl}_2$  solution (shown in Figure 4.9b).

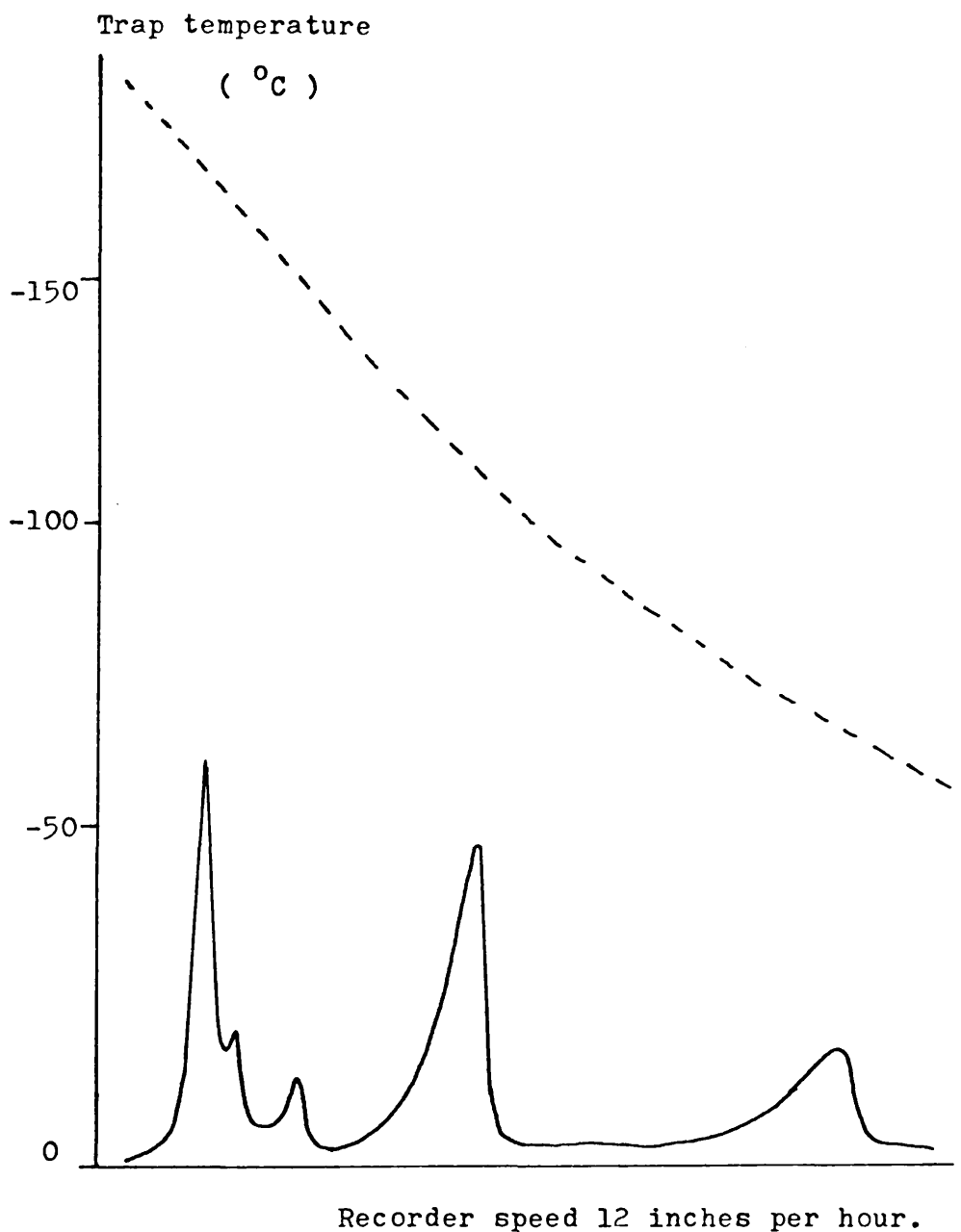


FIGURE 4.11. Product trace from NMC 74 film,  
cast from  $\text{CH}_2\text{Cl}_2$  solution and  
irradiated for a period of  
 $1.1 \times 10^4$  seconds.

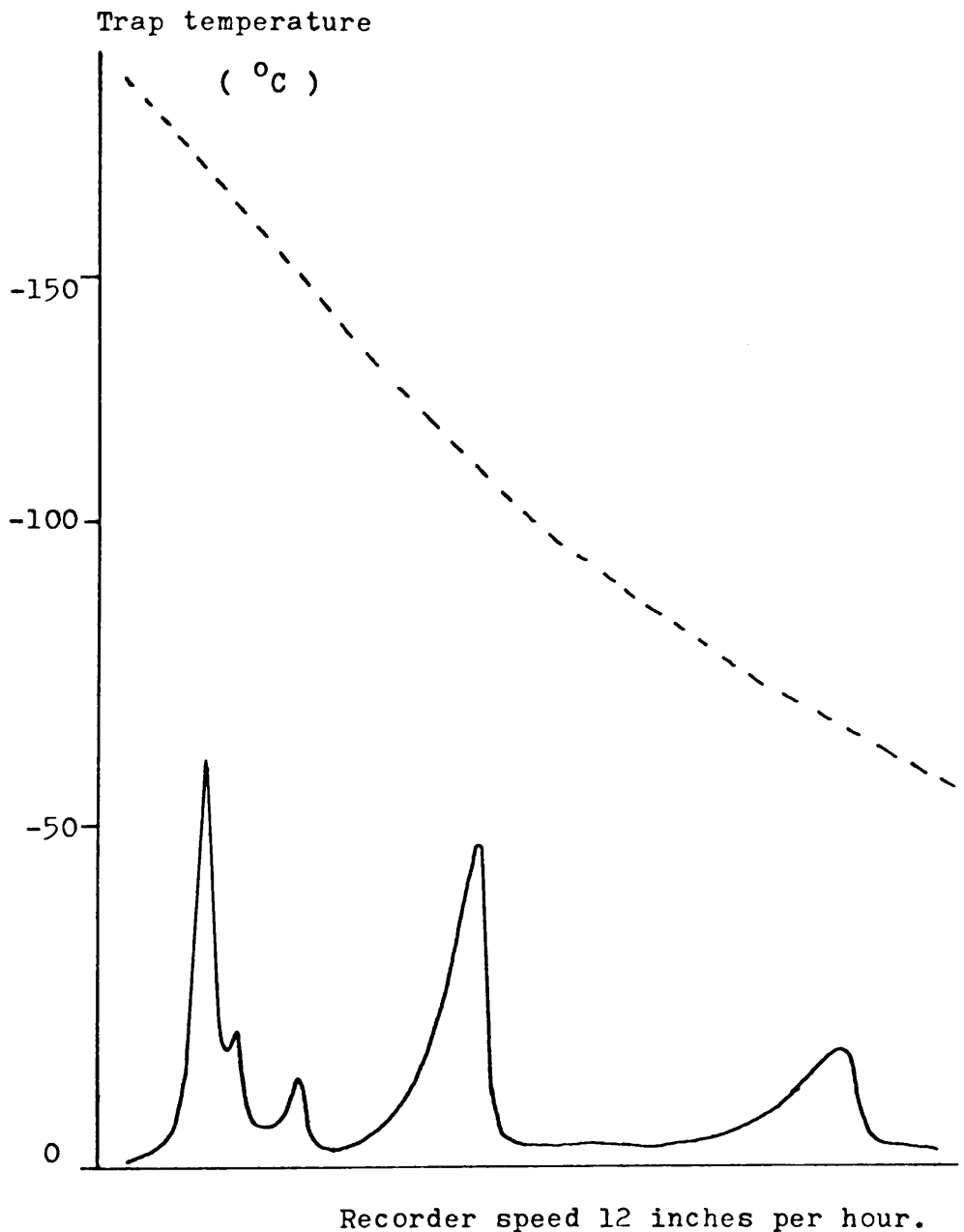


FIGURE 4.11. Product trace from NMC 74 film,  
cast from  $\text{CH}_2\text{Cl}_2$  solution and  
irradiated for a period of  
 $1.1 \times 10^4$  seconds.

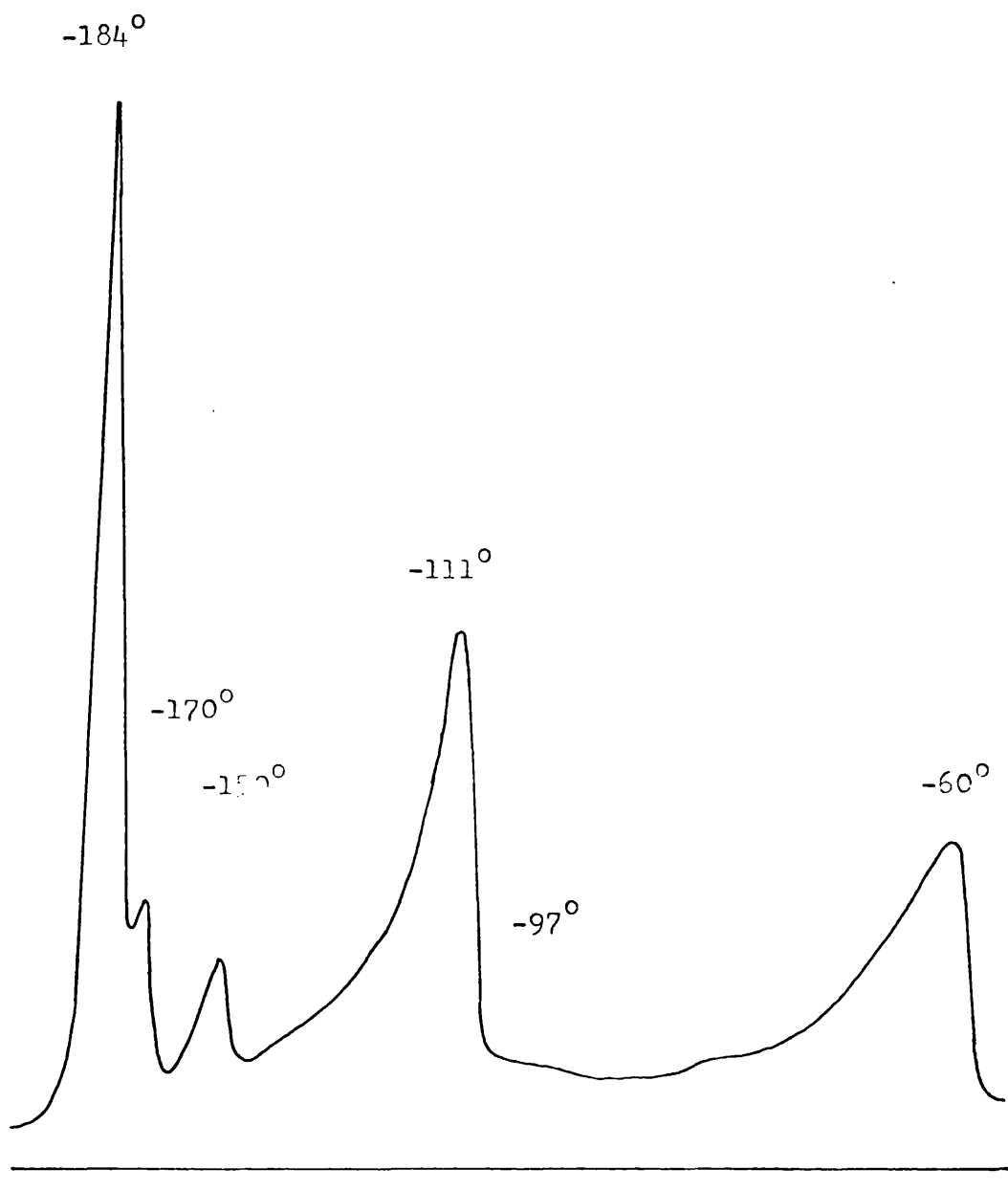
analysis no evidence of any new product was obtained during the exposure periods although product traces indicated small concentrations of CAN monomer.

#### 4.4 PRODUCT ANALYSIS.      II. PERMANENT GASES.

It is generally accepted that the photodegradation of poly(methyl methacrylate) results in the production of carbon monoxide, methane and hydrogen, all of which would pass through liquid nitrogen traps without condensing because of their very low boiling points. A different system was therefore employed to measure the amount of permanent gases produced. The apparatus is described in Chapter Two. A M<sup>c</sup>Leod Gauge was used to measure pressure of gas evolved and a Topler Pump down-line served to remove the product for analysis. This was, essentially, a static system. In order to eliminate secondary photo-reactions in the flux from the ultra-violet lamp, two liquid nitrogen traps were placed between the photolysis cell and the M<sup>c</sup>Leod Gauge thus removing condensable products.

The permanent gases obtained from photolysis of MMC 100 and MMC 90 films were found to be identical. Within the accuracy of the experiment the total pressure of gases from MMC 90 was measurably greater than that from MMC 100. A sample of MMC 50 film was similarly degraded and the products analysed by mass spectrometry. The spectrum showed no significant increase in carbon monoxide over the background but both methane and hydrogen were detected as products.

On this evidence it is reasonable to assume that the increase observed in pressure of products from MMC 90 is



Recorder speed 12 inches per hour.

FIGURE 4.12 Product trace from MMC 50 film, cast from dichloromethane solution, after an exposure period of  $3.4 \times 10^4$  seconds.

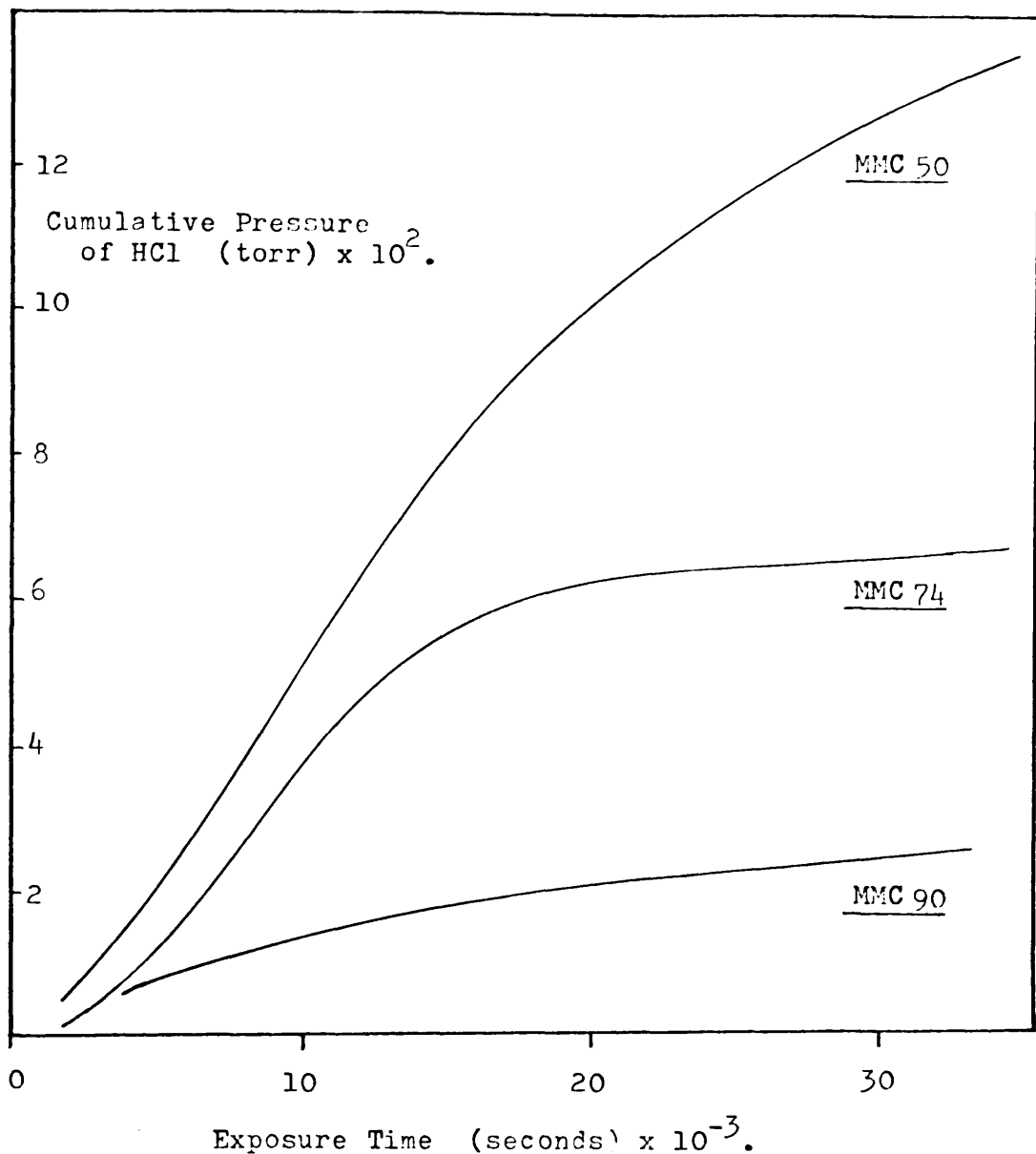


FIGURE 4.13 The evolution of HCl from irradiated films of MMC 90, MMC 74 and MMC50 cast from dichloromethane solution.

not due to carbon monoxide formation.

#### 4.5 VARIATION OF PRODUCT EVOLUTION RATE WITH COPOLYMER SYSTEM.

##### 4.5.1 Introduction.

The procedure for the step-wise, quantitative analysis of volatiles is described in Chapter Two. As the Pirani Gauge is preset to record dry nitrogen, the relationship between the Pirani response and the true pressure of product was determined initially and calibration charts were constructed. This technique involves the use of a McLeod Gauge and is, therefore, suitable only for carbon dioxide and hydrogen chloride. Products with higher boiling points are recorded as direct pressure readings on the gauge and only relative pressures are obtainable.

##### 4.5.2 Hydrogen chloride production.

Copolymer samples of similar mass and area were degraded under identical conditions and the cumulative pressure of hydrogen chloride recorded for each. Typical results are shown in Tables 4.4, 4.5 and 4.6. Graphs obtained by expressing cumulative pressure of hydrogen chloride as a function of time are displayed in Figure 4.13. The most convenient measure of product evolution is in terms of pressure. The temperature and volume of the system can be measured and the mass of gas present calculated as described previously.

From the results shown the total mass of hydrogen chloride produced in a degradation period of  $3.6 \times 10^4$  secs.

from MMC 90, MMC 74 and MMC 50 is in the ratio 1 : 2.5 : 5.1. This corresponds closely with the proportion of hydrogen chloride which is theoretically available in the copolymers if solvent contamination is discounted. The small quantity of methyl chloride formed accounts for some of the available chlorine.

From the data in Table 4.7 it is clear that only a small fraction of the available hydrogen chloride is produced during this degradation period. However, from Figure 4.13 the evolution rate from each copolymer has passed the maximum and appears to be approaching a limiting value.

#### 4.5.3 Carbon dioxide production.

The only source of carbon dioxide in a pure copolymer is the methyl methacrylate unit. It is formed by scission of the ester group from the polymer backbone and subsequent decomposition (4). It follows that, as the amount of CAN in the copolymer is increased, the proportion of carbon dioxide available decreases.

The evolution of carbon dioxide was monitored together with hydrogen chloride in the experiments described in the previous section. Results obtained after a degradation period of  $3.6 \times 10^4$  seconds are summarised in Table 4.8. The production of carbon dioxide is enhanced in the case of MMC 50 film. In contrast, the other products derived from methyl methacrylate units decrease with increasing CAN content.

#### 4.5.4 Methyl chloride production.

The quantity of methyl chloride collected during

TABLE 4.4.Production of Hydrogen Chloride by MMC 90.

Time of Exposure (seconds)	Cumulative pressure of HCl (torr)
$3.6 \times 10^3$	0.006
$14.4 \times 10^3$	0.018
$25.2 \times 10^3$	0.022
$28.8 \times 10^3$	0.024
$32.4 \times 10^3$	0.026
$36.0 \times 10^3$	0.027

TABLE 4.5.Production of Hydrogen Chloride by MMC 74.

Time of Exposure (seconds)	Cumulative pressure of HCl (torr)
$1.2 \times 10^3$	0.001
$4.8 \times 10^3$	0.010
$9.1 \times 10^3$	0.031
$12.7 \times 10^3$	0.051
$16.3 \times 10^3$	0.061
$19.9 \times 10^3$	0.063
$30.7 \times 10^3$	0.066
$34.3 \times 10^3$	0.067
$36.0 \times 10^3$	0.068

TABLE 4.6Production of HCl from MMC 50 Film.

Time of Exposure (seconds)	Cumulative Pressure of HCl (torr)
$0.9 \times 10^3$	0.002
$1.8 \times 10^3$	0.005
$3.6 \times 10^3$	0.014
$5.4 \times 10^3$	0.024
$19.8 \times 10^3$	0.100
$21.6 \times 10^3$	0.106
$32.4 \times 10^3$	0.132
$34.2 \times 10^3$	0.136
$36.0 \times 10^3$	0.137

TABLE 4.7

Percentage Yield of HCl after an Exposure Period of  $3.6 \times 10^4$  s.

Copolymer Reference	HCl Evolved (g)	HCl Available (g)	Efficiency (%)
MMC 90	$0.57 \times 10^{-4}$	$2.57 \times 10^{-3}$	2.2
MMC 74	$1.43 \times 10^{-4}$	$6.86 \times 10^{-3}$	2.1
MMC 50	$2.93 \times 10^{-4}$	$1.38 \times 10^{-2}$	2.1

TABLE 4.8

Percentage Yield of CO<sub>2</sub> after an Exposure Period of  $3.6 \times 10^4$  s.

Copolymer Reference	CO <sub>2</sub> Evolved (g)	CO <sub>2</sub> Available (g)	Efficiency (%)
MMC 90	$2.9 \times 10^{-5}$	$2.74 \times 10^{-2}$	0.10
MMC 74	$2.6 \times 10^{-5}$	$2.34 \times 10^{-2}$	0.11
MMC 50	$3.0 \times 10^{-5}$	$1.67 \times 10^{-2}$	0.18

degradation was found to increase with the chlorine content of the copolymer. Only trace amounts of methyl chloride could be detected after irradiation of MMC 90 film for a period of  $3.6 \times 10^4$  seconds.

Methyl chloride has been identified by Mikheyev and co-workers (66) as a product of the reaction between poly(methyl methacrylate) and ferric chloride under ultra-violet radiation. Mass spectrometric analysis of the system pointed to scissioning of the ester group from the polymer chain initiated by chlorine radicals produced by the photolysis of ferric chloride. The subsequent decomposition of the ester group leads to a methyl radical and carbon dioxide. The methyl radical was thought to abstract a chlorine atom from ferric chloride in preference to hydrogen from the polymer. Both methyl chloride and hydrogen chloride were detected in the mass spectrum.

#### 4.6 SPECTRAL CHANGES OCCURRING DURING DEGRADATION.

##### 4.6.1 Ultra-violet Region.

The absorbance of copolymer films in the ultra-violet region was measured before and after irradiation. Significant changes were observed in all copolymers. The spectra in Figure 4.14 of MMC 90 film after three successive exposure periods show that a progressive increase in absorption occurs. It can be reasonably assumed that new chromophores are being formed during degradation.

An increase in absorbance by poly(methyl methacrylate) during photodegradation has been reported by Fox (33).

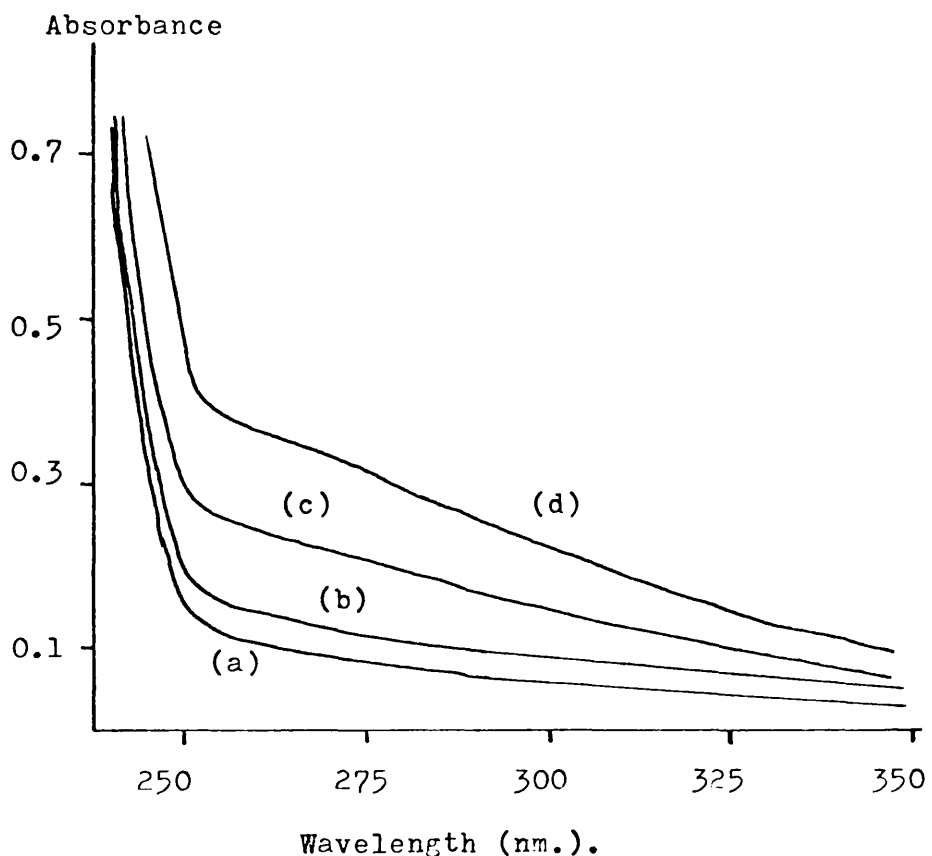


FIGURE 4.14. Ultra-violet absorption spectrum of MMC 90 film cast from chloroform solution and irradiated under the conditions described in Chapter 3 :

- (a) prior to degradation,
- (b) exposed for  $1.8 \times 10^4$  seconds,
- (c) exposed for  $7.2 \times 10^4$  seconds and
- (d) exposed for  $1.08 \times 10^5$  seconds.

However, by degrading MMC 100, MMC 90 and MMC 74 films of similar thickness under similar conditions, the rate of increase in absorbance was found to depend on the proportion of CAN in the copolymer as is shown in Figure 4.15.

One observation which arose from spectroscopic studies was the enhancement of polymer absorbance when benzene was the casting solvent. Benzene had been considered as a photolysis solvent but, as it absorbs ( $\epsilon$  204) at 254 nm, alternative solvents were used in scissioning and product analysis experiments. When two MMC 90 films with different amounts of residual benzene present, as shown by the strong benzene absorption in Figure 4.16, were irradiated under identical conditions, there was considerable disparity in the absorption spectra of the respective, degraded films. New absorptions are recorded at 319 nm, 334 nm and 349 nm in each case. Contrasting this with the spectrum obtained from MMC 90 film cast from ethyl acetate and degraded under identical conditions (Figure 4.17) there is little doubt that the solvent is participating in the reaction.

#### 4.6.2 Visible Region.

After exposure to long periods of irradiation the copolymer films acquire a yellow tint. This occurs more rapidly as the CAN content is increased and regardless of the nature of the solvent used for casting films. This coloration is due to an increase in absorption in the blue-violet region of the spectrum which is a "tail" of the absorption in the ultra-violet. Reference to Figure 4.15 reveals that, at the

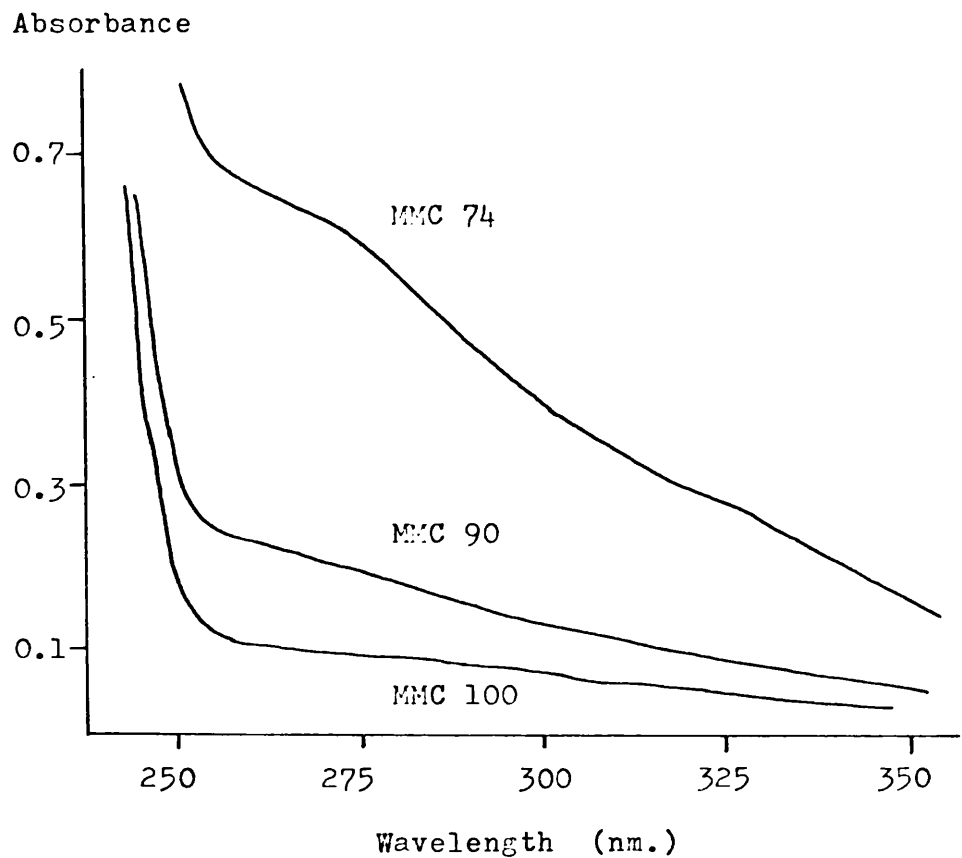
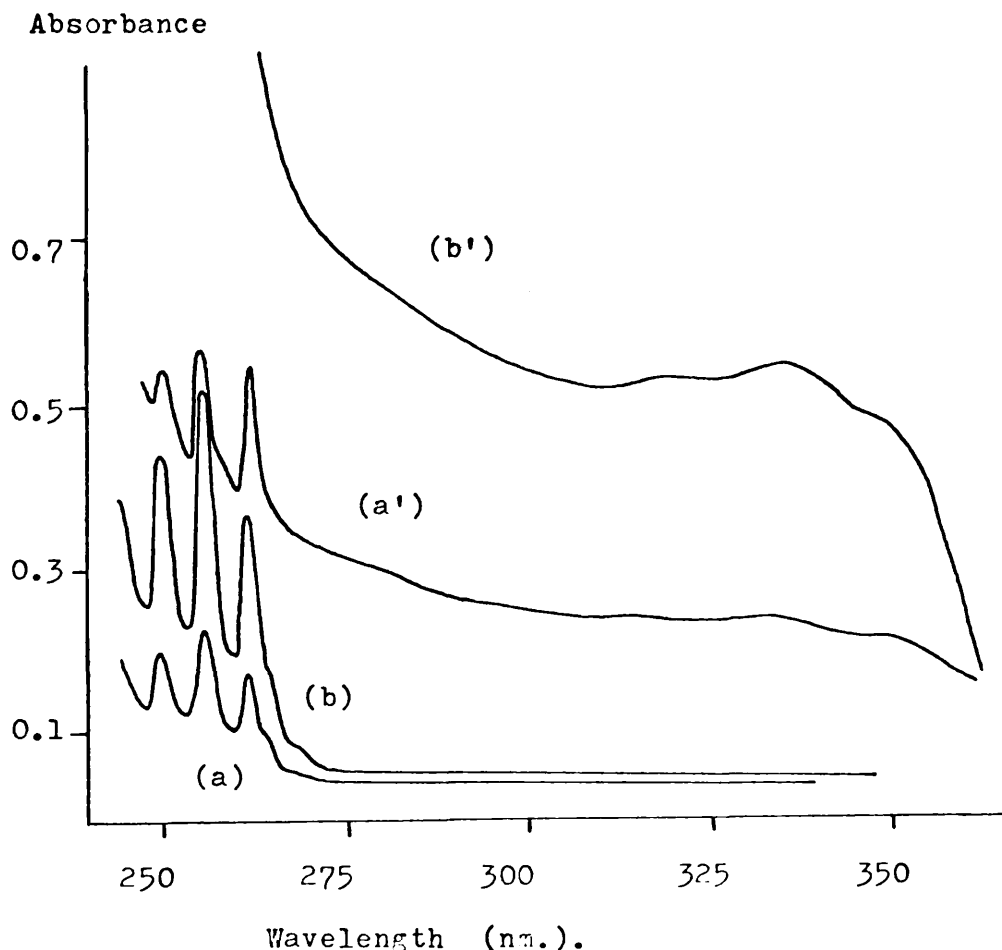


FIGURE 4.15. Ultra-violet spectra of MMC 100, MMC 90 and MMC 74 films cast from ethyl acetate solution and degraded under identical conditions for the same period.



**FIGURE 4.16.** Ultra-violet spectra of MMC 90 film cast from benzene solution. Two films with different residual benzene content gave spectra (a) and (b) respectively. After an identical exposure period under the same conditions spectra (a') and (b') were obtained.

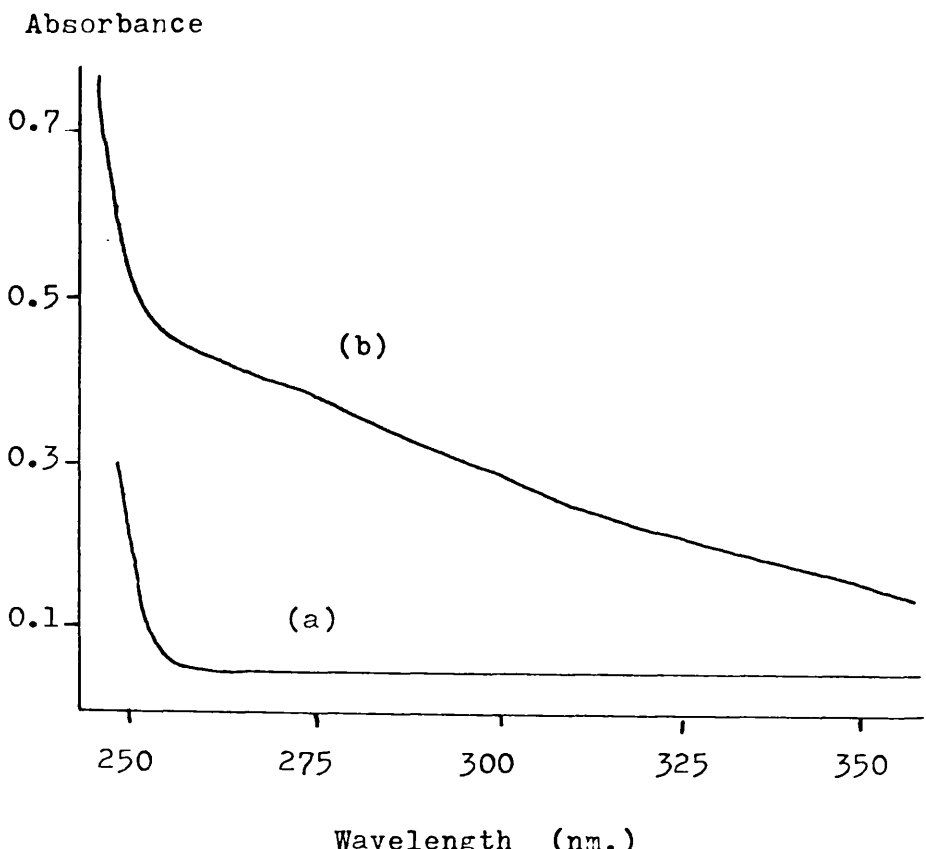


FIGURE 4.17. Ultra-violet spectrum of MMC 90 film cast from ethyl acetate solution ;  
(a) prior to degradation,  
(b) irradiated under identical  
conditions to the films in  
Figure 4.16.

lower energy region of the ultra-violet, the spectrum of the copolymer with the highest CAN content passes into the blue-violet region with the strongest absorption.

Colour in organic compounds is usually associated with unsaturated groups such as  $-C=C-$ ,  $-C=O$ ,  $-C=N$  etc. Approximately six groupings in conjugation are sufficient for coloration in aliphatic systems.

#### 4.6.3 Infrared Region.

In all the copolymers examined a new absorption appeared in the nitrile region as a shoulder on the  $2240\text{ cm}^{-1}$  band and increased with progressive exposure. Spectra obtained from irradiated MMC 50 film cast from dichloromethane solution are shown in Figure 4.18 together with a scale expansion between  $2220\text{ cm}^{-1}$  and  $2300\text{ cm}^{-1}$ . This result is consistent with the observation of previous workers (48) who noted a similar peak during thermal degradation and attributed it to unsaturated nitrile structures in the polymer.

By monitoring the absorption by the aliphatic C - H bond at its stretching frequency of  $2840\text{ cm}^{-1}$  and the absorption at  $2240\text{ cm}^{-1}$  during degradation, it would appear that, within experimental accuracy, there is a relative increase in the nitrile band. As the chlorine atom has a quenching effect on the nitrile absorption (59), its loss and replacement by an equivalent structure such as a saturated hydrocarbon grouping enhances the  $2240\text{ cm}^{-1}$  band. The increase observed at both the shoulder at  $2220\text{ cm}^{-1}$  and the  $2240\text{ cm}^{-1}$  bands is a measure of the rate of loss of chlorine.

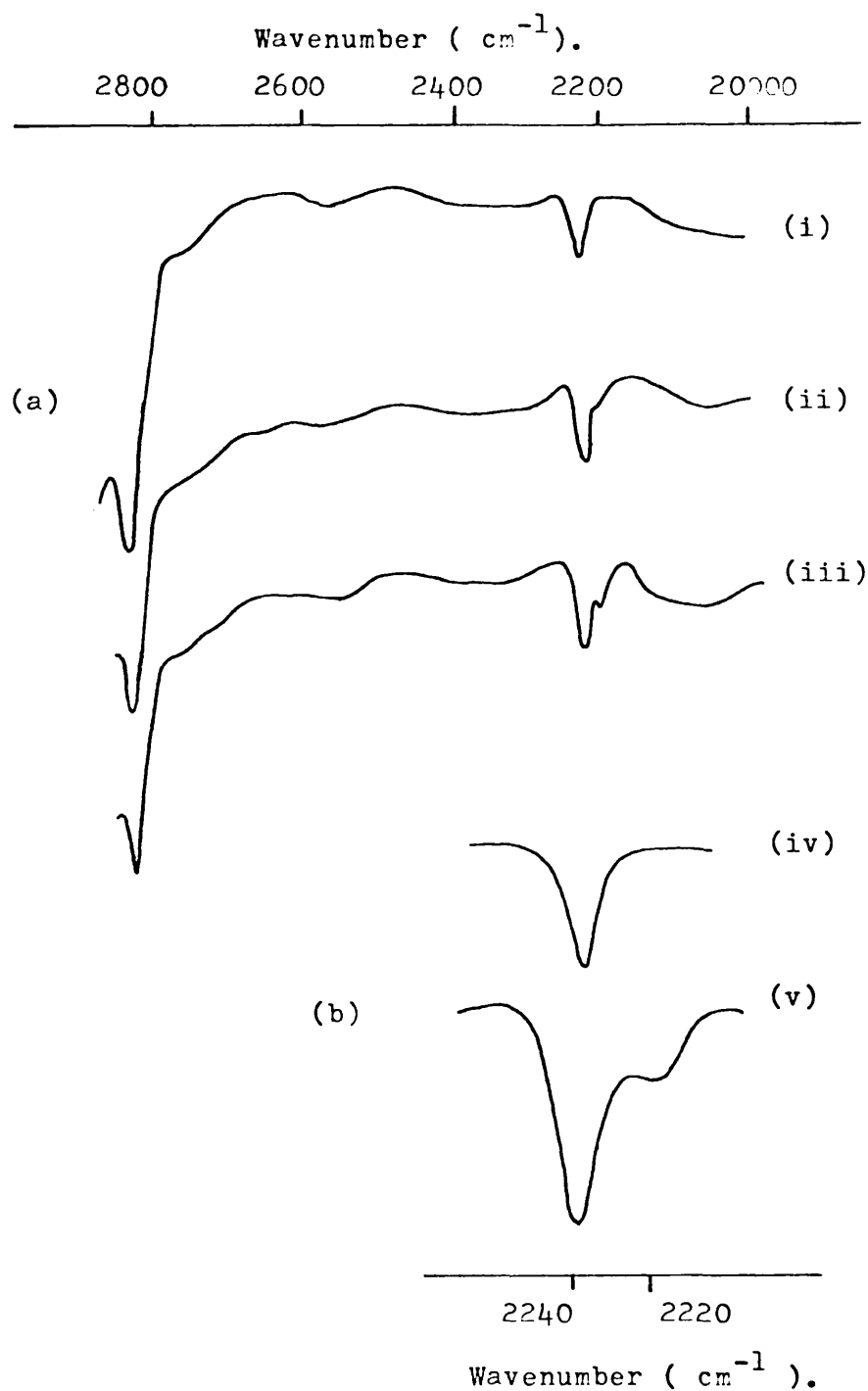


FIGURE 4.18. MC 50 film from  $\text{CH}_2\text{Cl}_2$  solution,

(a) (i) undegraded,

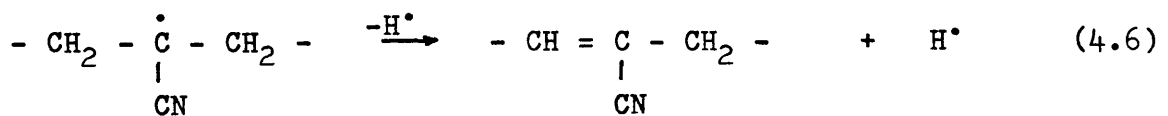
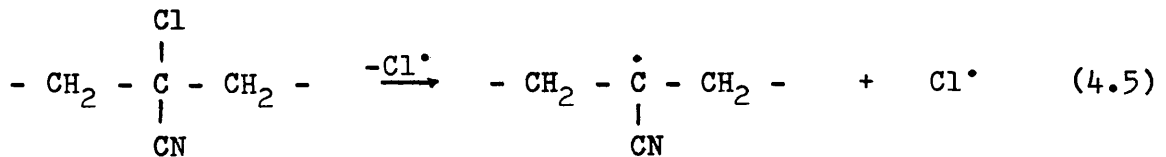
(ii) irradiated for  $3 \times 10^4$  seconds.

(iii) " "  $6 \times 10^4$  "

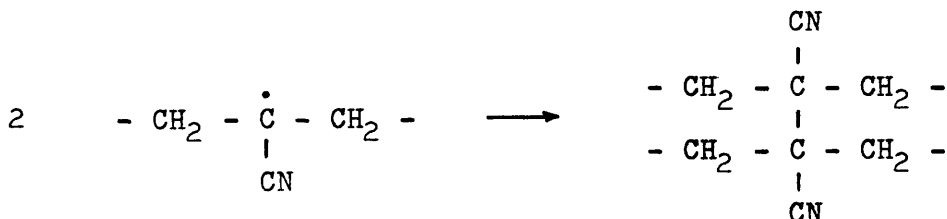
(b) (iv) scale expansion of (i)

(v) scale expansion of (iii).

The mechanism of the reaction may be similar to that previously suggested (48) for the degradation of copolymers of CAN in which C - Cl bond scission produces chlorine atoms and polymer radicals. The former may abstract hydrogen atoms from the polymer matrix to form HCl and unsaturated structures,



while combination of polymer radicals formed in reaction (4.5) results in cross-linking,



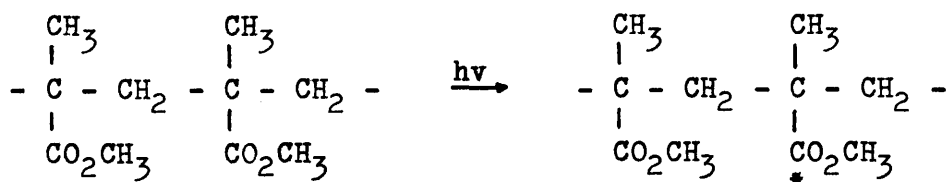
#### 4.7 DISCUSSION.

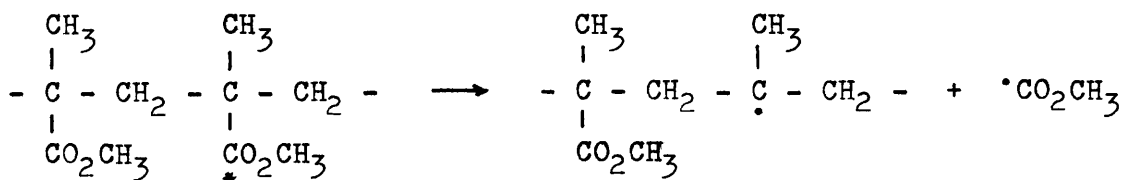
From experimental results and observations on the copolymer system a general trend begins to emerge. By and large, as more CAN units are inserted into the poly(methyl methacrylate) structure, the difference in behaviour between the homopolymer and copolymers becomes greater. This is illustrated by the movement away from chain-scissioning to cross-linking reactions

or substituent reactions and by the more rapid development of absorption in the ultra-violet and visible regions. The growth in the proportion of CAN - related products such as hydrogen chloride and residual unsaturated structures, as demonstrated by the shift in the nitrile absorption band in the infrared region, is accompanied by a decline in the production of methyl formate, methanol and methyl methacrylate. There is evidence of increasing interaction between CAN units and methyl methacrylate units, based on methyl chloride production and unexpected increases in the yield of carbon dioxide.

Any photolysis mechanism proposed for this copolymer system must satisfy the experimental evidence and account for the trends observed. At low levels of CAN incorporation the copolymer degradation mechanism must be expected to have a large contribution from photolysis reactions associated with pure poly(methyl methacrylate). Alternatively, any deviation from the well-established photodegradation mechanism of this homopolymer can be attributed to the effect of CAN units.

Photodegradation of poly(methyl methacrylate) is initiated by absorption at the carbonyl group of the ester side chain and subsequent scission of the weakest bond:





The ester radical gives rise to volatile products. The corresponding polymer radical can undergo chain scissioning resulting in depolymerisation over short zip lengths and the formation of monomer.

As CAN units are introduced into poly(methyl methacrylate) there is a gradual reduction in the rate of chain scissioning. It is, therefore, reasonable to assume that chain-scissioning is hindered by CAN units. This contrasts with the work of Grassie and Farish (67) on the photodegradation at high temperatures of a similar copolymer system, that of methyl methacrylate and acrylonitrile. Their findings supported the view that incorporation of acrylonitrile into the poly(methyl methacrylate) structure, up to an extent of ten per cent, leads to an increase in the rate of chain scissioning. The degradation mechanism was thought to comprise initiation by absorption of radiation at the acrylonitrile unit and subsequent depolymerisation, terminating at the next acrylonitrile unit along the chain.

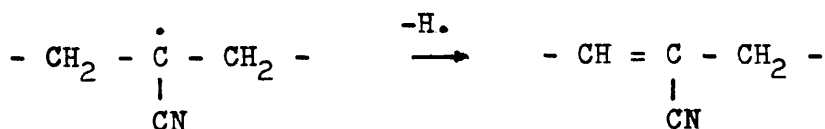
As shown in Chapter One the photodegradation of poly(methyl methacrylate) at ambient temperatures follows a different course from that at elevated temperatures as a result of increased chain mobility and decreased viscosity under the latter conditions. It is reasonable to expect that copolymers

derived largely from methyl methacrylate will, likewise, display temperature-dependent behaviour.

Another difference between these two copolymer systems is the relative weakness of the carbon-chlorine bond. The inclusion of hydrogen chloride in the degradation products is indicative that carbon-chlorine bond scission, in fact, occurs at CAN units. The energy for bond cleavage may be absorbed at the CAN unit itself or may reach the CAN by energy migration along the polymer chain from an absorbing chromophore such as the carbonyl group. Scissioning at CAN produces a chlorine radical and a polymer radical,

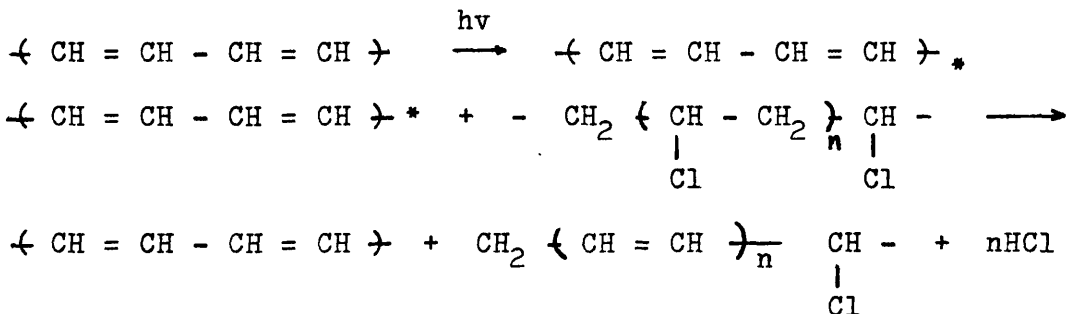


The chlorine radical can abstract an adjacent hydrogen atom to form HCl. The polymer radical, by virtue of the location of the nitrile group, is more stable than the corresponding radical produced on methyl methacrylate units and will thus tend to undergo chain scissioning less readily. Hence radicals formed at CAN units are more susceptible to cross-linking reactions. Alternatively, loss of hydrogen from the polymer radical and formation of a double bond in conjugation with the nitrile group is highly favoured by energy considerations.



This step was first postulated by Grassie (68) in his work on the thermal degradation of poly(CAN).

Gibb and MacCallum (69) have shown that radiation emitted at 254 nm is responsible for initiating the photo-degradation of samples of poly(vinyl chloride) and that only dienes and trienes can absorb significant amounts of the radiation. This means that further decomposition is caused by energy transfer from these sites, along the polymer chains, to other parts of the system:



A similar situation can be imagined at unsaturated CAN units. Absorption of radiation and subsequent energy transfer would promote further degradation in other parts of the copolymer and thus accelerate the normal degradation process.

The more rapid development of absorption observed in the ultra-violet spectra of films with higher CAN contents can also be attributed to unsaturation at the CAN units. Here, the possibility of a "skin effect" occurring cannot be overlooked. During the photolysis of poly(vinyl chloride) films Gibb and MacCallum (70) found that, as the number of unsaturated structures near the irradiated surface increased by dehydrochlorination reactions, the effective penetration

of ultra-violet radiation was gradually reduced to a thin surface layer. This was reflected in the rate of evolution of hydrogen chloride which passed through a maximum value and faded to a negligibly small limiting rate. Only a small percentage of the available hydrogen chloride was produced. On directing the incident radiation to the obverse surface of the film a similar result was obtained. This situation appears to prevail in the degradation of MMC 50 film during which hydrogen chloride production follows the same pattern but the experimental data do not allow a decision to be made regarding the other copolymers.

So far, the copolymer system could be said to be behaving like two separate homopolymers, with the production of hydrogen chloride, cross-linking and unsaturated nitrile structures associated with CAN units and chain scissioning and the volatile products typical of methyl methacrylate units. However, the formation of methyl chloride requires the interaction of both monomer units. Further, the rate of production of carbon dioxide which, within the limits of experimental accuracy, was found to be relatively greater for MMC 50 films than MMC 90 films can be associated with methyl chloride formation.

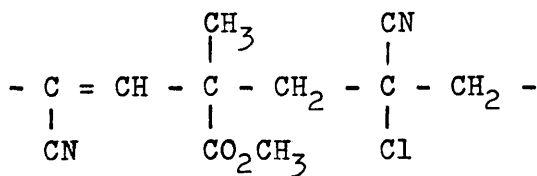
Carbon dioxide is formed during the photolysis of poly (methyl methacrylate) by a mechanism comprising scissioning of the ester group from the main chain and subsequent decomposition of the  $\text{CH}_3\text{OOC}\cdot$  radical.



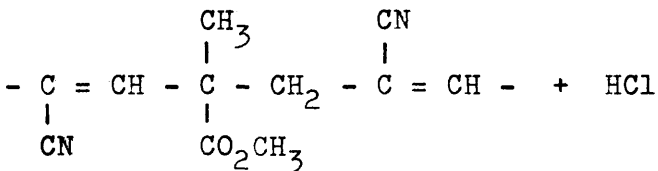
Mikheyev and coworkers (66) conducted experiments on the photolysis of poly(methyl methacrylate) in the presence of ferric chloride. They observed that methyl radicals formed in the above decomposition process are less active in abstracting hydrogen from the polymer than in removing chlorine from ferric chloride.

As the CAN content of the copolymer is increased, the availability of chlorine for reaction with the methyl group of the ester moiety is greater. However, the production of hydrogen chloride also increases significantly and is a strongly competitive reaction for chlorine consumption. It is reasonable to assume that the formation of methyl chloride is dependent upon the occurrence of favourable combinations of monomer units and may, in fact, require a stereospecific arrangement. This "combination" appears to occur more frequently at higher CAN contents and with reference to Chapter Three is possibly associated with the CAN - MMA - CAN trimer which is present in the MMC 50 copolymer to a much greater extent than in the MMC 90 and MMC 74 systems.

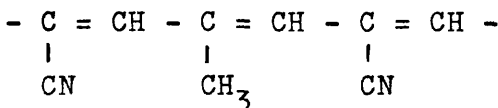
Absorption at this structure and subsequent scissioning at the weakest bond may result in the production of hydrogen chloride and the following unsaturated unit:



By further absorption at the trimer and subsequent scissioning, increased unsaturation can develop:



A more stable structure could be achieved by extending the conjugation to include the methyl methacrylate unit as shown below:

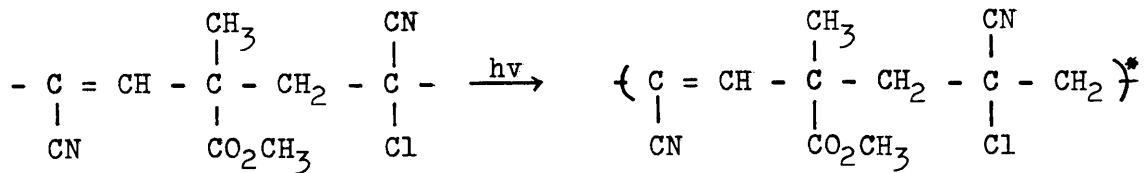
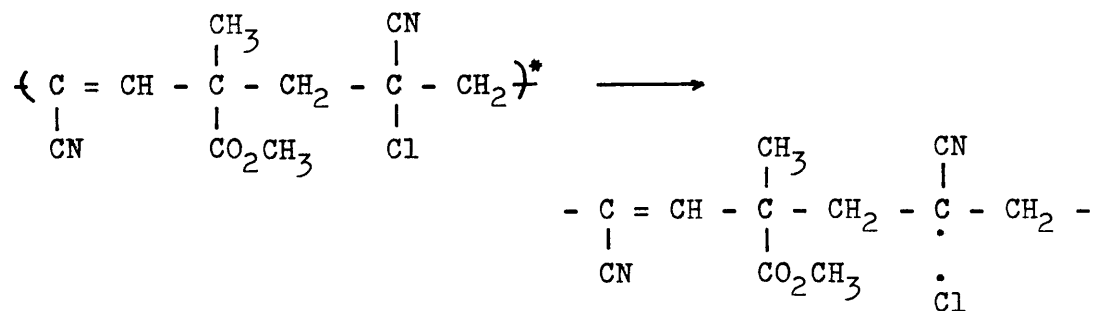
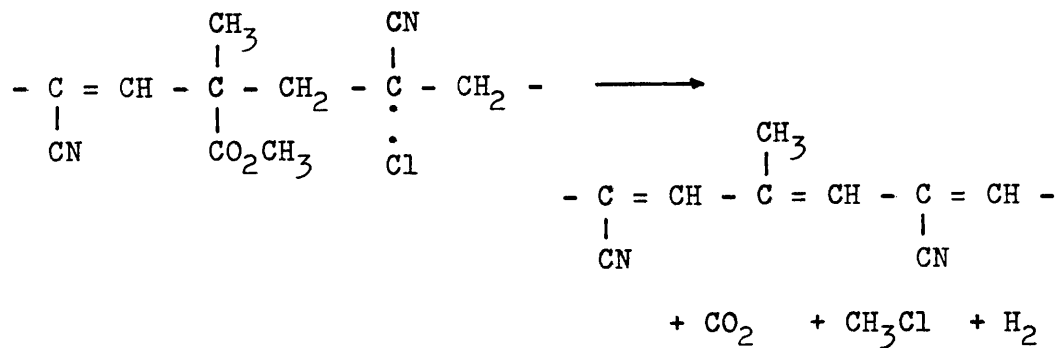


The coloration of copolymer films which is more evident at higher CAN concentrations suggests the presence of extended conjugation. The degradation mechanism shown in Scheme 1 may account for both the production of methyl chloride and the formation of structures which are responsible for the polymer coloration. Carbon dioxide is also produced in the course of reaction which, by virtue of the requirement of CAN - MMA - CAN sequences has a greater probability of occurring by this method at higher CAN contents. The mechanism requires specific orientation of the reacting groups in Stage 3 and the resonance stabilisation of the radical at the methyl methacrylate unit in Stage 3b by an adjacent, unsaturated nitrile structure.

An alternative explanation for the origin of colour in copolymer films is provided by analogy with the photodegradation of poly(CAN). Films of poly(CAN) cast from acetone solution were found to rapidly discolour when exposed to ultra-violet radiation. The absorption spectrum of the degraded film extended into the blue-visible region. It is reasonable to assume that the type of structure responsible for the

absorption is highly conjugated and is formed from long sequences of dehydrochlorinated CAN units. As the proportion of CAN in the copolymer increases, the probability of encountering such sequences must rise and hence be responsible for the observed coloration.

The formation of cyclic structures through the nitrile group is less probable at ambient temperatures than at higher temperatures above the glass transition temperature but polycyclic sequences would be terminated at methyl methacrylate units. Ring structures involving the  $-C=N-$  linkage have characteristic infrared absorptions (1) which were not present in the copolymer spectra. Inclusion of the methyl methacrylate unit in a cyclic structure is generally achieved by expulsion of an  $\cdot OCH_3$  radical which combines with hydrogen to form methanol. With increasing CAN content the production of methanol by this process should increase accordingly. This was not found to be the case.

SCHEME 1.Stage 1 :Stage 2 :Stage 3 :

CHAPTER FIVEPHOTODEGRADATION OF COPOLYMERS OF STYRENE WITH  
2,2-CHLOROACRYLONITRILE.5.1 INTRODUCTION.

A study of the mechanism of photodegradation of copolymers of styrene with 2,2- chloroacrylonitrile (CAN) requires a knowledge of the products of reaction and the inter-relationships of products. Accordingly, copolymers in film form were degraded by ultra-violet radiation and the products were characterised by spectroscopic techniques following separation by the procedure described in Chapter Two. The degraded films were examined by infrared and ultra-violet spectroscopy in order to determine structural changes.

5.2 PRODUCT ANALYSIS.

The photolysis apparatus and conditions and the techniques of product collection, separation and identification have been described in detail in previous chapters. As before, films were prepared from solution, residual solvent being removed by treatment in a vacuum oven. Dichloromethane was preferred as casting solvent although some work was based on films from benzene solution. As described in Chapter Four, products were first separated according to their physical state at liquid nitrogen temperature under low pressure conditions.

### 5.2.1 Condensable Products.

The products from the photodegradation of STC 875 film, collected separately from two consecutive irradiation periods, formed the traces shown in Figure 5.1. The dashed line indicates the response of the chromel - alumel thermocouple as the temperature in the collection trap gradually increases during the differential distillation process. The low boiling species ( -5.4 mV, -184°C at peak maximum) was identified from its characteristic absorption in the infrared region at  $3050\text{ cm}^{-1}$  -  $2600\text{ cm}^{-1}$  as hydrogen chloride.

After the removal of hydrogen chloride by the separation procedure, the remaining products were examined by mass spectroscopy. The spectrum obtained is shown in Figure 5.2 together with spectra of dichloromethane and styrene respectively from liquid samples. It would appear that the spectrum of the degradation products can be built up from contributions from casting solvent and styrene allowing for background interference. No evidence was found for the existence of any other significant product.

Further exposure of the STC 875 film to radiation results in a gradual diminution of the hydrogen chloride peak as is illustrated in Figure 5.1, until the production reaches a limiting value. However, on inverting the film so that incident radiation enters at the obverse surface, a significant increase in the rate of evolution of hydrogen chloride is found. This anomalous behaviour is illustrated in Figure 5.3 where the cumulative pressure of hydrogen chloride is plotted as a

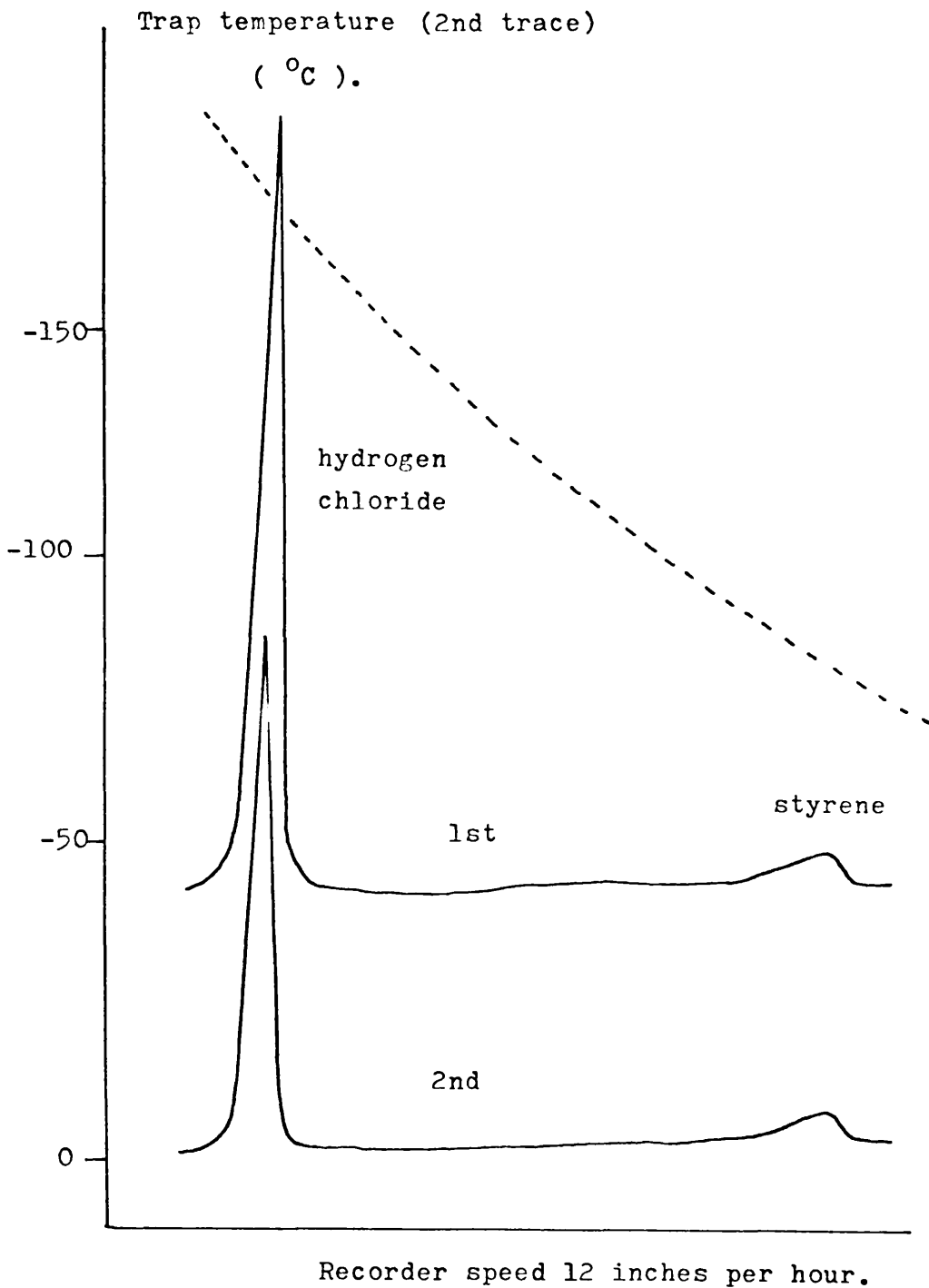
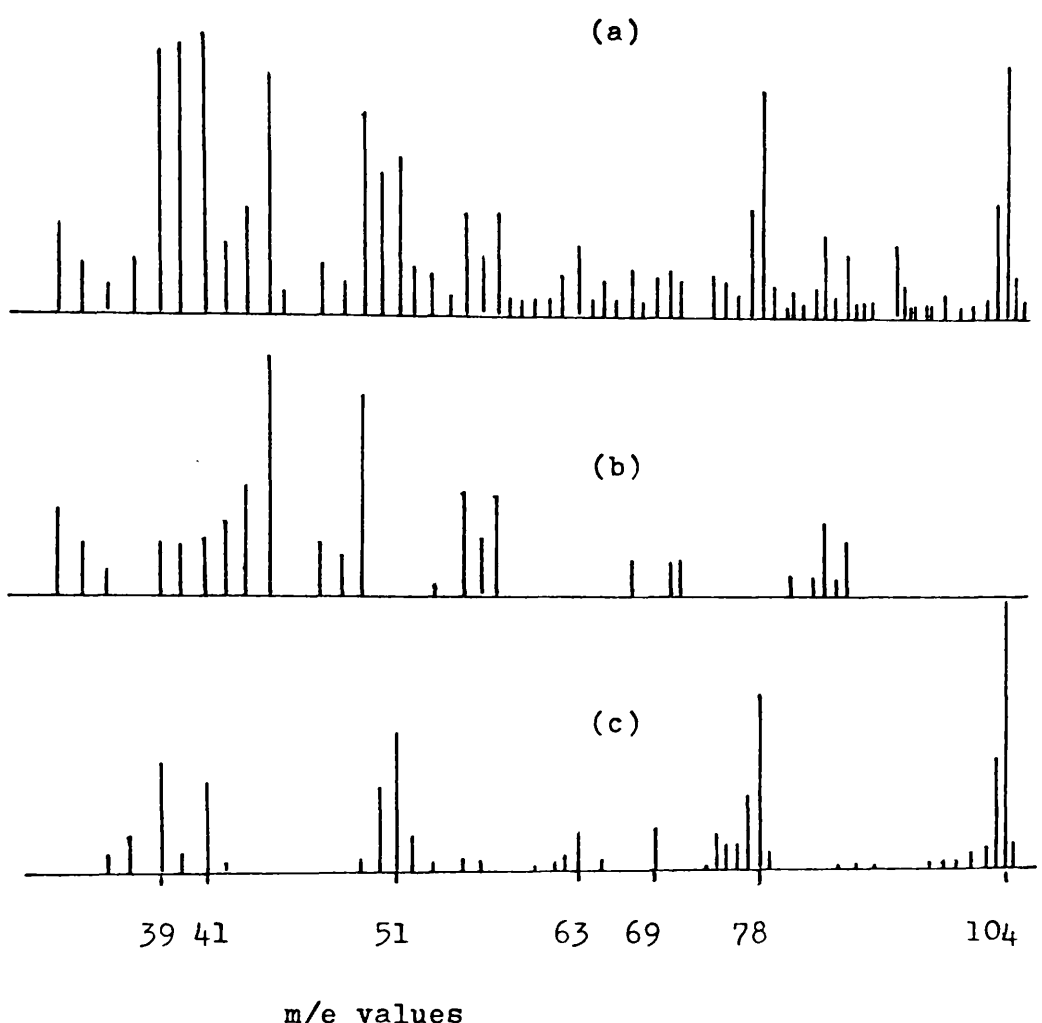
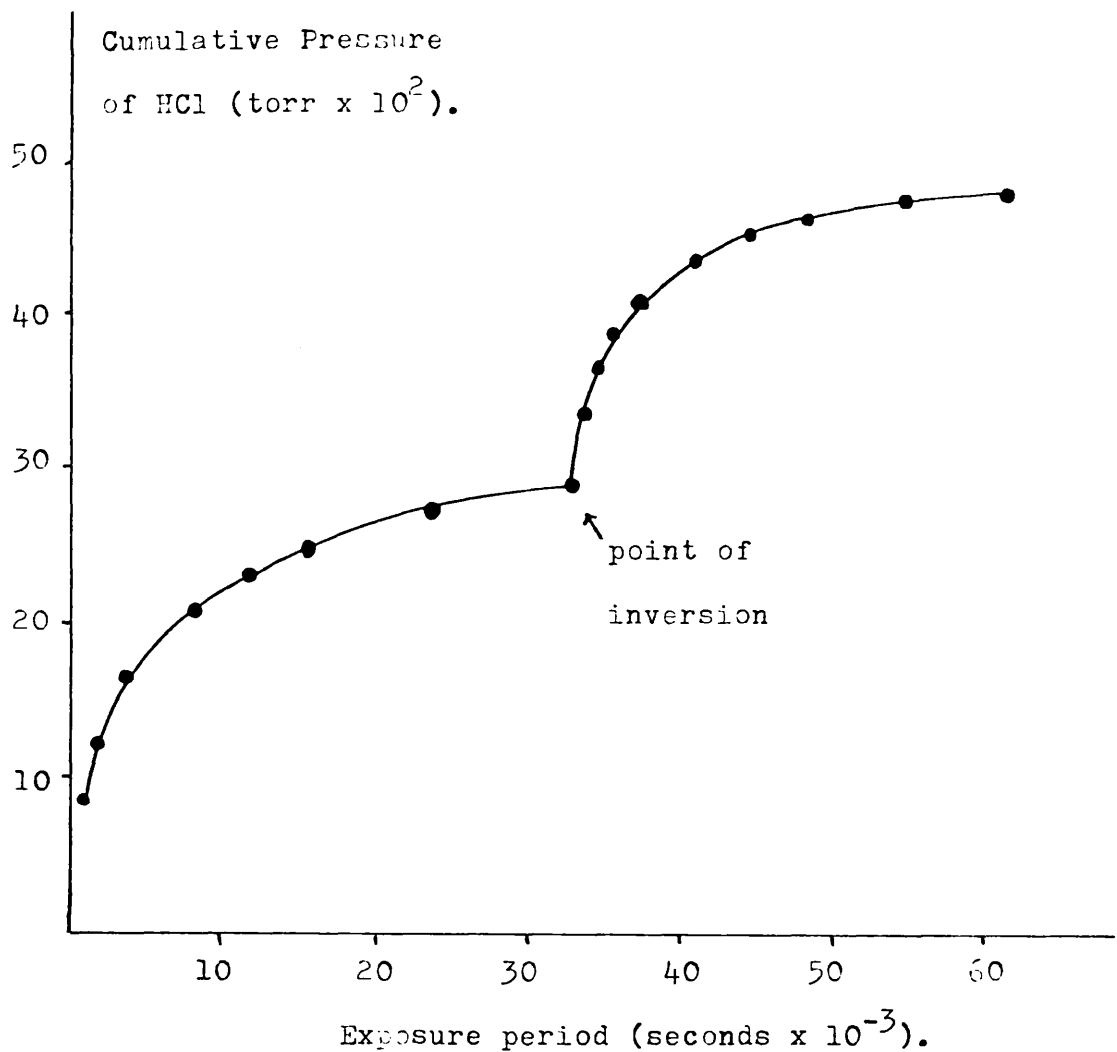


FIGURE 5.1. Product traces from two consecutive exposure periods of  $9 \times 10^2$  seconds of STC 875 film cast from  $\text{CH}_2\text{Cl}_2$  solution.

$10^8$



**FIGURE 5.2** (a) Mass spectrum of the photodegradation products of STC 875 film after separation and removal of HCl.  
(b) Mass spectrum of casting solvent and background.  
(c) Mass spectrum of liquid styrene.



**FIGURE 5.3** Evolution curve for HCl from STC 375 film cast from dichloromethane solution.

The film was irradiated at one surface, inverted and irradiated at the other.

function of time of exposure. When the film is inverted, a marked deviation is apparent in the evolution curve. On closer examination it appears that the evolution rate of hydrogen chloride, on irradiating at the first surface, is almost reproduced by the subsequent application of radiation to the obverse surface.

The product trace obtained from the degradation of STC 75 film cast from dichloromethane solution, as shown in Figure 5.4, consists of peaks corresponding to hydrogen chloride, casting solvent, styrene and a fourth species which gave rise to the infrared spectrum in Figure 5.5. This spectrum is characteristic of CAN. A similar product trace was obtained from STC 69 film ( Figure 5.6 ).

The hydrogen chloride evolution curve for the photodegradation of STC 75 ( Figure 5.7 ) follows the same pattern as that established previously, having a marked deviation at the inversion point. The origin of the hydrogen chloride formed during the course of photodegradation can be wholly associated with the polymer as no trace was found after irradiation of STC 100 film cast from dichloromethane, although undegraded solvent was present in the products.

#### 5.2.2 Dependence of HCl evolution rate on Sample Weight and Area.

Samples of STC 75 film cast from dichloromethane solution were degraded under identical conditions and HCl evolution was measured in the normal manner. The casting procedure resulted in samples with one optically flat surface but an overall semi-

Trap temperature ( $^{\circ}\text{C}$ ).

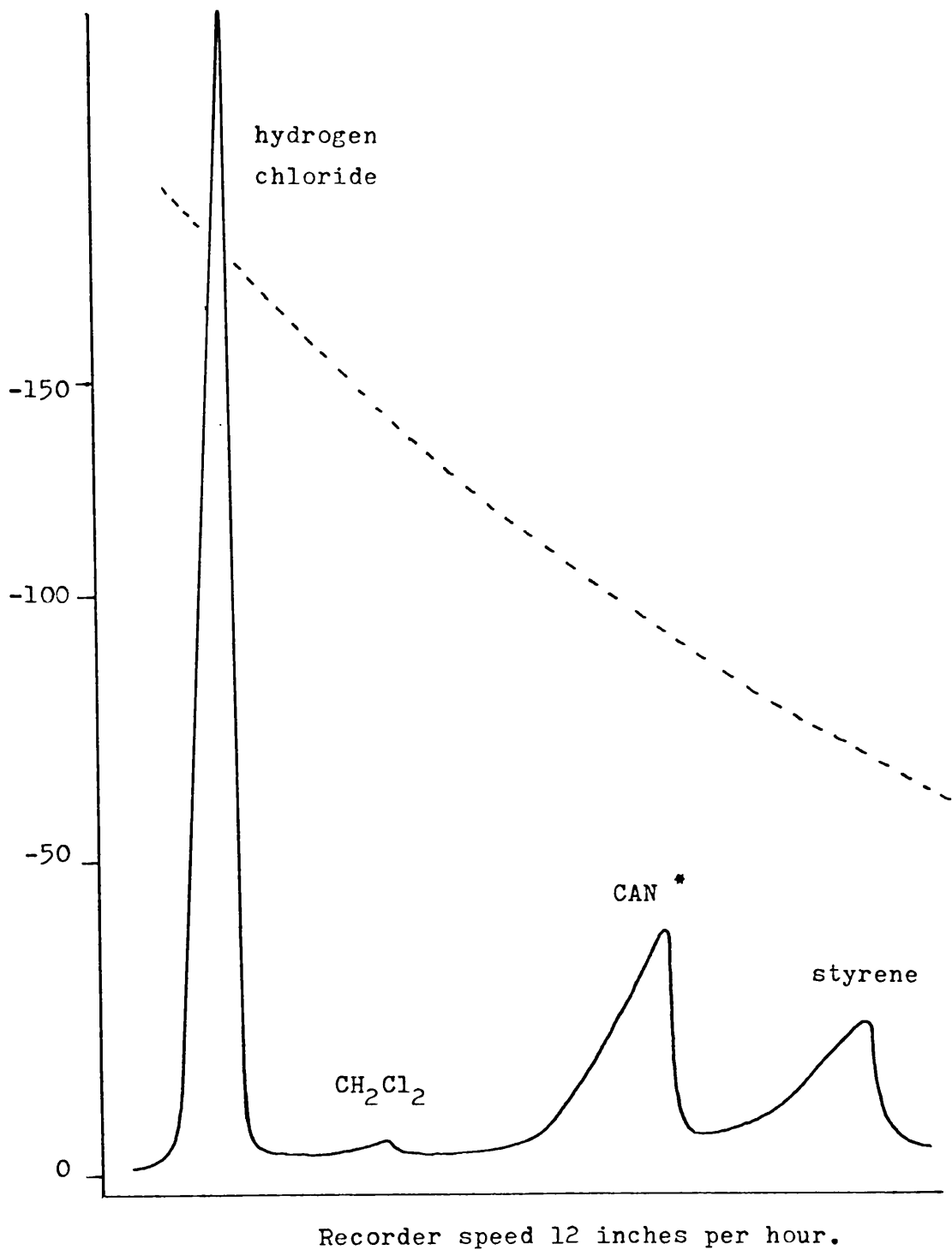


FIGURE 5.4. Product trace from STC 75 film cast from  $\text{CH}_2\text{Cl}_2$  solution irradiated for a period of  $1.4 \times 10^4$  seconds.

\* see FIGURE 5.5.

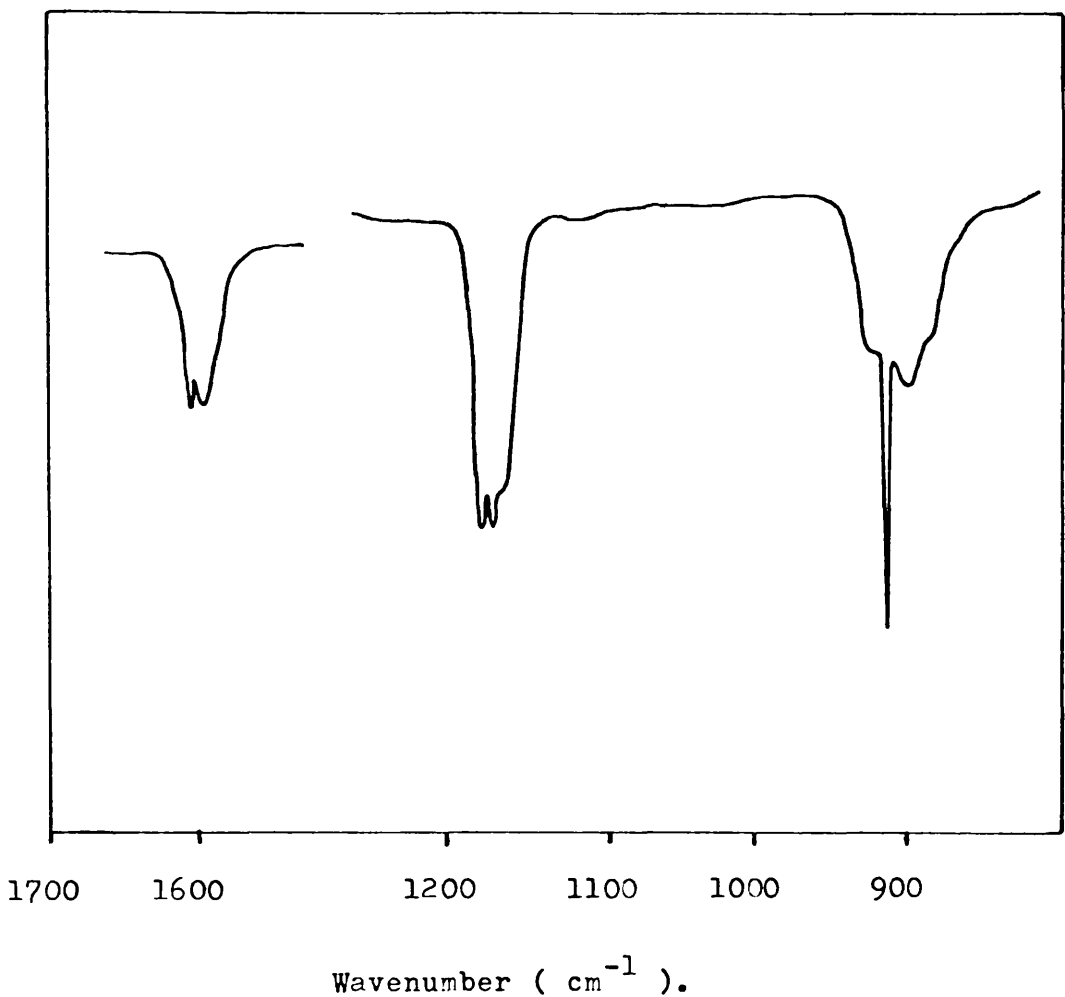


FIGURE 5.5. Infrared spectrum (gas phase) obtained from a separated peak in the product trace from the photodegradation of STC 75 film (see FIGURE 5.4). The product was identified as CAN monomer (cf. FIGURE 6.2 of Chapter Six).

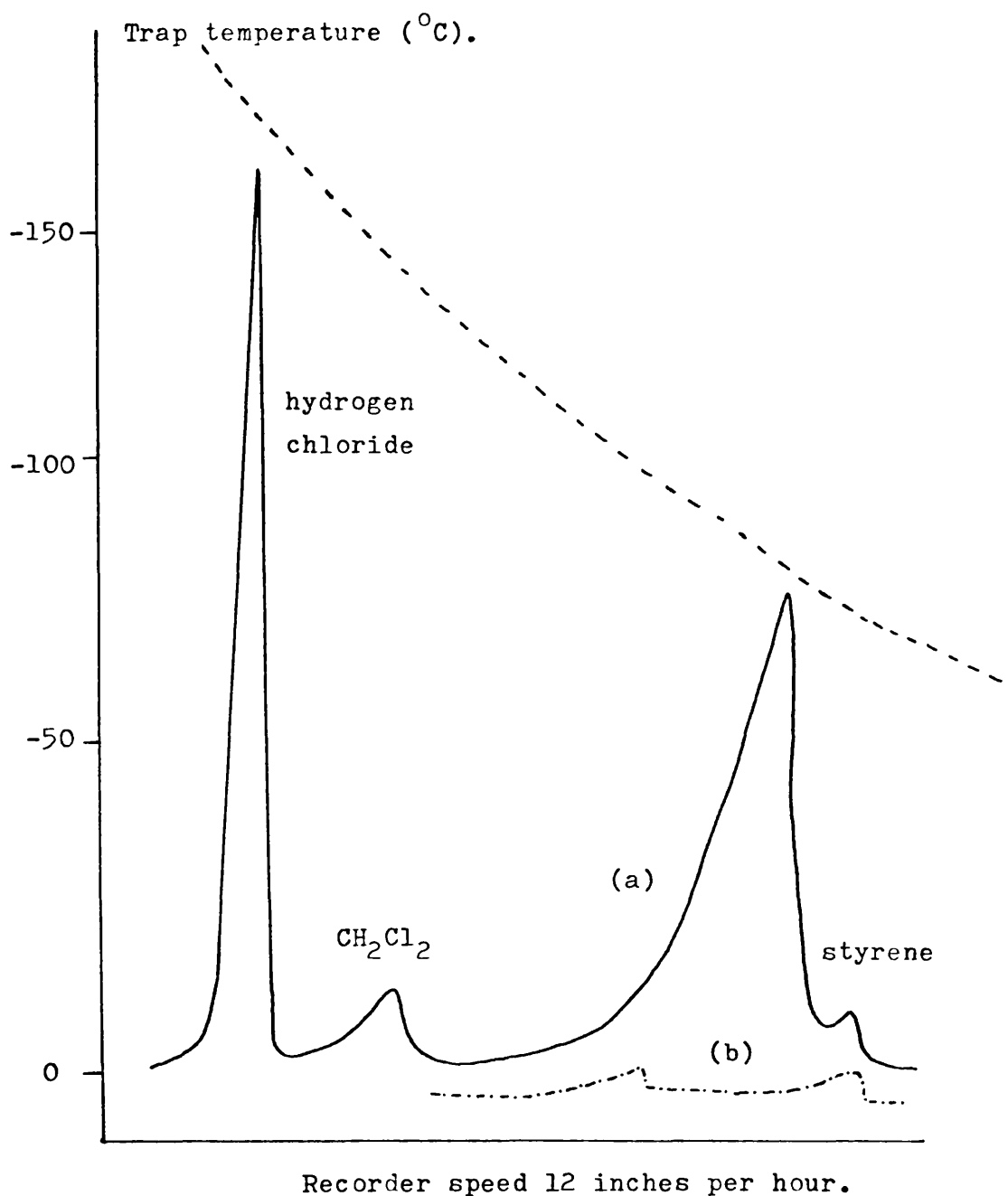


FIGURE 5.6. (a) Product trace from STC 69 film cast from  $\text{CH}_2\text{Cl}_2$  solution.  
 (b) Trace obtained from CAN and styrene monomer.

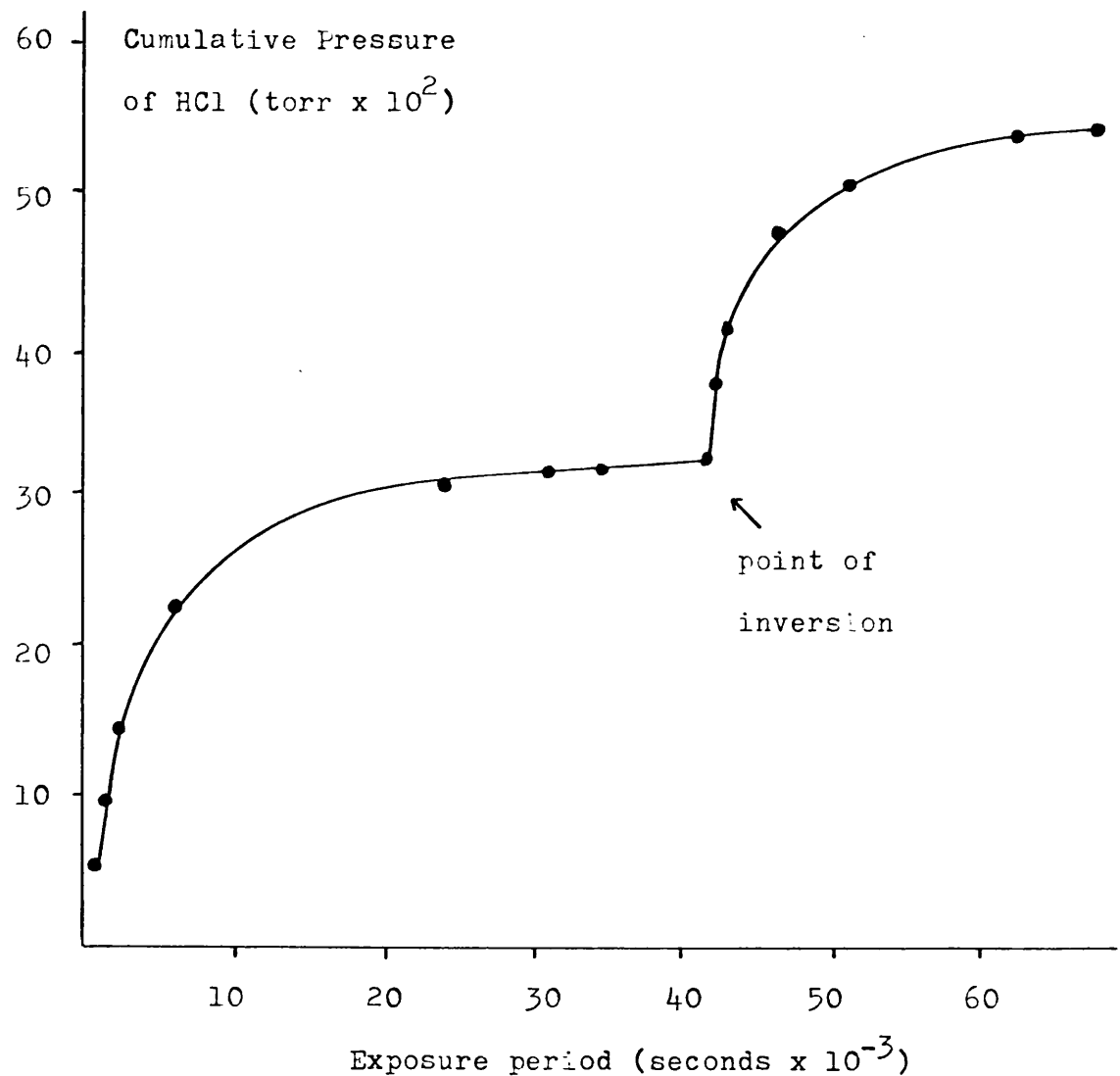


FIGURE 5.7 Evolution curve for HCl from STC 75 film cast from dichloromethane solution.

The film was irradiated at one surface, inverted and irradiated at the other.

lenticular shape. In order to minimise optical deviations the film thickness was kept to a minimum. In Table 5.1 the ratios of sample weights and areas are shown for three samples as is the HCl evolution ratio. The data is derived from the graphs in Figure 5.8. The films were denoted "A", "B" and "C".

From the A : B : C ratio it is apparent that, as the photolysis reaction proceeds, the initial dependence of HCl formation on the sample weight is replaced by a marked dependence on sample area. Assuming a constant film density throughout, it would appear that, after an initial period of degradation, the sample thickness plays little part in determining the quantity of HCl produced.

### 5.2.3 Non-condensable Products.

The products of photodegradation of the copolymer film which were condensable at liquid nitrogen temperature were trapped during degradation and the non-condensable products were removed from the system by means of a Topler pump. The procedure is described in detail in Chapter Four.

Transfer to a mass spectrometer and subsequent analysis revealed that hydrogen was the only significant product. The cumulative pressure of hydrogen formed during degradation was measured on a McLeod Gauge. The evolution curves obtained from samples of STC 100 and STC 69 films of similar weight and area are shown in Figure 5.9.

In both cases the rate of hydrogen evolution decreases from an early maximum value as the degradation proceeds. Data from Figure 5.9 indicate that the pressure of hydrogen

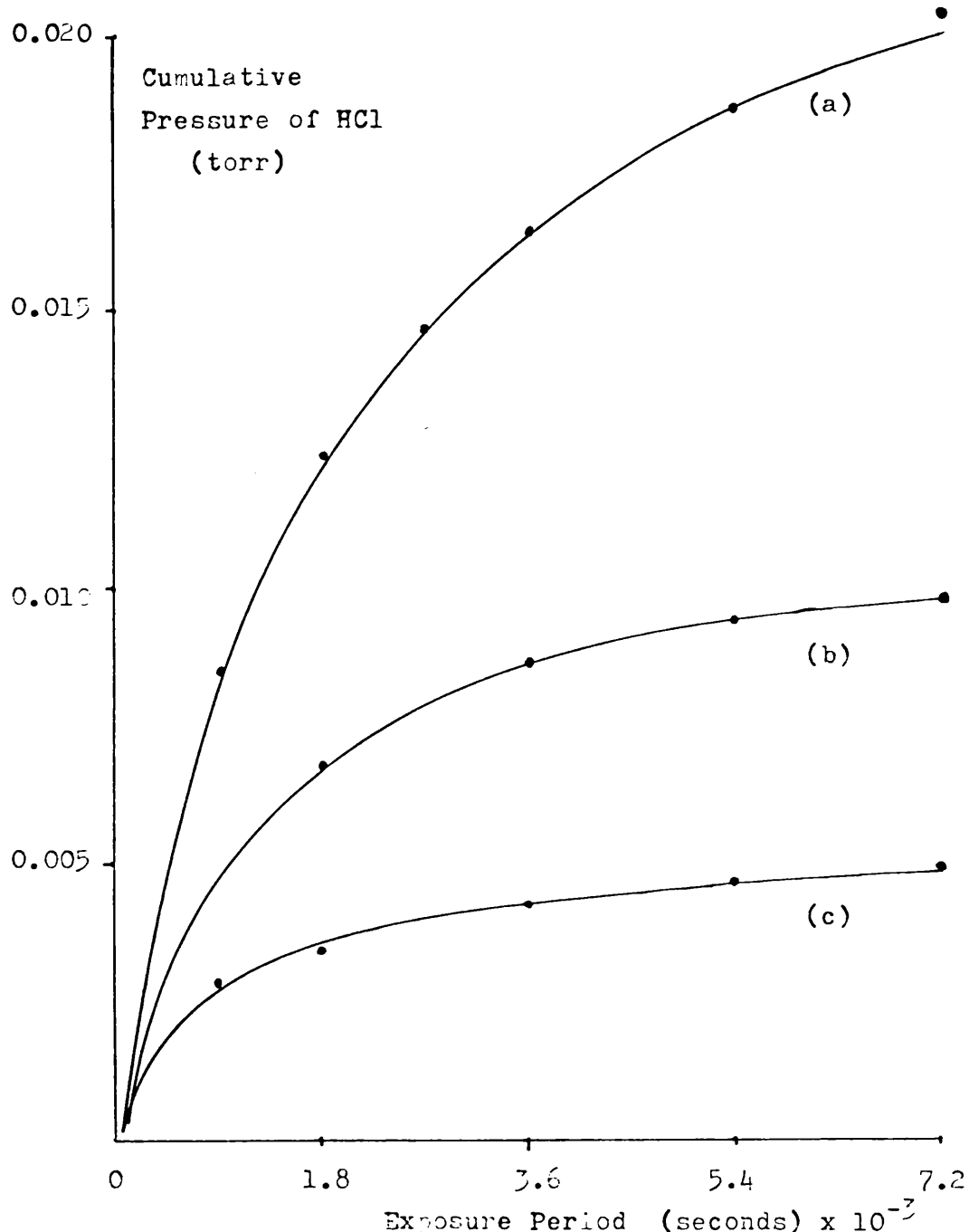


**FIGURE 5.8** Evolution of HCl during the photodegradation of STC 875 film of cross-sectional area  
 (a)  $21.20 \text{ cm}^2$  (b)  $7.07 \text{ cm}^2$  (c)  $3.53 \text{ cm}^2$ .

TABLE 5.1.

Dependence of HCl Production from STC 75 Film on Sample Weight  
and Area.

(a)	Sample Reference	A	B	C
	Sample Weight (g)	0.0590	0.0338	0.0174
	Sample Area (cm <sup>2</sup> )	21.204	7.068	3.534

(b)	A	:	B	:	C
	Weight Ratio	3.4	1.94	1	
	Area Ratio	6	2	1	

(c)	<u>Exposure Period</u>	<u>HCl Evolution Ratio</u>		
( from Fig. 5.8 )				
	seconds $\times 10^{-3}$	A	:	C
	0 to 1.8	3.62	2	1
	1.8 to 3.6	4.67	2	1
	3.6 to 5.4	5.5	2	1
	5.4 to 7.2	6.0	1.46	1

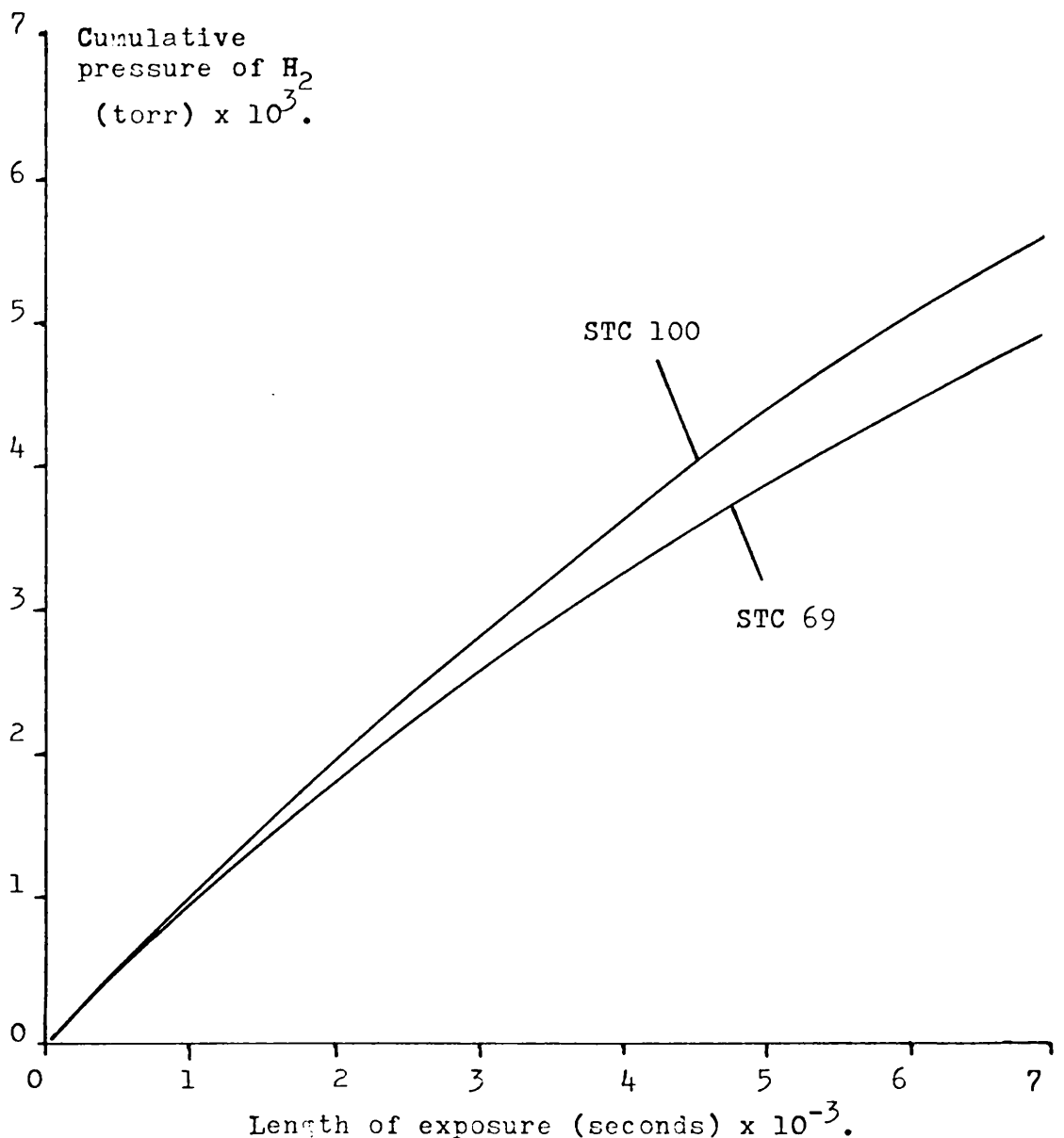


FIGURE 5.9 Production of hydrogen during the early stages of the photodegradation of films of STC 100 and STC 69 cast from  $\text{CH}_2\text{Cl}_2$ .

formed, both in the initial and final stages of the respective curves corresponding to STC 100 and STC 69 over identical irradiation periods is in the ratio 1 : 0.9. However, the ratio of hydrogen on the respective polymers which is theoretically available for abstraction and combination under the degradation conditions can be calculated as approximately 1 : 0.8. Thus the formation of hydrogen from the copolymer appears to be uninfluenced by the considerable demand placed on resources by the formation of hydrogen chloride.

### 5.3 SPECTRAL CHANGES DURING PHOTODEGRADATION.

#### 5.3.1 Infrared Region.

As in the case of copolymers of methyl methacrylate with CAN the only structural change detectable by infrared spectroscopic analysis of STC 875, STC 75 and STC 69 films as a result of photodegradation relates to the nitrile group absorption. The peak is initially observed at  $2240\text{ cm}^{-1}$  but, as degradation proceeds, a strong shoulder develops at  $2220\text{ cm}^{-1}$  resulting in a shift in the apparent maximum to a lower energy.

No evidence was found for the  $825\text{ cm}^{-1}$  peak referred to by Fox (3) which had been observed during the photodegradation of polystyrene film.

#### 5.3.2 Ultra-violet and Visible Regions.

The ultra-violet spectrum of the copolymers increased featurelessly during degradation as is illustrated for STC 75 film in Figure 5.10. The absorption intensified in the 250 - 400 nm region and the encroachment into the blue region

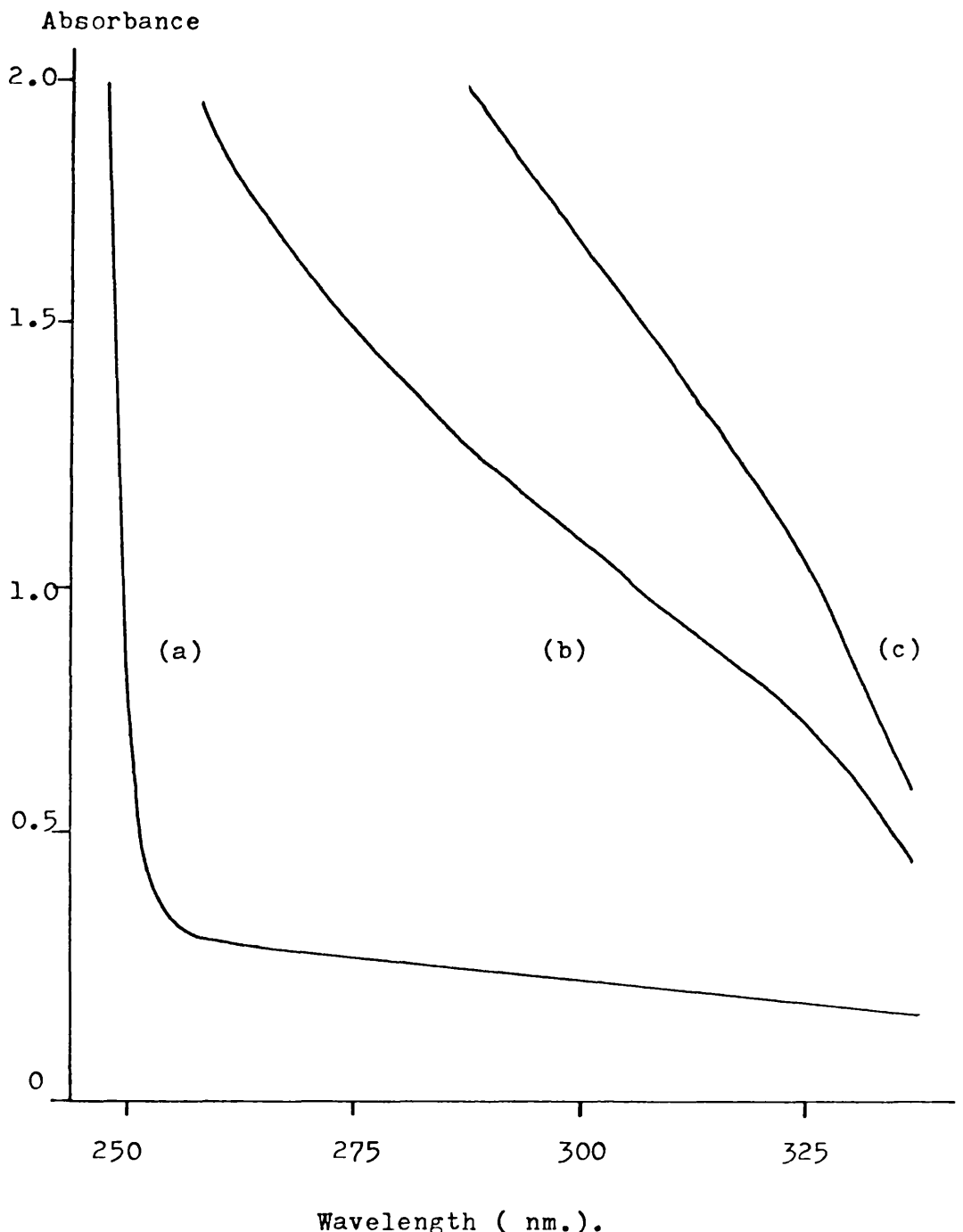


**FIGURE 5.10.** Ultra-violet spectrum of STC 75 film cast from benzene,  
(a) prior to irradiation  
(b) after an exposure of  $2.9 \times 10^4$  seconds,  
(c) after an exposure of  $7.2 \times 10^4$  seconds.

gave rise to yellowing of the films. The yellow colour intensified with further degradation.

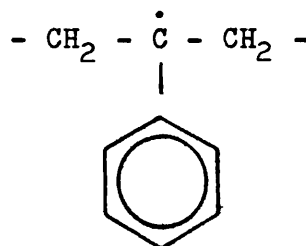
#### 5.4 MOLECULAR WEIGHT ANALYSIS.

After short exposure periods the copolymer films were found to be only partially soluble in toluene. Thus molecular weight measurements by conventional membrane osmometry were made impracticable. Sol-gel analyses (65) of the degraded films were attempted after extraction in a Soxhlet apparatus. However, as the results obtained were of low reproducibility the procedure was discontinued.

It is reasonable to assume that the copolymer films undergo crosslinking reactions during photodegradation.

#### 5.5 DISCUSSION.

Polystyrene absorbs strongly at 254 nm. However, it is considered that the radical yield is relatively low (4), possibly because energy is readily dissipated by the benzene rings. In E.S.R. studies at 77K, Browning and his coworkers (71) tentatively attributed a broad singlet to phenyl radicals but investigations by Selivanov (45) revealed that, in fact, the origin of the spectrum was radical structure I.



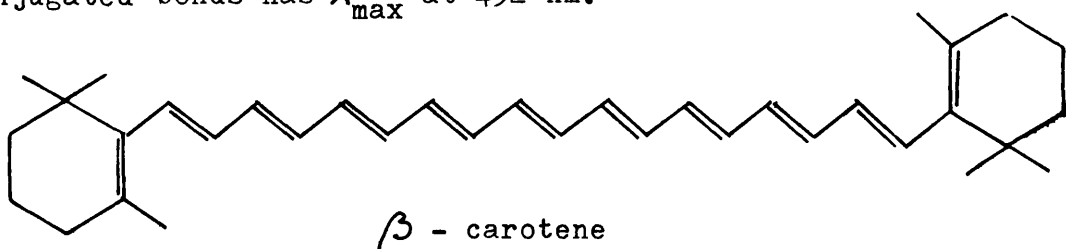
I

which resulted from the scission of a tertiary hydrogen - carbon bond.

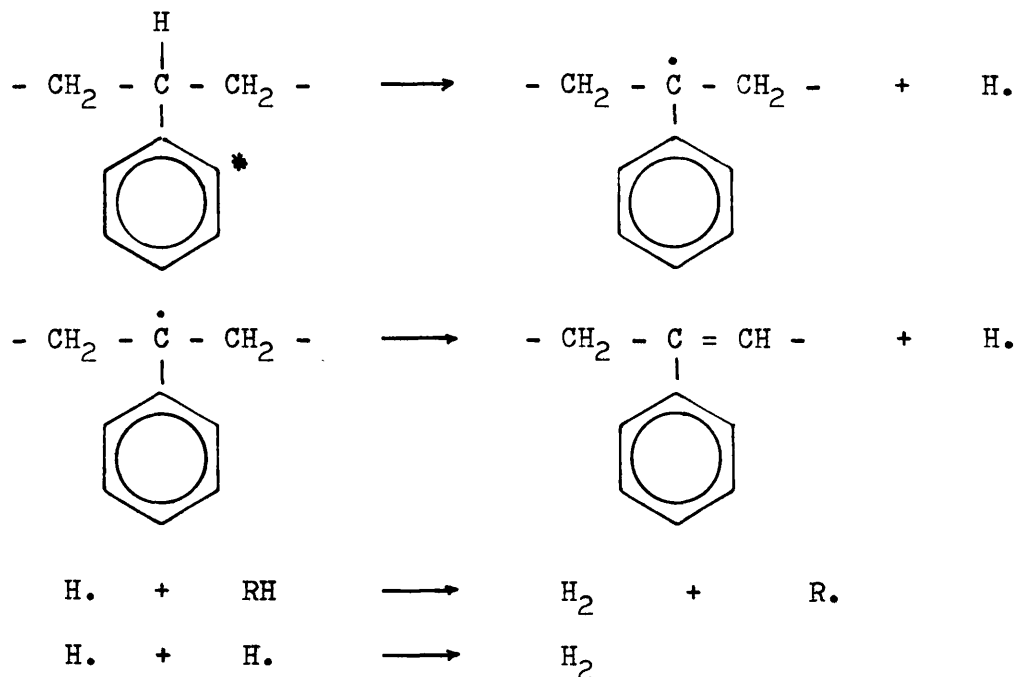
The only volatile degradation product of the pure polymer reported by Grassie and Weir (40) in their comprehensive study of polystyrene photodegradation was hydrogen. This finding was endorsed by Fox and his coworkers (44).

Grassie and Weir observed that films of polystyrene turned yellow on exposure to ultra-violet radiation at ambient temperatures but, as the degradation progressed, no further bathochromatic shift occurred. Instead, the yellow colour increased in intensity. This they regarded as evidence that unsaturated structures had been formed but were of low conjugation length.

As a simple analogy the  $R - (CH = CH)_n - R$  series can be considered. The absorption spectrum of members of the series when  $R = CH_3$  consists of several peaks, the most intense of which has  $\lambda_{max}$  at approximately 270 nm when  $n = 3$  and 420 nm when  $n = 8$  (72). The effect of further conjugation on the polyene chromophore is to shift the position of  $\lambda_{max}$  to a lower energy. However, at  $n > 8$  the extent of penetration of  $\lambda_{max}$  into the visible region is subject to a limiting value. The structure (shown below) of  $\beta$ -carotene with eleven conjugated bonds has  $\lambda_{max}$  at 452 nm.

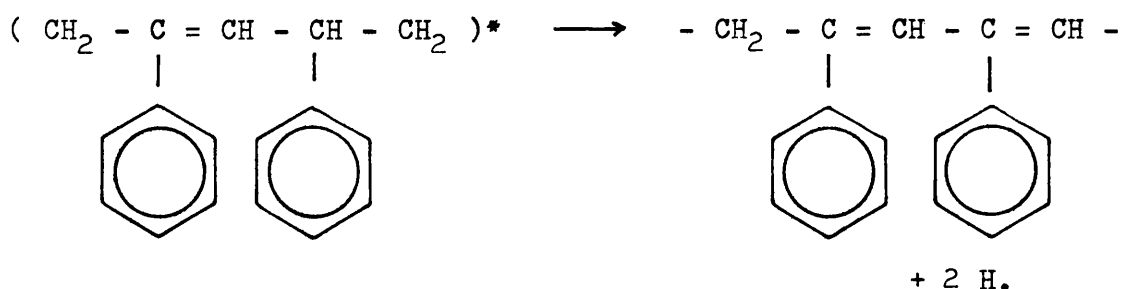


The observations of Grassie and Selivanov can be embodied in the following reaction:



The initial scission is thought to occur at the tertiary carbon - hydrogen bond where the activation energy required for this step is obviously lowered by the resonance stabilisation afforded by the benzene ring. Hydrogen molecules are formed either by direct combination of hydrogen radicals in a concerted reaction or by the abstraction of a second hydrogen atom from the polymer structure. In both cases the formation of an unsaturated structure is possible.

Further absorption at this site may result in an extension to the conjugation since the tertiary carbon - hydrogen bond on the adjacent unit is weakened by allylic resonance stabilisation:



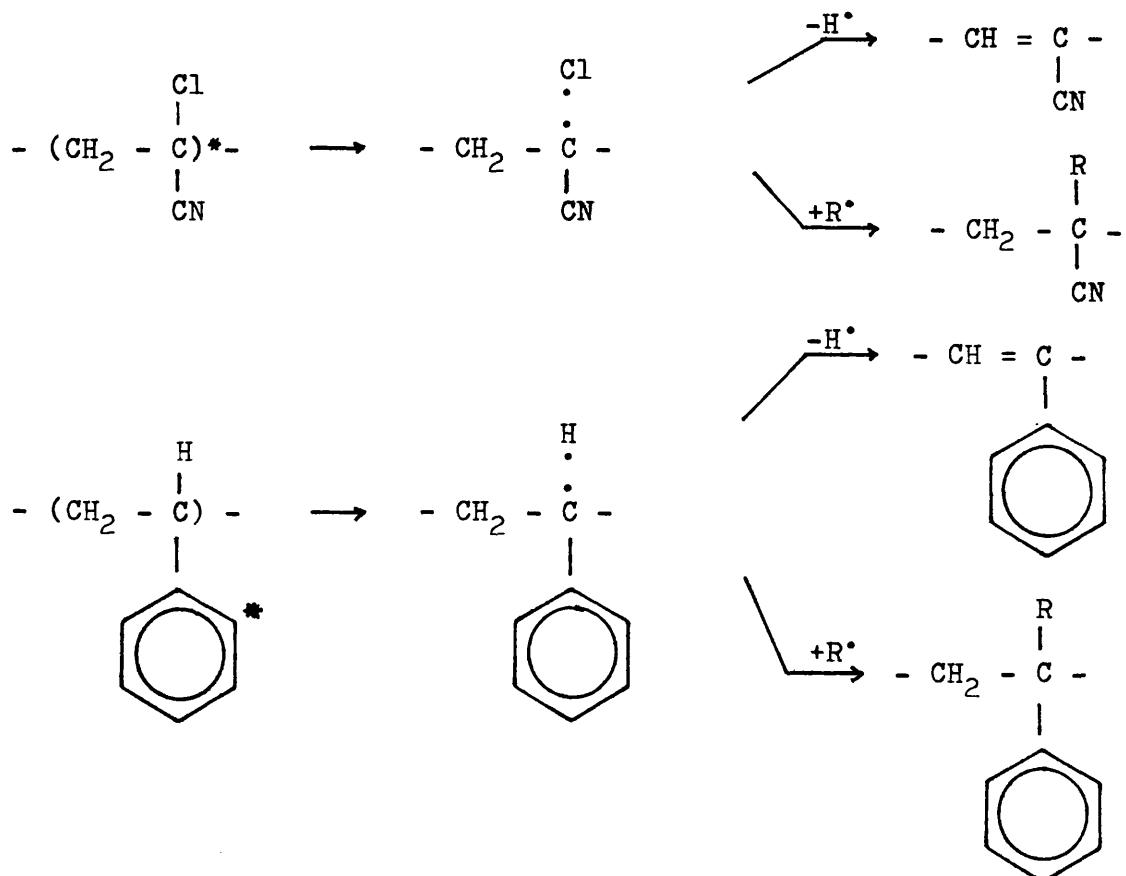
There is an obvious pattern for further extension of the conjugation as degradation progresses.

A similar situation is found in degradation studies on poly(vinyl chloride) in which Gibb and MacCallum (69) observed that, of the unsaturated structures formed by elimination of HCl from the polymer backbone, only dienes and trienes absorbed significant amounts of radiation of wavelength 254 nm. They suggested that a proportion of the high energy radiation absorbed caused reaction in non-absorbing parts of the polymer as a result of energy transfer.

As discussed in Chapter One, there is considerable scope for energy transfer. Guillet (73) in systematic studies on various polymer systems has shown that energy absorbed from incident radiation is mobile and does not necessarily remain at the absorbing chromophore.

The initial scissioning reaction, regardless of the site of absorption of radiation, which gives rise to structure I can also proceed to crosslinking reactions. Grassie and Weir suggested that crosslinks in polystyrene were most probable between radicals formed by the scission of tertiary carbon - hydrogen bonds, owing to the increased stability of the radical centre provided by the benzene ring.

The results obtained in Chapter Four demonstrated that incorporated CAN units provide crosslinking sites in copolymers with methyl methacrylate. Thus it is reasonable to assume that the crosslinking reactions associated with STC 875, STC 75 and STC 69 films can be initiated at both styrene and CAN units in the copolymer. Both initiation sites can result in unsaturated structures:



The progress of degradation will depend on the proportion of each initiation site in the copolymer film and the probability of bond scission at each.

The low values for the reactivity ratios of CAN and styrene

in the copolymer equation (57,58) suggest a strong alternating tendency at low conversion. At equimolar concentrations of monomers this could lead to a predominance of STY - CAN - STY - CAN sequences. However, as the copolymers in this work lie within the 60 - 100 per cent styrene range, a substantial proportion of STY - STY - STY sequences has to be expected.

N.M.R. studies in this work and by Gaylord and Patnaik (62) have confirmed that this is the case. It is reasonable to assume that the characteristics of degradation in the copolymers with high styrene content, e.g. STC 875, will be similar to those of polystyrene. As the proportion of CAN units is increased, the degradation may be expected to grow in complexity.

However, the shape of the HCl evolution curves from the copolymer degradation studies are similar in profile. In fact, this type of curve was obtained by Gibb and MacCallum (70) in their photodegradation studies on poly(vinyl chloride) in which the fall-off in evolution of HCl was shown to be caused by the build-up of a thin, absorbing surface layer which effectively prevented the penetration of destructive radiation. They accredited the absorbing effect of the layer to polyene structures formed by the elimination of HCl from the polymer backbone. On inverting the film the pattern is repeated with a second surface layer being formed.

Geuskens (74) has shown that the high coefficient of absorption of polystyrene results in 50 per cent of the incident energy being absorbed in a surface layer  $2\mu$  thick and at least 90 per cent of the energy being absorbed by a  $5 - 6\mu$  thick

layer.

As the films studied in this work were  $30 - 60\mu$  in thickness and had a high styrene content ( $>60$  per cent), the probability of a skin effect occurring is very high. A pointer to this type of behaviour by the copolymer films is that HCl evolution displays a marked area dependence as the degradation proceeds.

The formation of a polyene network is suggested by the expansion of the absorption spectra obtained from the copolymers during degradation. The extent of penetration into the visible region in the case of polystyrene appears to reach a limiting value.

In Chapter Four the production of HCl from the photo-degradation of copolymers of CAN with methyl methacrylate was investigated. It is possible to compare the HCl evolution data from copolymers of CAN with styrene and CAN with methyl methacrylate which contain similar proportions of CAN, provided that the sample weights and areas are closely matched and the degradation conditions are identical. This is represented in Table 5.2.

There is a sharp contrast in the evolution rates of HCl from the two copolymer systems. The formation of HCl from copolymers derived from styrene occurs more rapidly and efficiently than from the corresponding copolymers with methyl methacrylate. Thus it would appear that the absorption of radiation by the co-monomer and its transference to the CAN unit, either via intermolecular or intramolecular pathways

TABLE 5.2.

Comparison of HCl Evolution Behaviour from MMA - CAN and STY - CAN Copolymers Degraded under Identical Conditions.

(a) MMC 90 and STC 875.

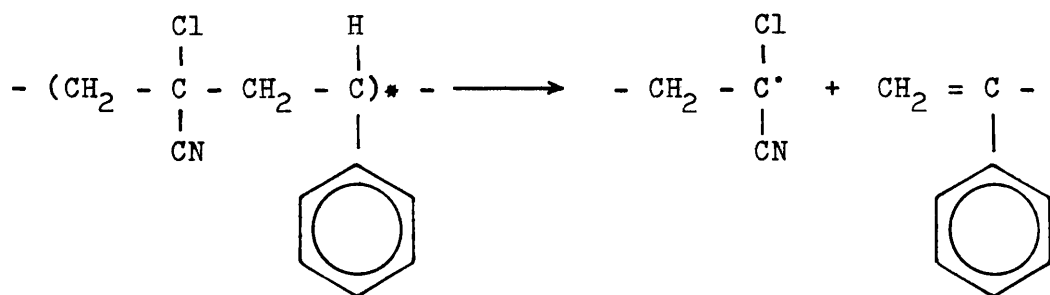
Time of Exposure (seconds)	Cumulative Pressure of HCl (torr)	
	MMA - CAN	STY - CAN
$3.6 \times 10^3$	0.006	0.165
$14.4 \times 10^3$	0.018	0.258
$25.2 \times 10^3$	0.022	0.283
$28.8 \times 10^3$	0.024	0.288

(b) MMC 74 and STC 75.

Time of Exposure (seconds)	Cumulative Pressure of HCl (torr)	
	MMA - CAN	STY - CAN
$1.2 \times 10^3$	0.001	0.125
$4.8 \times 10^3$	0.010	0.216
$9.1 \times 10^3$	0.031	0.272
$16.3 \times 10^3$	0.061	0.301
$30.7 \times 10^3$	0.066	0.321

is the critical distinguishing factor. In this case styrene is the more effective co-monomer at promoting the degradation of the CAN unit.

Another distinguishing feature between the two reactions is the appearance of CAN in the photodegradation products of styrene - CAN copolymers. It is possible that monomeric CAN molecules become trapped as inclusions in the polymer matrix and survive the reprecipitation procedure perhaps by hydrogen-bonding to the styrene units, and the degradation mechanism provides scope for their escape from the system. A similar explanation may account for the presence of styrene monomer among the products. Alternatively, scissioning may occur in the polymer backbone resulting in the depolymerisation to monomer over short zip lengths.



However, scissioning of the carbon - chlorine bond is more favourable than main - chain scissioning in terms of dissociation energies and would be expected in the majority of cases.

There is apparently some overlap between the degradation characteristics associated with styrene and those associated with CAN. The energy absorbed by styrene serves to enhance the production of HCl. The absence of any sharp drop in hydrogen

production from STC 69 film suggests that hydrogen formation involving the tertiary hydrogen atom of the styrene unit is also enhanced perhaps by the allylic unsaturation resulting from HCl elimination on an adjacent CAN unit.

CHAPTER SIXTHERMAL DEGRADATION OF PRE-IRRADIATED COPOLYMER FILMS.**6.1 INTRODUCTION.**

The photodegradation of polymers often results in structural changes such as the development of unsaturation, the formation of shorter chain lengths or the production of a crosslinked network. The physical properties of the polymer can be radically altered by these changes. The behaviour of the polymer in further stress situations may also be affected. In many applications polymers are exposed to several degradative agencies during their functional span; particularly common are heat and light, either consecutively or simultaneously. It is of practical importance, therefore, to examine the effect of photodegradation on the thermal behaviour of the polymer. In certain cases it is often possible to discern useful information about the mechanism of photodegradation by examining discrepancies in the subsequent thermal degradative pattern.

The behaviour of the polymer during thermal degradation can be monitored by the techniques of thermogravimetric (TG) analysis, thermal volatilisation analysis and differential condensation thermal volatilisation analysis (DCTVA), all of which are described in Chapter Two.

In this, the final chapter, the normal thermal degradation behaviour of each copolymer, as characterised by the above techniques, is compared to that of a pre-irradiated copolymer

sample in order to determine the effect of pre-irradiation on thermal degradation. The cause of any discrepancy in behaviour is examined in order to throw light on the photodegradation processes involved.

## 6.2 EXPERIMENTAL RESULTS.

### 6.2.1 Apparatus and Conditions.

The apparatus employed for DCTVA is described in Chapter Two. The heating rate was maintained at  $10^{\circ}\text{C}$  per minute throughout. The temperatures quoted in DCTVA traces refer to the sample and not the oven. Depending on the availability of material sample weights varied between 20mg and 50mg. The trap temperatures were set as follows:

$0^{\circ}\text{C}$	}	dashed line on trace,
$-45^{\circ}\text{C}$		
$-75^{\circ}\text{C}$		unbroken line on trace,
$-100^{\circ}\text{C}$		dotted line on trace,
$-196^{\circ}\text{C}$		alternate dash-dot line on trace.

TG data were obtained in a dynamic nitrogen atmosphere (80ml per minute) and at a heating rate of  $10^{\circ}\text{C}$  per minute using 3 - 5mg film samples accommodated in a platinum holder. Again, the technique and apparatus are described in Chapter Two.

The pre-irradiation of the copolymer films was carried out under conditions described in the respective Chapters on copolymer photodegradation.

### 6.2.2 Product Analysis.

Before discussing the DCTVA traces of various copolymers it is essential first to identify the products formed by thermal degradation. As the quantity of volatiles obtained for a given sample weight is considerably greater than that formed in photolysis studies, infrared spectroscopy is generally regarded as a reliable method of detection.

The products obtained from the series of methyl methacrylate - CAN copolymers are summarised in Table 6.1. Pre-irradiation of the copolymers was found to have no effect on the nature of the products.

In previous studies on this copolymer system Grant (57) detected CAN amongst the degradation products. In Figure 6.1 the infrared spectrum of the degradation products from MMC 50 film is reproduced. By comparison with Figure 6.2 it would appear that there is no correlation between the spectrum of products and that of CAN. A similar result was obtained by comparison of the total mass spectrum of the products with that of CAN as is shown in Figure 6.3. It is possible, however, that the sample size available (30mg) was insufficient for detectable quantities of CAN to be formed.

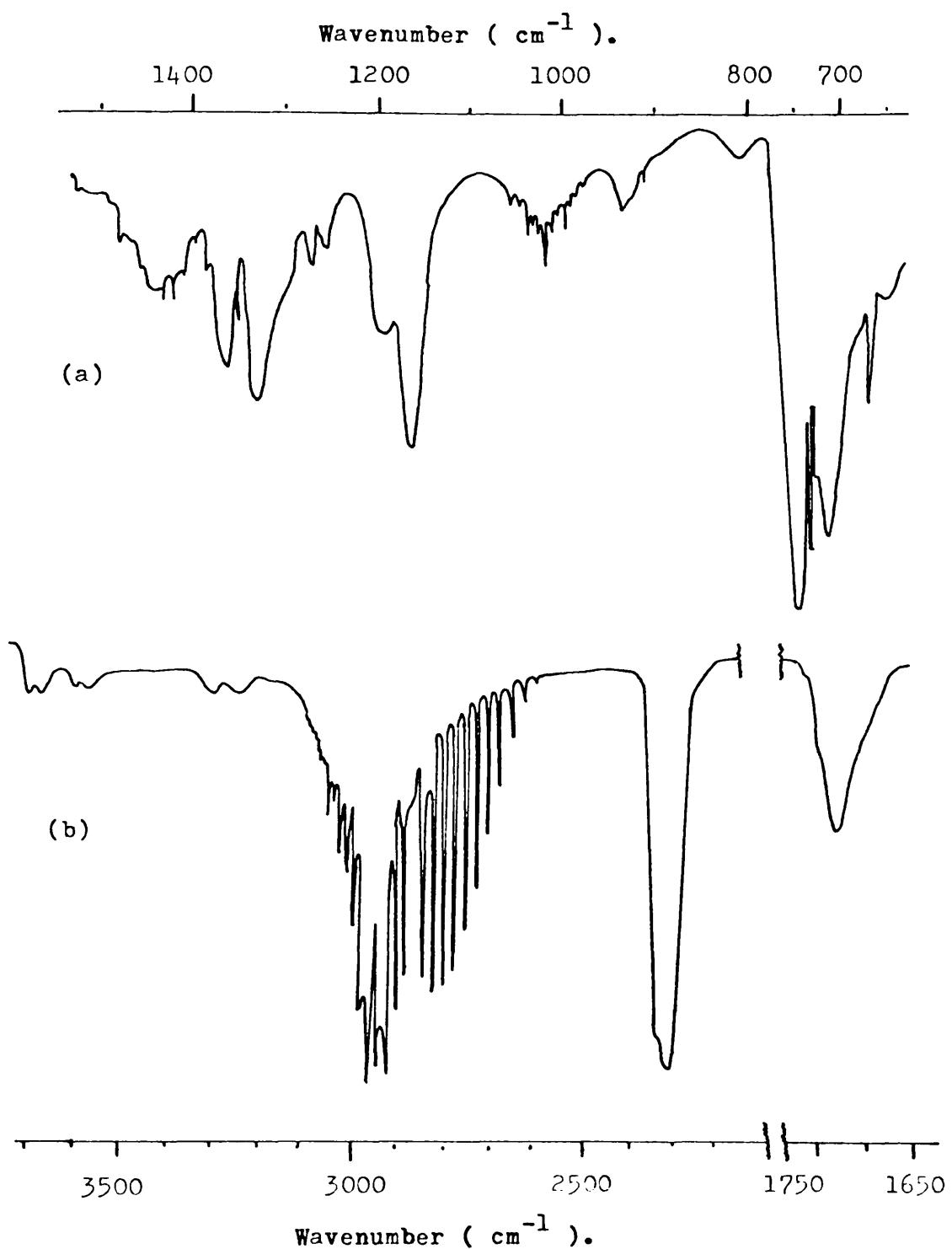
In the case of the styrene copolymers hydrogen chloride was found to be the major product. Trace amounts of hydrogen cyanide (infrared absorption at  $714 \text{ cm}^{-1}$ ) were also detected. Mass spectrometric studies were not attempted on the product sample.

TABLE 6.1.

Thermal Degradation Products (condensable at -196°C) from  
Methyl methacrylate - CAN Copolymers.

<u>Product</u>	<u>MMC 90</u>	<u>MMC 74</u>	<u>MMC 50</u>
Methyl methacrylate	s	s	m
Hydrogen chloride	w	s	s
Carbon dioxide	w	m	m
Methyl chloride	-	w	m
Hydrogen cyanide	w	w	m

Subjective analysis:      w = weak  
 based on relative      s = strong  
 amount of product      w    m    s  
 in the three spectra.



**FIGURE 6.1** Infrared spectrum (a)  $650 - 1500 \text{ cm}^{-1}$ , (b)  $1650 - 3700 \text{ cm}^{-1}$ ) of thermal degradation products from MMC 50 film cast from dichloromethane solution and pre-irradiated for  $3.96 \times 10^4$  seconds.

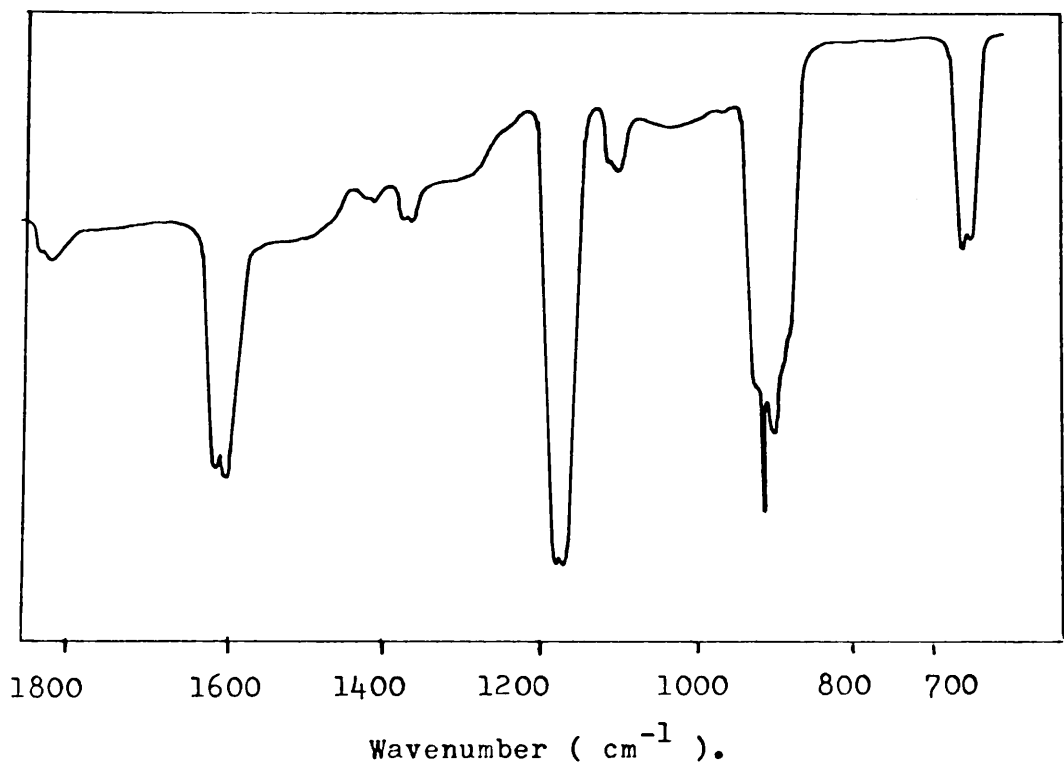
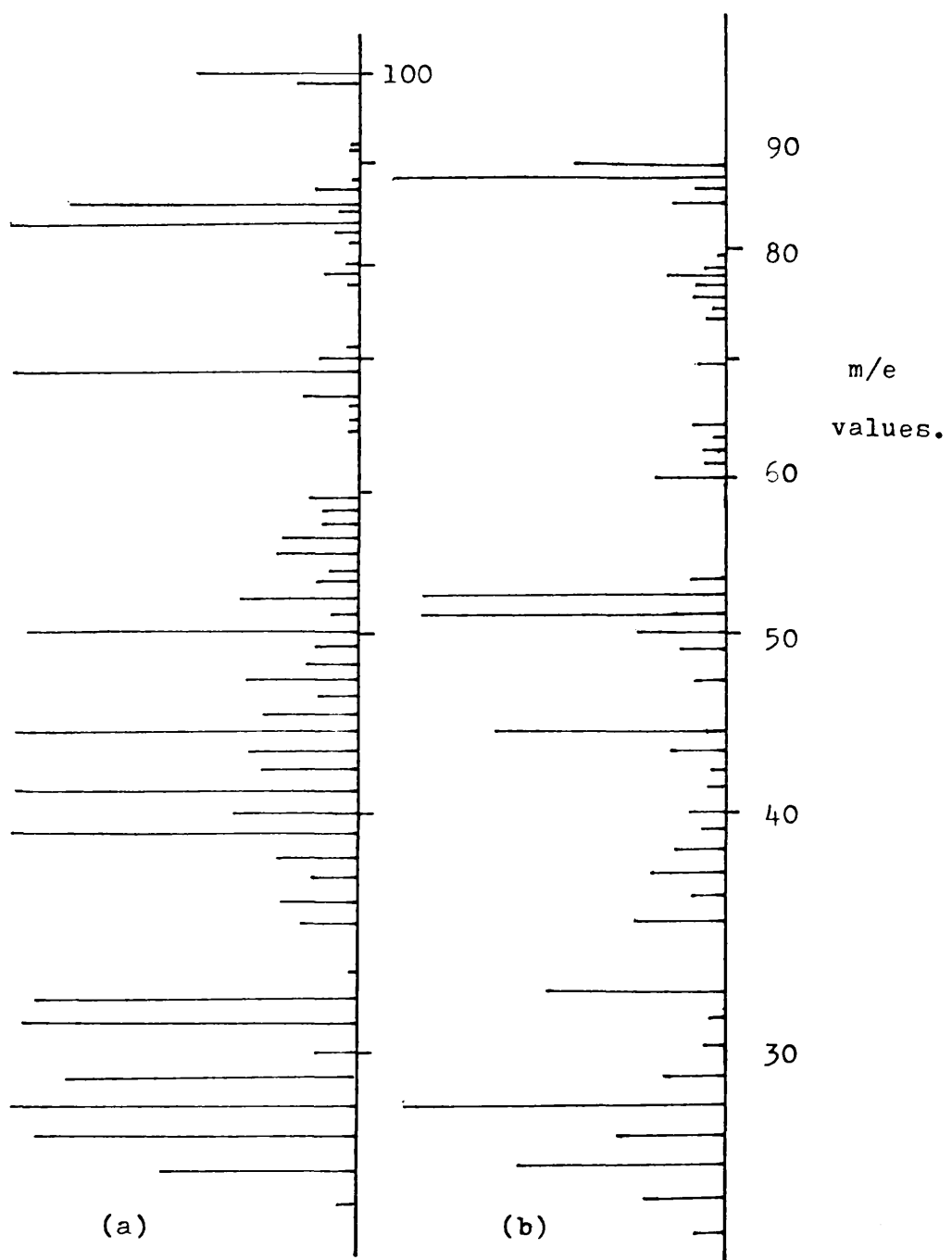


FIGURE 6.2 Infrared Spectrum of 2,2-chloroacrylonitrile.



**FIGURE 6.3** (a) Mass spectrum of products from the thermal degradation of MMC 50 film cast from dichloromethane solution.  
(b) Mass spectrum of 2,2-chloroacrylonitrile.

### 6.2.3 DCTVA Results.

#### (a) Styrene - CAN copolymer system.

Two stages of reaction can be distinguished in the DCTVA trace from STC 75 as shown in Figure 6.4a. In the main stage, commencing at  $240^{\circ}\text{C}$ , volatile products are formed which are almost totally non-condensable at  $-100^{\circ}\text{C}$ . In the second stage of reaction (above  $310^{\circ}\text{C}$ ) the products are, for the main part, condensed at  $-100^{\circ}\text{C}$  and, in the latter stages, exhibit a limiting rate at  $-75^{\circ}\text{C}$ . The pre-irradiated sample has a similar profile (allowing for the non-linearity of Pirani response and the difference in sample sizes).

The main products detected were hydrogen chloride, a trace of hydrogen cyanide and, from the limiting rate at above  $400^{\circ}\text{C}$  in the  $-75^{\circ}\text{C}$  trace, styrene was strongly suspected (75). Hydrogen chloride is not condensed at  $-100^{\circ}\text{C}$ , but fully condensed at  $-196^{\circ}\text{C}$  (55). It would appear that the main product in the first stage of reaction is hydrogen chloride with styrene formed at higher temperatures.

In both samples a  $T_{\max}$  of  $280 \pm 3^{\circ}\text{C}$  was recorded for the first stage. The other copolymers in this series, STC 69 and STC 875 displayed similar DCTVA traces. However, the  $T_{\max}$  for the first stage occurred at lower temperatures in STC 69 ( $276^{\circ}\text{C}$ ) and at higher temperatures in STC 875 ( $283^{\circ}\text{C}$ ).

#### (b) Methyl methacrylate - CAN copolymer series.

The DCTVA traces obtained from the thermal degradation of MMC 90, MMC 74 and MMC 50 copolymers and pre-irradiated samples (in film form) of these copolymers are reproduced in Figures

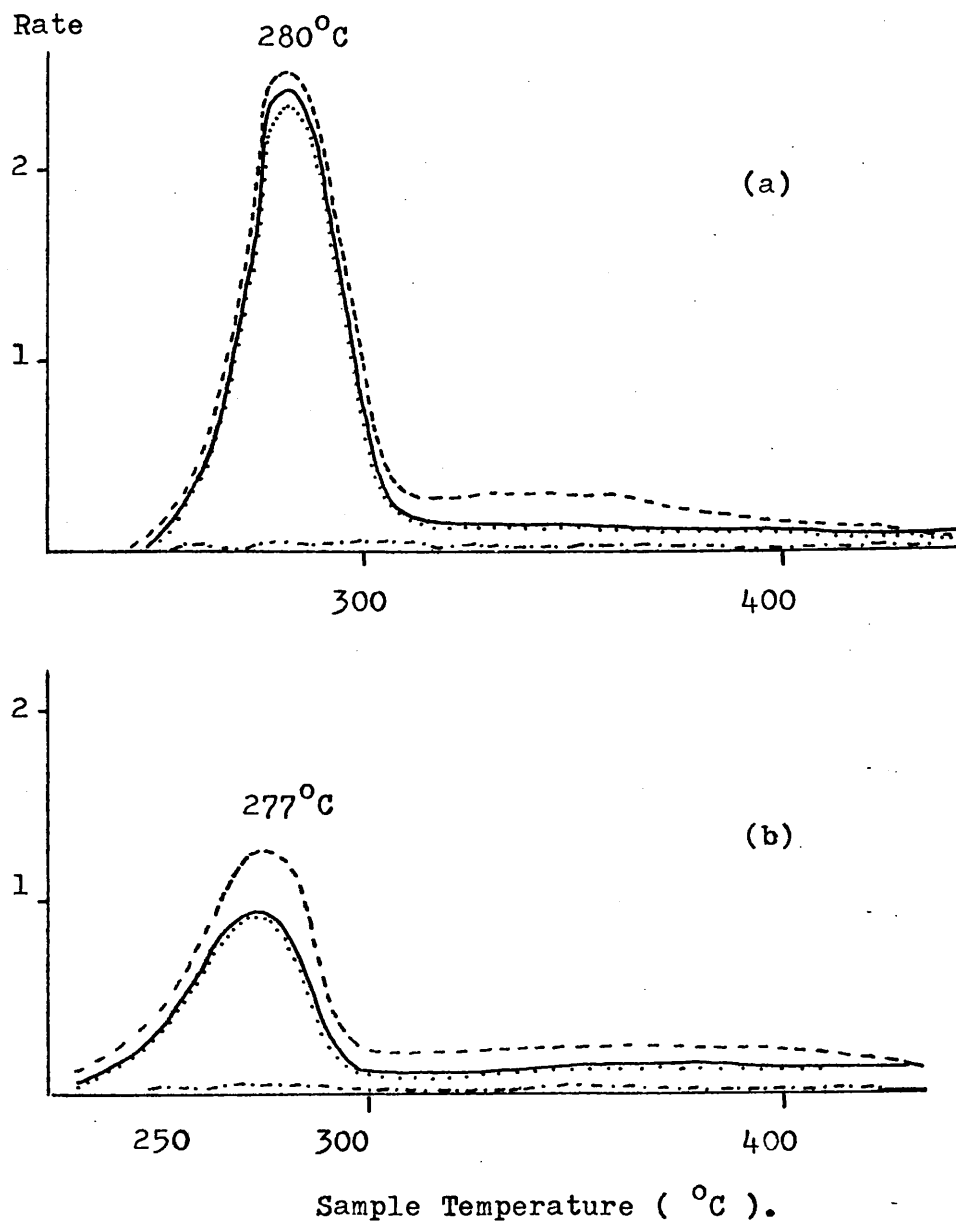


**FIGURE 6.4** DCTVA traces obtained from  
 (a) STC 75 film cast from  $\text{CH}_2\text{Cl}_2$   
 (b) STC 75 film cast from  $\text{CH}_2\text{Cl}_2$   
 and pre-irradiated for a period  
 of  $3.42 \times 10^4$  seconds.

6.5, 6.6, 6.7, 6.8, and 6.9, respectively.

The initial reaction stage in the degradation of MMC 90 commences below 200°C. From previous work (48) it is known that methyl methacrylate and hydrogen chloride are liberated virtually simultaneously. This is consistent with the trace shown in Figure 6.5. The monomer formed is trapped at -75°C but not fully condensed since it distils into the -196°C trap at a steady, limiting rate. It is, however, fully condensed at -100°C. Hydrogen chloride is volatile at -100°C but fully condensed at -196°C.

Also included in Figure 6.5 is the corresponding TG curve obtained by placing the sample on the pan of a Cahn balance which is situated within the degradation tube. It is apparent that methyl methacrylate evolution during this initial reaction stage accounts for the major part of the total weight loss.

In Figure 6.6 the DCTVA trace for a pre-irradiated sample of MMC 90 has a similar overall appearance. The most obvious change resulting from pre-irradiation is the much greater amount of material volatile at -100°C. Thus it appears that the contribution from methyl methacrylate has decreased. Also a greater proportion of products volatile at -196°C are present in the later stages of reaction.

The MMC 74 copolymer behaves in a similar manner as is shown in Figures 6.7 and 6.8. The proportion of methyl methacrylate in the initial reaction stage is apparently smaller in the pre-irradiated sample. Again, the occurrence of products

Residual weight  
as percentage of  
the initial weight.

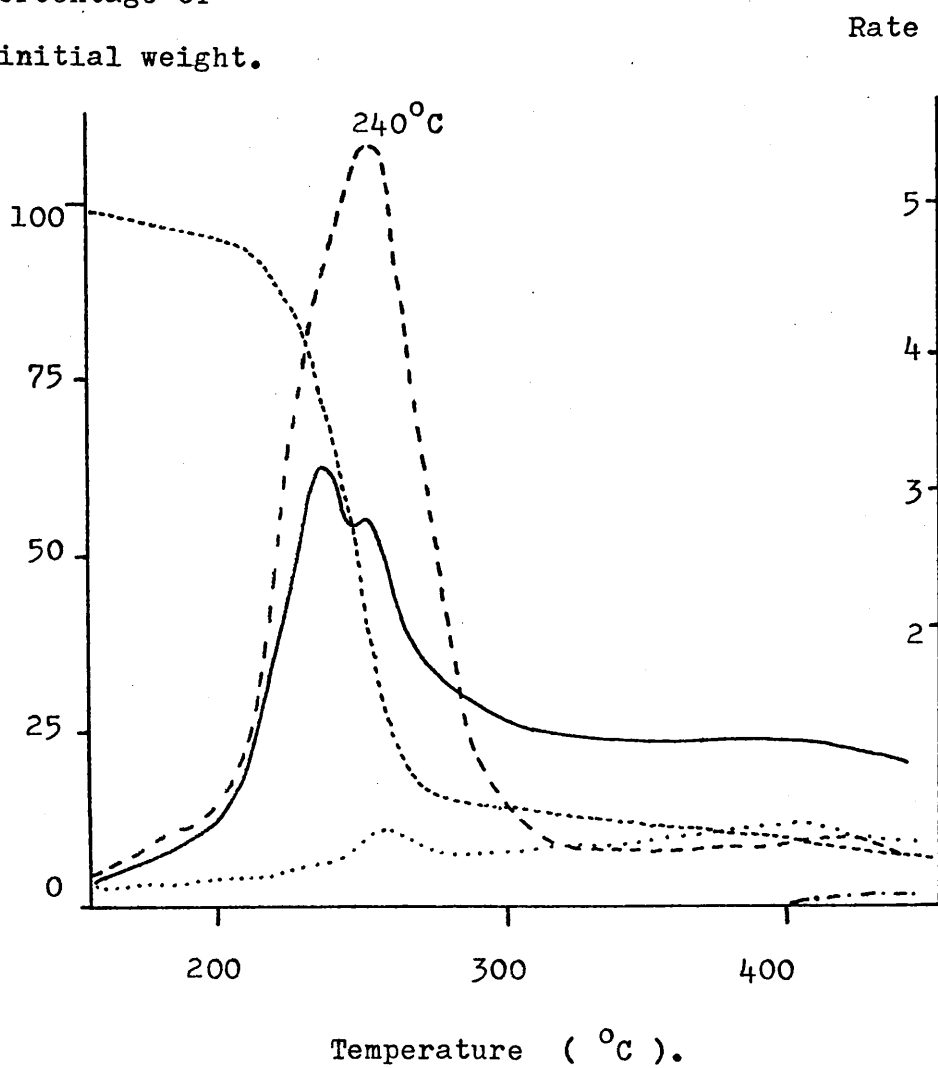


**FIGURE 6.5** DCTVA trace from the degradation of  
MMC 90 in powder form.  
Superscribed on the trace is the TG curve  
which was obtained simultaneously.

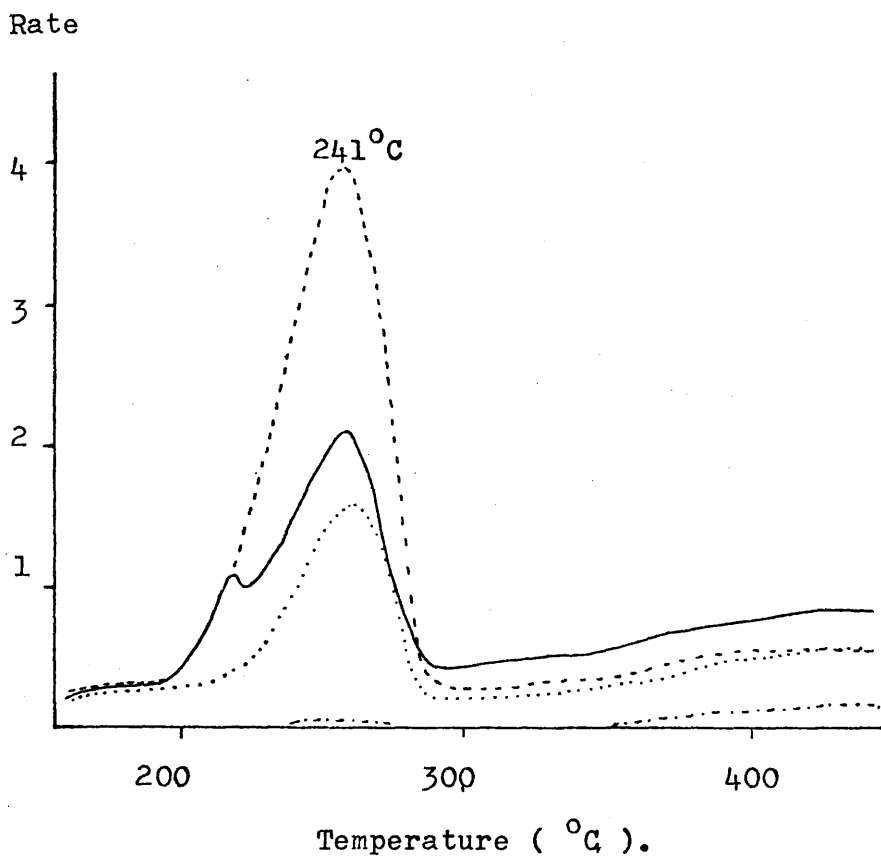


FIGURE 6.6. DCTVA trace from the degradation of MMC 90 film cast from dichloromethane and pre-irradiated for  $3.6 \times 10^4$  seconds.

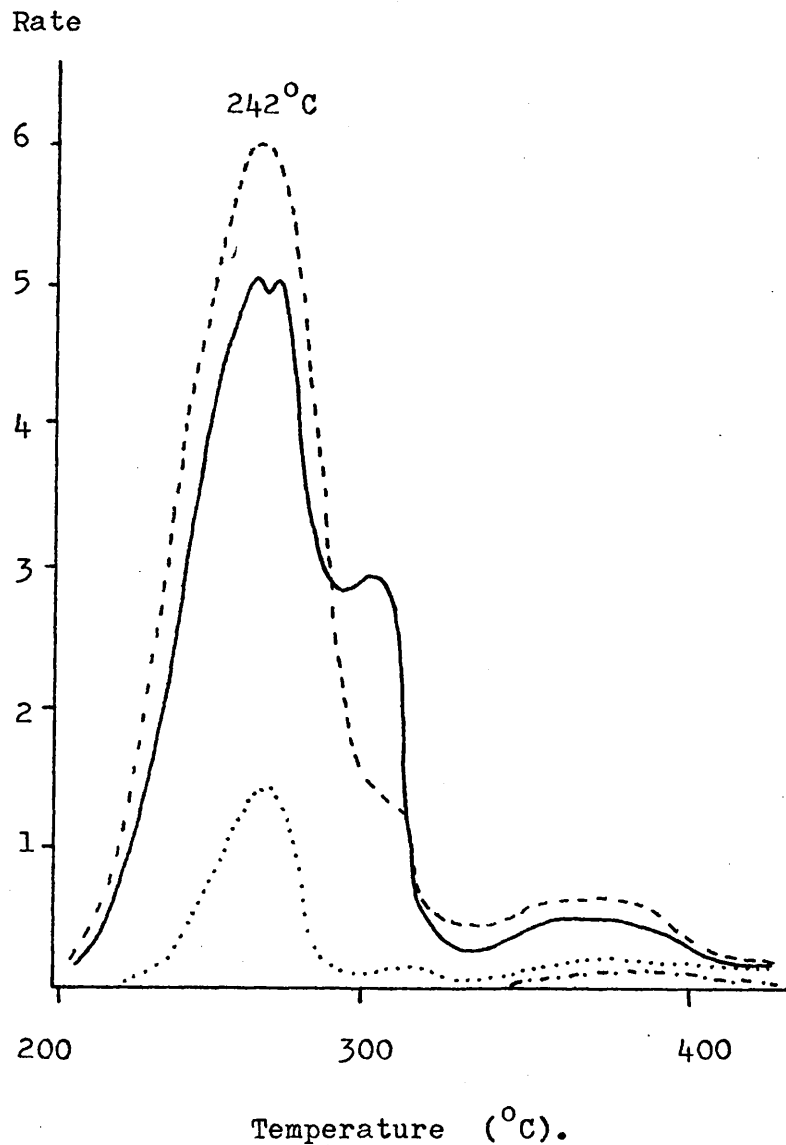
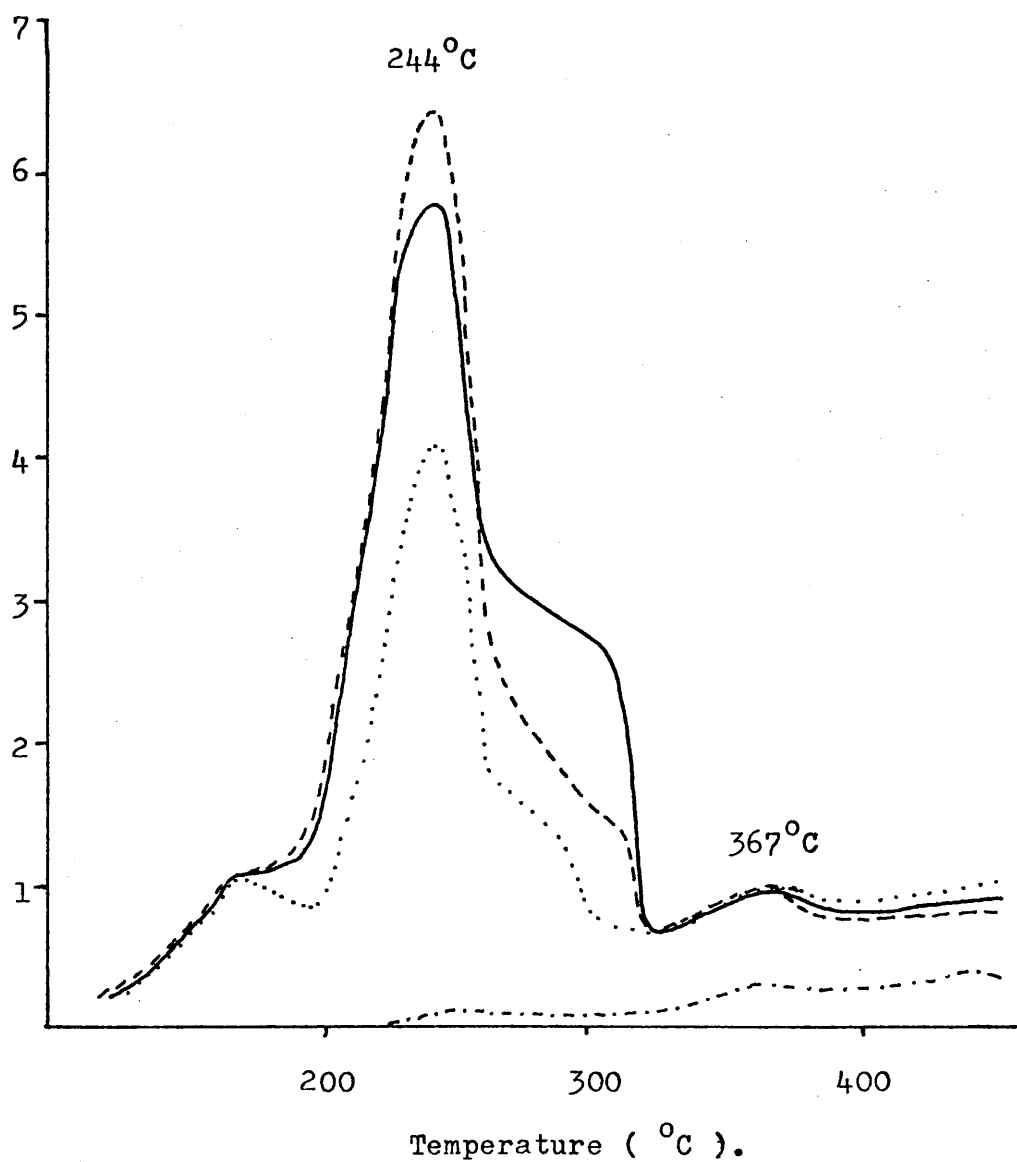
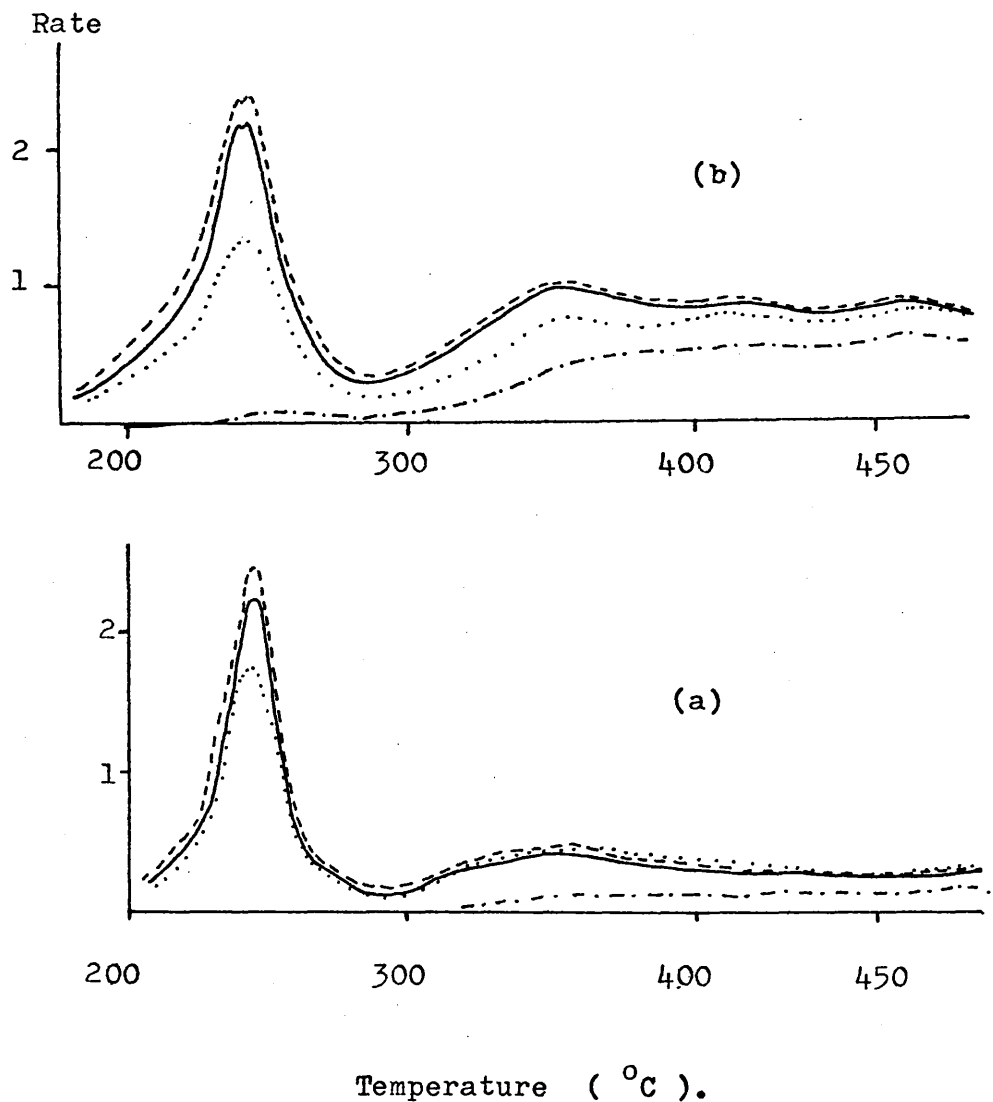


FIGURE 6.7 DCTVA trace from the degradation of  
MMC 74 (in powder form).

Rate



**FIGURE 6.8** DCTVA trace from the degradation of  
MMC 74 film, cast from dichloromethane  
solution and pre-irradiated for a period  
of  $3.6 \times 10^4$  seconds.



**FIGURE 6.9.** DCTVA trace from the thermal degradation of  
 (a) MMC 50 film cast from dichloromethane  
 and (b) MMC 50 film cast from dichloromethane  
 and pre-irradiated for a period of  
 $3.96 \times 10^4$  seconds.

volatile at  $-196^{\circ}\text{C}$  is more marked. This pattern is repeated in the MMC 50 copolymer as is illustrated in Figure 6.9.

The temperature of the first rate maximum in each copolymer examined occurred at  $240 \pm 2^{\circ}\text{C}$ . The reaction was initiated at temperatures below  $200^{\circ}\text{C}$  and in all cases involved the evolution of hydrogen chloride and methyl methacrylate (although other products may be present).

A second maximum temperature is discernable which is apparently little affected by pre-irradiation but dependent on the CAN content of the copolymer. Thus in MMC 90, MMC 74 and MMC 50 the second  $T_{\max}$  occur at  $380 \pm 2^{\circ}\text{C}$ ,  $367 \pm 2^{\circ}\text{C}$  and  $352 \pm 2^{\circ}\text{C}$  respectively.

The MMC 50 copolymer exhibits further rate maxima temperatures at  $410^{\circ}\text{C}$  and  $459^{\circ}\text{C}$  suggesting further stages of reaction. It is possible that these stages occur in the other copolymers to a lesser degree.

#### 6.2.4 Thermogravimetric Analysis.

##### (a) Styrene - CAN Copolymer System.

Pre-irradiation of the STC 75 copolymer had no significant effect on the normal TG curve as is shown in Figure 6.10. It is of interest to note that only a 30 per cent weight loss occurs between  $200^{\circ}\text{C}$  and  $300^{\circ}\text{C}$ , whereas in DCTVA traces, admittedly under vacuum conditions, this region appears to house the major stage. The STC 69 copolymer behaved in similar fashion. The STC 875 copolymer was not tested in this manner.

##### (b) Methyl Methacrylate - CAN Copolymer System.

In contrast to styrene copolymers the TG curve for MMC 90

Residual weight  
as percentage of  
initial weight.

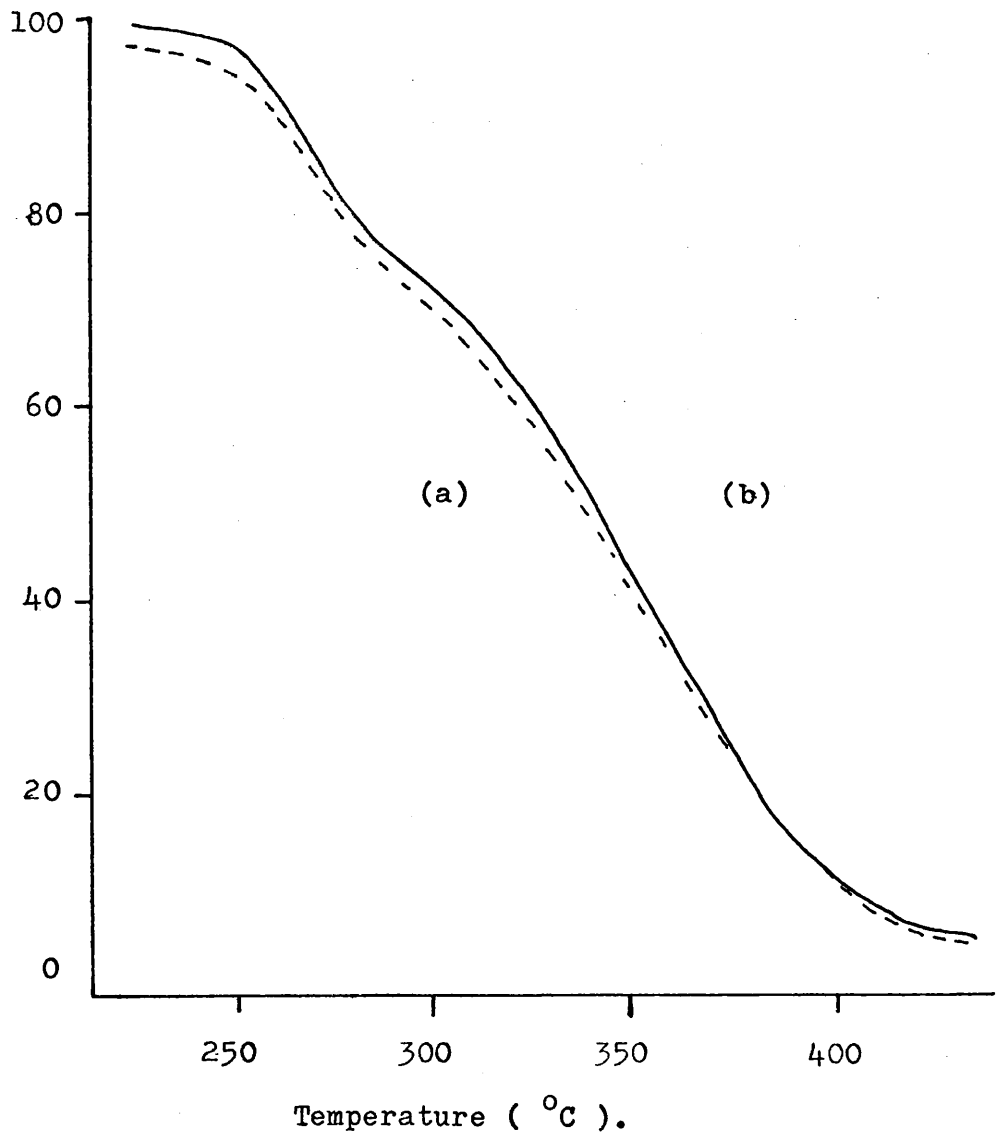


FIGURE 6.10 TG curve for STC 75 film cast from dichloromethane solution.  
(a) unirradiated  
and (b) pre-irradiated for  $3.6 \times 10^3$  seconds.

was significantly restructured by pre-irradiation. As the exposure period was increased the effect was enhanced. This is shown in Figure 6.11. The major weight loss in the copolymer is caused by methyl methacrylate liberation (48). In all three TG curves the maximum rate of weight loss occurs below 250°C. However, in comparing the residual weights at 250°C, the effect of pre-irradiation is established. Whereas 20 per cent of the original mass of copolymer remains at the 250°C stage under normal conditions, pre-irradiation periods of 5 hours and 20 hours result in residual masses of 40 per cent and 60 per cent respectively of the original.

In the case of the MMC 74 copolymer the effect of pre-irradiation is less marked. Exposure periods of 6 hours 12 hours and 22 hours respectively resulted in residual masses at 270°C (Figure 6.12) of 20 per cent, 23 per cent and 26 per cent of the original.

Residual weight  
as percentage of  
initial weight.

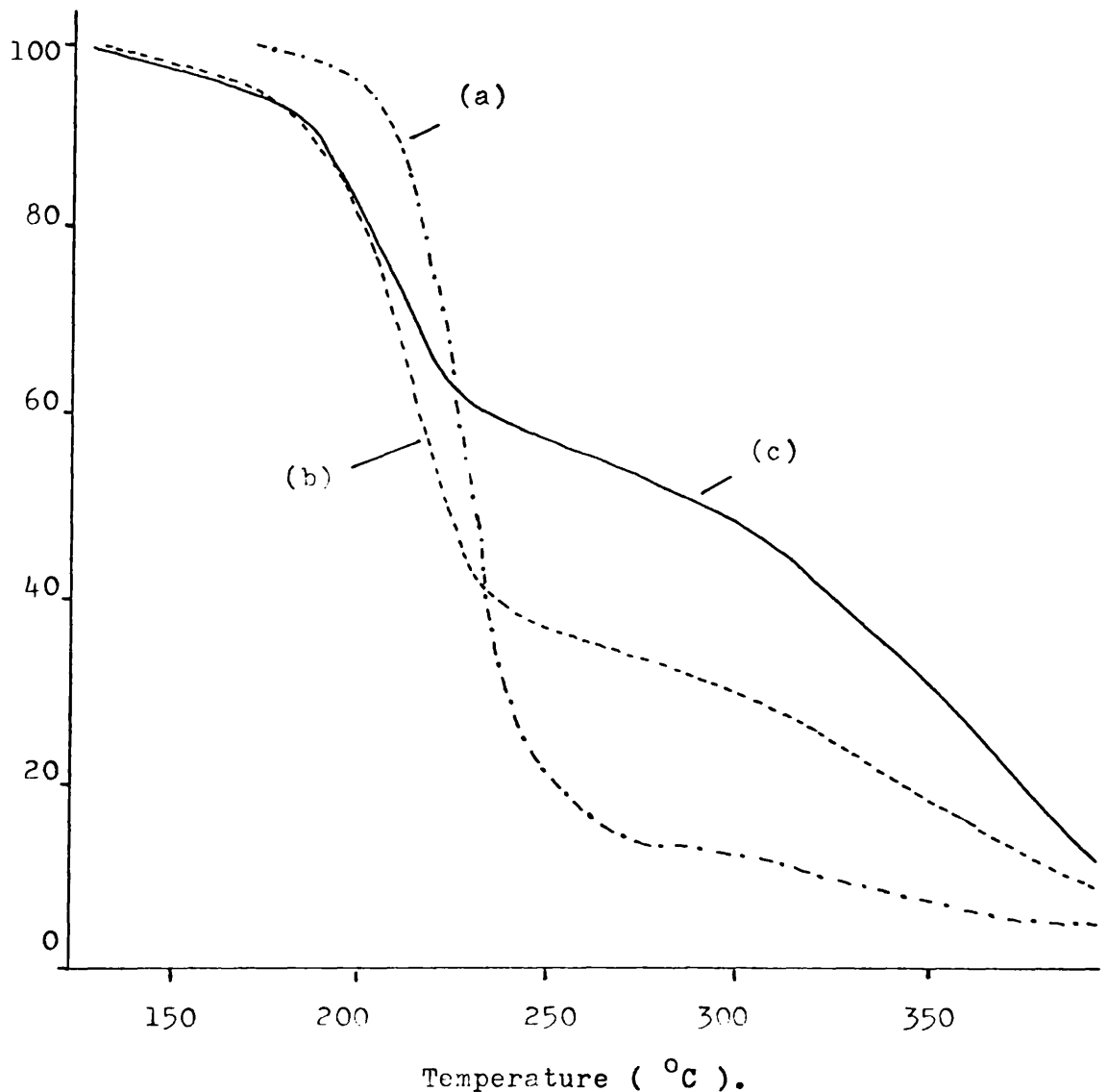
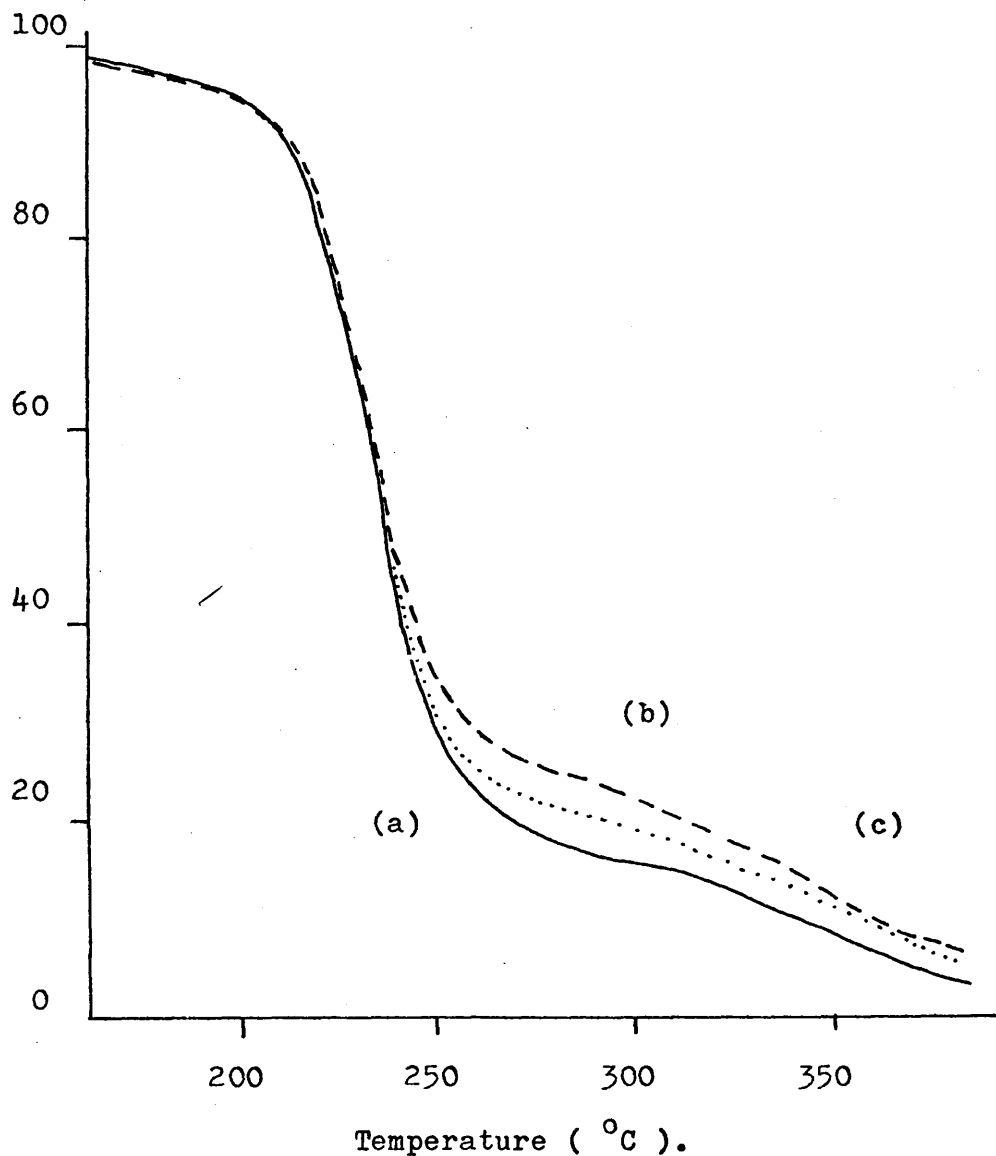


FIGURE 6.11 TG curve for MMC 90 film cast from dichloromethane solution

- (a) unirradiated,
- (b) pre-irradiated for  $1.8 \times 10^4$  seconds
- and (c) pre-irradiated for  $7.2 \times 10^4$  seconds.

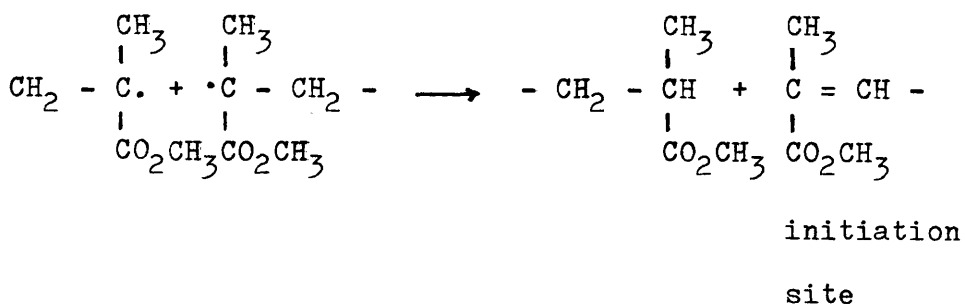
Residual weight as  
percentage of initial weight.



**FIGURE 6.12.** TG curve for MMC 74 film cast from dichloromethane solution and pre-irradiated for:  
(a)  $2.16 \times 10^4$  seconds,  
(b)  $4.32 \times 10^4$  seconds and  
(c)  $7.92 \times 10^4$  seconds.

### 6.3 DISCUSSION.

The thermal degradation of poly(methyl methacrylate) results in a quantitative yield of monomer (76). The depolymerisation reaction is thought to be initiated specifically at the unsaturated chain ends formed in the disproportionation termination process during polymerisation:



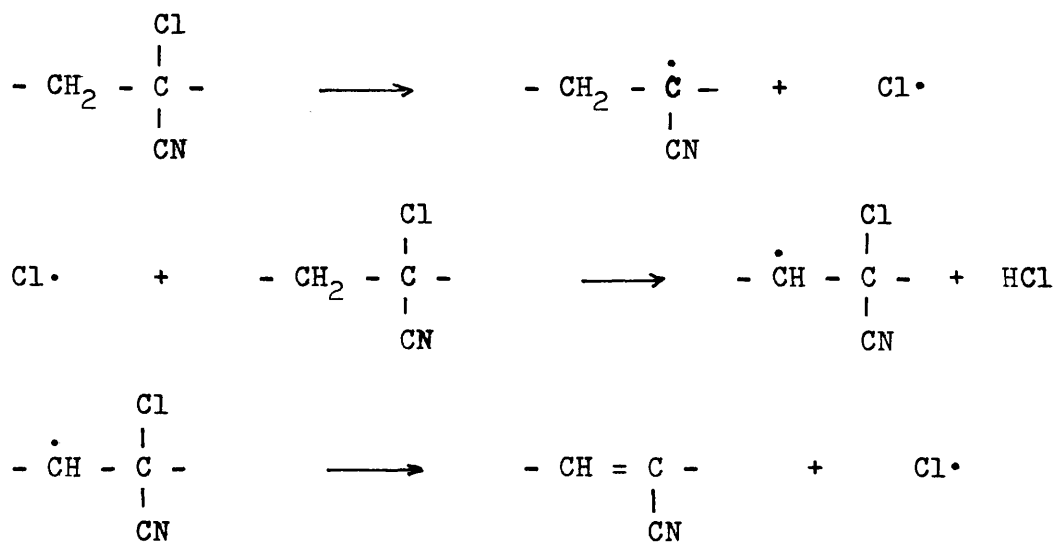
When these structures are eliminated by degradation, the residual terminally saturated polymer is more stable and can only be further degraded at a higher temperature through a random scission process.

The effect of pre-irradiation on the thermal degradation behaviour of poly(methyl methacrylate) prepared by free radical polymerisation has been investigated by Mackinnon(47) employing the DCTVA technique. The normal trace consists of two peaks with  $T_{max}$  at approximately  $307^{\circ}\text{C}$  and  $373^{\circ}\text{C}$  respectively. It is generally accepted that the low temperature peak results from monomer liberated by chain-end initiated depolymerisation and the second peak from monomer released by random scissioning.

The DCTVA trace from the degradation of poly(methyl methacrylate) film, cast from toluene solution and pre-irradiated by 254 nm radiation, was found to contain the same two peak maxima but with the  $307^{\circ}\text{C}$  peak greatly enhanced.

This was attributed to the formation of unsaturated structures within the polymer.

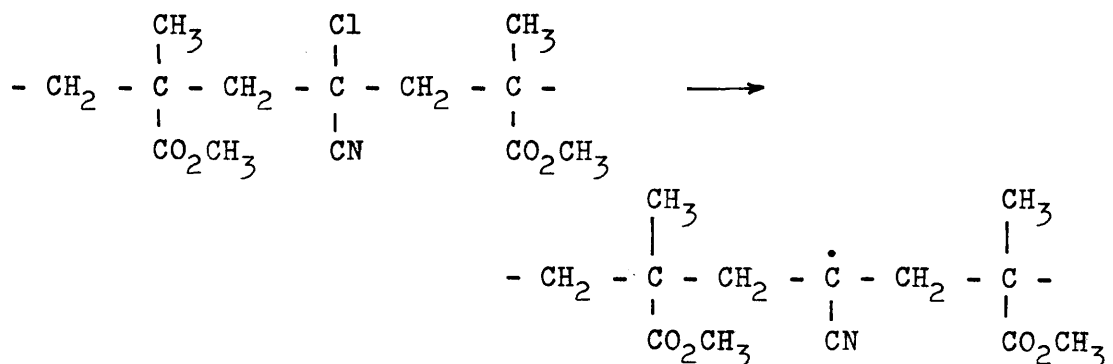
The thermal degradation mechanism of poly(CAN) was first studied by Grant (57). This belongs to the substituent or non-chain scissioning group of degradation reactions. Hydrogen chloride is evolved and unsaturation develops in the main chain:



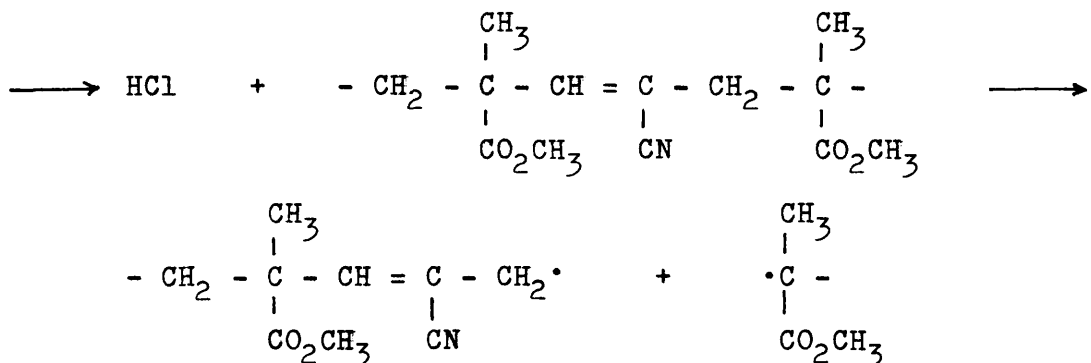
The effect of pre-irradiation on the thermal behaviour of this polymer has also been investigated (47). The DCTVA trace for poly(CAN) was found to consist of one dominant peak with  $T_{max}$  at  $240^{\circ}\text{C}$ . This was attributed to hydrogen chloride evolution. A sample of the polymer was pre-irradiated by 254 nm radiation and subsequently thermally degraded. It was concluded that pre-irradiation had no significant effect on thermal degradation behaviour.

The thermal degradation of copolymers of methyl methacrylate with CAN was also studied by Grant (57). The main feature of interest was the appearance of volatile products, consisting of hydrogen chloride and the two monomers, at

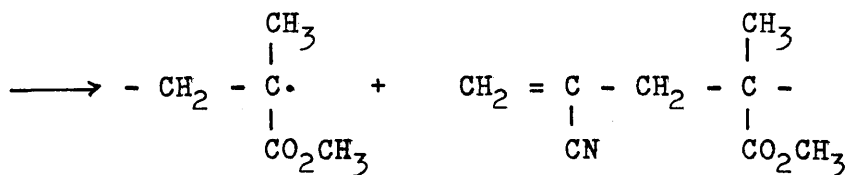
temperatures around  $150^{\circ}\text{C}$ . This is the same temperature region at which hydrogen chloride is first evolved during the degradation of poly(CAN). The results of the copolymer studies suggested that the degradation process was initiated by carbon - chlorine bond scissioning, with resulting evolution of hydrogen chloride, followed by random scissioning to produce the two monomers. Two possible reaction pathways were proposed:



Path 1.

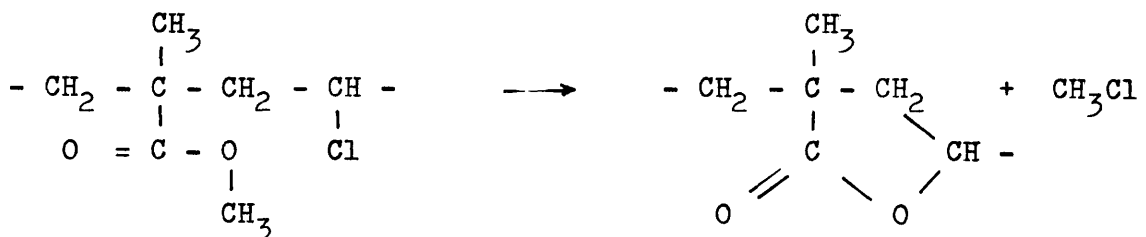


Path 2.



In each case the resulting polymer radical is capable of depolymerisation.

As methyl chloride, hydrogen chloride and carbon dioxide become significant products when the proportion of CAN in the copolymer is increased, it is necessary to account for their formation. When an analogous copolymer system, that of methyl methacrylate and vinyl chloride, was investigated by Zutty and Welch (77), it was discovered that, in the region of  $150^{\circ}\text{C}$ , a purely intramolecular lactonisation reaction occurred in which  $\alpha$ -methyl- $\gamma$ -butyrolactone groups were formed together with the quantitative elimination of methyl chloride:

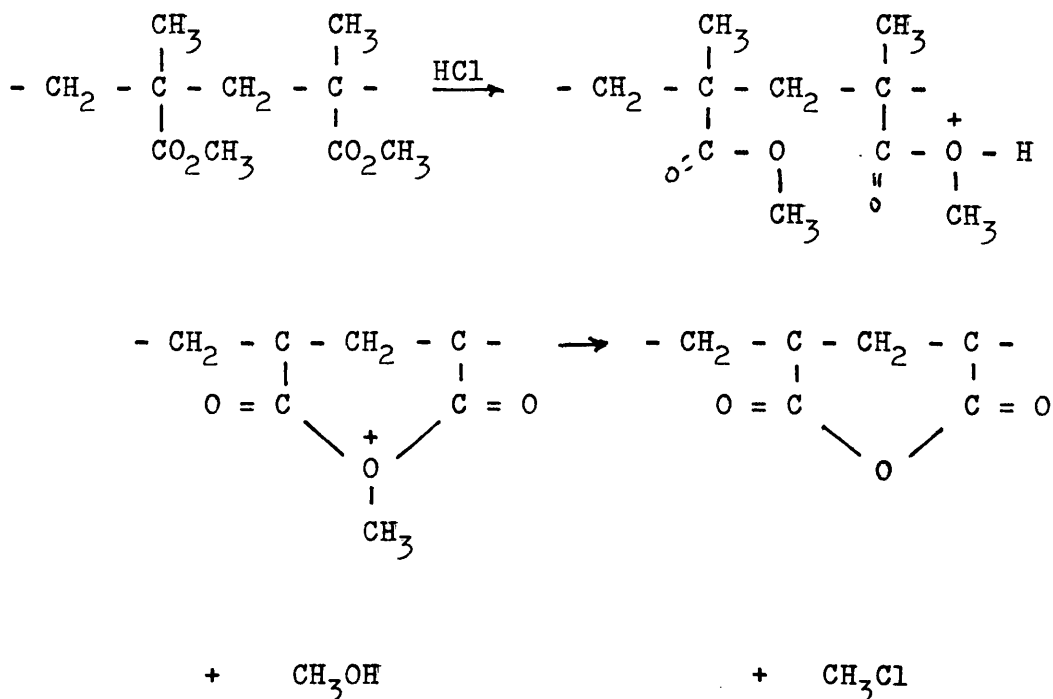


This was taken further by Straiton (78) who established, using the DCTVA technique, that the lactonisation reaction in the methyl methacrylate - vinyl chloride system occurred with  $T_{\max}$  at  $206^{\circ}\text{C}$ . In the same work interaction between hydrogen chloride and ester groups was observed at higher temperatures in copolymers of intermediate composition reaching a maximum extent in the copolymer with approximately 60 per cent vinyl chloride. The overall reaction could be subdivided into temperature dependent stages.

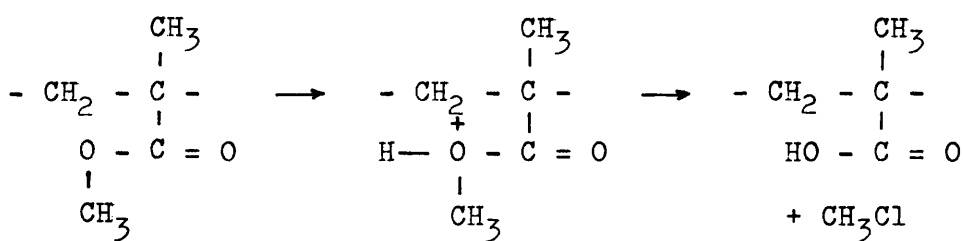
Thus between  $100^{\circ}\text{C}$  and  $200^{\circ}\text{C}$  the primary products were methyl chloride from lactonisation, hydrogen chloride and benzene (from vinyl chloride units). Between  $200^{\circ}\text{C}$  and  $300^{\circ}\text{C}$  methyl methacrylate from chain - end initiation, hydrogen chloride and methyl chloride from the interaction of

hydrogen chloride with ester were formed. Finally, above  $300^{\circ}\text{C}$ , methyl methacrylate from random scissioning, carbon dioxide and hydrocarbons were reported.

As an extension of this work Straiton investigated the thermal degradation of copolymers of vinyl chloride with methacrylic acid. Three stages of reaction were observed by DCTVA. Hydrogen chloride was evolved with  $T_{\max}$  at  $168^{\circ}\text{C}$  and, again, with  $T_{\max}$  at  $319^{\circ}\text{C}$ , while anhydrous structures formed at  $249^{\circ}\text{C}$  degrade with  $T_{\max}$  at  $444^{\circ}\text{C}$ . McNeill (79) was able to show that similar anhydride structures may be formed when poly(methyl methacrylate) is degraded in the presence of a hydrogen chloride source such as poly(vinyl chloride). Two possible mechanisms were suggested by McNeill for the anhydride formation. In the first both methanol and methyl chloride are formed:

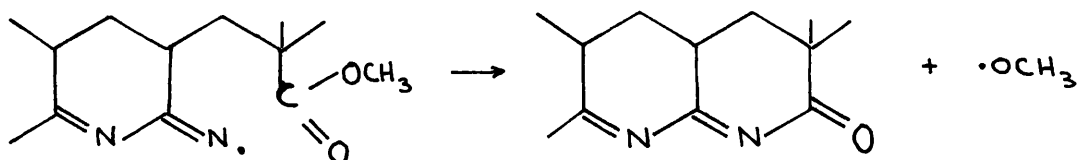


In the second, however, hydrogen chloride converts the ester groups to carbonyl groups with the evolution of methyl chloride:



with the subsequent formation of the anhydride by dehydration of pairs of methacrylic acid units.

Another analogous copolymer system is that of acrylonitrile with methyl methacrylate. Grassie and McGuchan (80) investigating the effect of incorporating small amounts of methyl methacrylate units into polyacrylonitrile, found that they were capable of participating in ring-forming reactions :



The formation of cyclic structures during the thermal degradation of polyacrylonitrile is a well-established feature but the nature of the structures has provoked much discussion (80,21,81). The degradation products have been studied by the same workers. Hydrogen cyanide and ammonia are detected in the 300 - 400°C region. The former arises from acrylonitrile units isolated between cyclic structures, the latter during aromaticisation of the rings. Also in this region the appearance of hydrogen and methane was noted.

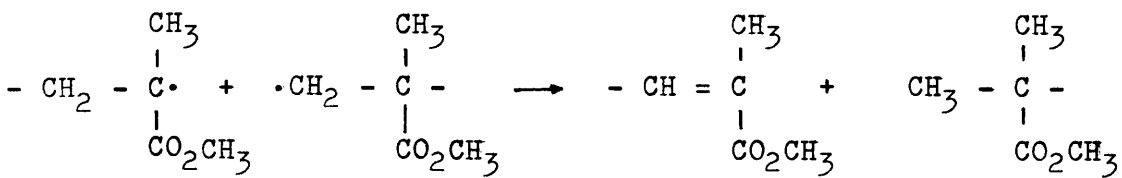
DCTVA studies on polyacrylonitrile (47) indicate two rate maxima at 319°C and 414°C respectively.

It appears from the range of products collected during DCTVA experiments on MMC 90, MMC 74 and MMC 50 that various

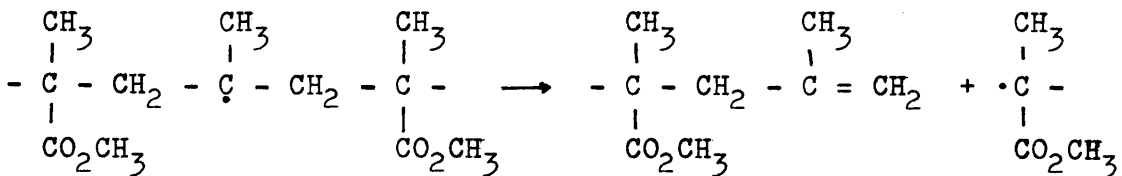
reactions are capable of occurring in the copolymer system and that the proportion of each type of reaction is governed by the arrangement of monomer units within the copolymer which, in turn, is a reflection of the molar composition. Grassie and Grant have determined the interaction between the liberation of hydrogen chloride and the depolymerisation to monomer at unusually low temperatures. The appearance of methyl chloride among the products suggests lactone or anhydride formation as in the case of vinyl chloride-methyl methacrylate copolymers. The elimination of hydrogen cyanide from isolated acrylonitrile units between cyclised structures in polyacrylonitrile may apply equally well to CAN units under the same circumstances within the copolymer or, alternatively, at crosslinked sites or on lactone rings. Similarly, the formation of carbon dioxide may occur at isolated methyl methacrylate units along the chain, or as a decomposition product of lactone or anhydride structures.

The pre-irradiation of copolymer samples had no observable effect on the nature of the products obtained by thermal degradation but resulted in perturbation of the normal TG curves and DCTVA traces. This was most marked in the MMC 90 copolymer.

As discussed in Chapter Four, the major characteristic of the photodegradation of copolymers such as MMC 90, which may be regarded as poly(methyl methacrylate) with a 10 per cent impurity level, is the rapid decrease in molecular weight. This is generally associated with either random scissioning which can be followed by disproportionation;



or with methyl formate formation and subsequent scissioning of the residual polymer radical;



By either route an unsaturated structure is formed. However, Grassie determined that the type of chain end formed by the direct scissioning process is responsible for the low-temperature depolymerisation reactions observed in poly(methyl methacrylate). The end group formed by the methyl formate process would be expected to be thermally more stable.

In their studies on the thermal degradation of this copolymer system Grassie and Grant were able to show that when a CAN unit was reached during the depolymerisation process, there is direct competition between its elimination as monomer and a termination process in which it is involved. In a photolytically degraded sample of copolymer a proportion of the CAN units will be in the unsaturated state following the elimination of hydrogen chloride from the unit or, alternatively, in the crosslinked state following radical combination as described in Chapter Four. As the extent of irradiation increases a higher proportion of mutant CAN units will be found in the copolymer. Consequently direct competition between termination and elimination reactions involving CAN units will be replaced

by an uncontested termination reaction at the mutant CAN unit.

A third factor arising from the photodegradation of MMC 90 is the hydrogen chloride lost during the reaction. Grassie and Grant deduced that hydrogen chloride formation results in a residual, unstable polymer radical which immediately undergoes scissioning reactions. Thus monomer is produced at lower temperatures than recorded in the homopolymer. As a proportion of the potential chlorine radicals are removed during photodegradation, a corresponding decrease in the extent of this premature depolymerisation can be expected.

In the case of the MMC 74 copolymer, increasing the photodegradation period has a far less pronounced effect on the TG and DCTVA traces. Whereas from MMC 90, 91 per cent of the total weight is methyl methacrylate, only 76 per cent is formed from MMC 74. Taking these figures into consideration it is reasonable to assume that a much more marked effect might be expected on the TG curve and the DCTVA trace by increased absorption of radiation.

As both hydrogen chloride and methyl methacrylate are detected among the products of the  $150^{\circ}\text{C}$  -  $250^{\circ}\text{C}$  stage of the thermal degradation, the same premature depolymerisation reaction is strongly implied. The possibility of lactone formation at this stage has been discussed previously, and this would be expected to be affected by the pre-irradiation in which a substantial proportion of hydrogen is eliminated. It is, therefore, unlikely that this reaction should influence the TG curve.

One possible explanation for this unexpected behaviour is the formation of a "protective" surface layer in the film during the early stages of photodegradation. This layer acts as a barrier to the passage of radiation into the film and reduces the degradative effect of radiation. In the event of a skin effect occurring the degradative results from a 6-hour, a 12-hour and a 22-hour period of exposure should differ only slightly. This appears to be the case with the TG curves.

The nature of barrier layers which form these skin effects has been discussed in Chapter Five. In this instance adjacent, unsaturated CAN units or unsaturated sequences of units involving methyl methacrylate units may be responsible.

A similar situation is proposed for MMC 50 in which the proportion of CAN units is even higher. In this case the formation of cyclised structures may be envisaged from the high temperatures required for the breakdown of the structure compared to MMC 90 and MMC 74. The formation of lactones or nitrogen - based structures would be little affected by pre-irradiation under the conditions of the skin effect.

REFERENCES

- (1) N. Grassie : "Degradation" In: "Polymer Science", edited by A.D. Jenkins, North-Holland Publishing Co. (1972).
- (2) P.R.E.J. Cowley and H.W. Melville : Proc. Roy. Soc. A210, 461 (1952).
- (3) R.B. Fox : "Photodegradation of High Polymers" In: "Progress in Polymer Science", Vol. 1, edited by A.D. Jenkins, Pergamon N.Y. (1967).
- (4) B. Ranby and J.F. Rabek : "Photodegradation, Photo-oxidation and Photostabilisation of Polymers", Wiley-Interscience (1975).
- (5) N.J. Turro : "Molecular Photochemistry", W.A. Benjamin Inc., N.Y. (1965).
- (6) W.M. Horspool : "Aspects of Organic Photochemistry", Academic Press, London (1976).
- (7) C. David, M. Piens and G. Geuskens : Europ. Polym. J. 8, 1019 (1972).
- (8) T. Hirayama : J. Chem. Phys. 42, 3163 (1965).
- (9) T. Hirayama, L.J. Basile and C. Kikuchi : Mol. Cryst., 4, 83 (1968).
- (10) J.G. Calvert and N.J. Pitts, Jr. : "Photochemistry", Wiley, N.Y. (1966).
- (11) O. Cicchetti : Advan. Polymer Sci. 7, 70 (1970).
- (12) K. Tsuji and T. Seiki : J. Polym. Sci. B 10, 139 (1972).

- (13) A.R. Burgess : Chem. Ind. (London) 78 (1952).
- (14) K. Tsuji : Advan. Polymer Sci. 12, 131 (1973).
- (15) N. Grassie : "Chemistry of High Polymer Degradation Processes", Interscience N.Y. (1956).
- (16) H.H.G. Jellinek : "Degradation of Vinyl Polymers" Academic Press N.Y. (1955).
- (17) H.H.G. Jellinek : J. Polymer Sci. 62, 281 (1962).
- (18) H.H.G. Jellinek : Pure and Applied Chem. 4, 419 (1962).
- (19) W.H. Gibb and J.R. MacCallum : Europ. Polym. J. 8, 1223 (1972).
- (20) N. Grassie and I.C. McNeill : J. Chem. Soc. 3929 (1956).
- (21) N. Grassie and I.C. McNeill : J. Polym. Sci. 27, 207 (1958)
- (22) N. Grassie and I.C. McNeill : J. Polym. Sci. 30, 37 (1958).
- (23) N. Grassie and I.C. McNeill : J. Polym. Sci. 33, 171 (1958).
- (24) N. Grassie and I.C. McNeill : J. Polym. Sci. 39, 211 (1959).
- (25) F.W. Billmeyer : "Textbook of Polymer Science", John Wiley & Sons (1962).
- (26) W.B.H. Leeming : Ph.D. Thesis, Glasgow Univ. (1973).
- (27) W.G. Leighton and G.S. Forbes : J. Am. Chem. Soc., 52, 3139 (1930).
- (28) G.S. Forbes and L.J. Heidt : J. Am. Chem. Soc., 56, 2363 (1934).
- (29) C.G. Hatchard and C.A. Parker : Proc. Roy. Soc.,

A235, 518 (1956).

- (30) E.E. Wegner and A.W. Adamson : J. Am. Chem. Soc., 88, 394 (1966).
- (31) R.B. Fox, L.G. Isaacs, S. Stokes and R.E. Kagarise : J. Polym. Sci. A 2, 2085 (1964).
- (32) J.R. MacCallum and C.K. Schoff : Trans. Faraday Soc., 75, 2383 (1971).
- (33) R.B. Fox, L.G. Isaacs and S. Stokes : J. Polym. Sci. A 1, 1079 (1963).
- (34) A.R. Shultz : J. Phys. Chem., 65, 967 (1961).
- (35) M.I. Frolova, L.V. Nevskii and A.V. Ryabov : Polym. Sci. USSR., 2, 703 (1962).
- (36) M. Iwasaki and Y. Sakai : J. Polym. Sci. A 1, 7, 1537 (1969).
- (37) Y. Kato and A Nishioko : Rept. Prog. Polym. Phys. Japan, 9, 477 (1966).
- (38) K. Tsuji : "ESR Study of Photodegradation of Polymers", In: Adv. Polym. Sci., 12, 131 (1973).
- (39) N. Grassie and N.A. Weir : J. Appl. Polym. Sci., 9, 963 (1965).
- (40) N. Grassie and N.A. Weir : J. Appl. Polym. Sci., 9, 975 (1965).
- (41) N. Grassie and N.A. Weir : J. Appl. Polym. Sci., 9, 987 (1965).
- (42) N. Grassie and N.A. Weir : J. Appl. Polym. Sci., 9, 999 (1965).
- (43) G. Loux and G. Weill : J. Chim. Phys. 61, 484 (1964).

- (44) R.B. Fox, L.G. Isaacs, R.E. Saalfeld and M.V. McDowell :  
U.S. Naval Res. Lab Report No. 6284 (1965).
- (45) P.I. Selivanov, E.I. Kirillova and V.L. Maksimov :  
Vysokomol. Soedin. 8, 1418 (1966).
- (46) J.F. Rabek and B. Ranby : J. Polym. Sci. A1 12, 273 (1974).
- (47) L.W. Mackinnon : B.Sc. Thesis, Univ. of Glasgow (1975).
- (48) N. Grassie and E.M. Grant : Europ. Polym. J., 2 255 (1966).
- (49) G.V. Schulz and G. Harborth : Agnew. Chem. A59, 90 (1949).
- (50) Massey and Potter : "Atmospheric Photochemistry",  
(R.I.C. Monograph) 1, 2 (1961).
- (51) G.D. Cooper and B.A. DeGraph : J. Phys. Chem., 75,  
2897 (1971).
- (52) L. Ackerman and W.J. McGill : J. S. Afr. Chem. Inst.,  
26, 82 (1973).
- (53) J. Yarwood : "High Vacuum Technique", Chapman and  
Hall (1975).
- (54) I.C. McNeill and D. Neill : "Thermal Analysis" Vol. 1  
Academic Press, London (1969).
- (55) I.C. McNeill : "Thermal Analysis" Vol 1, Academic  
Press, London (1969).
- (56) F.A. Bovey and G.V.D. Tiers : J. Polym. Sci., 44,  
173 (1960).
- (57) E.M. Grant : Ph.D. Thesis, Univ. of Glasgow (1965).
- (58) B. Yamada and T. Otsu : J. Macromol. Sci. - Chem.  
A3, 1551 (1969).
- (59) H.W. Thompson and P. Torkington : Trans. Far. Soc.,  
41, 254 (1945).

- (60) K.C. Ramey and J. Messick : J. Polym. Sci.,  
A4, 2, 155 (1966).
- (61) F.A. Bovey : Acc. Chem. Res., 1, 175 (1968).
- (62) N.G. Gaylord and B.K. Patnaik : J. Macromol. Sci. - Chem.  
A5, (5), 859 (1971).
- (63) N. Grassie, B.J.D. Torrance and J.D. Fortune :  
 Unpublished work
- (64) W.H. Gibb and J.R. MacCallum : Europ. Poly. J.  
9, 771 (1973).
- (65) A. Charlesby and S.H. Pinner : Proc. Roy. Soc.  
A249, 367 (1959).
- (66) Yu.A. Mikheyev, T.S. Popravko, L.L. Yashina and D.Ya.  
 Toptygin : Polymer Sci. USSR, 15, (11)  
 2797 (1973).
- (67) N. Grassie and E. Farish : Europ. Polym. J.,  
3, 627 (1967).
- (68) N. Grassie and E.M. Grant : J. Polym. Sci. C.,  
16, 591 (1967).
- (69) W.H. Gibb and J.R. MacCallum : Europ. Polym. J.,  
10, 529 (1974).
- (70) W.H. Gibb and J.R. MacCallum : Europ. Polym. J.,  
7, 1231 (1971).
- (71) H.L. Browning, H.D. Ackermann and H.W. Patton :  
 J. Polym. Sci. A1, 4, 1433 (1966).
- (72) S.F. Dyke, A.J. Floyd, M. Sainsbury and R.S. Theobald :  
 "Organic Spectroscopy : An Introduction",  
 Penguin Books, U.K. (1971).

- (73) J.E. Guillet : "Energy Transfer and Molecular Mobility in Polymer Photochemistry" In: "Degradation and Stabilisation of Polymers" edited by G. Geuskens, Applied Science Publ., London (1975).
- (74) G. Geuskens and C. David : "The Photo-oxidation of Polystyrene" In: "Degradation and Stabilisation of Polymers" edited by G. Geuskens, Applied Science Publ., London (1975).
- (75) I.C. McNeill : Europ. Polym. J. 6, 373 (1970).
- (76) N. Grassie and H.W. Melville : Proc. Roy. Soc. A199, 1 (1949).
- (77) N.L. Zutty and F.J. Welch : J. Polym. Sci. - A 1, 2289 (1963).
- (78) T. Straiton : Ph.D. Thesis, Univ. of Glasgow (1975).
- (79) I.C. McNeill and D. Neill : Europ. Polym. J., 6, 569 (1970).
- (80) N. Grassie and R. McGuchan : Europ. Polym. J., 8, 865 (1972).
- (81) N. Samson : Ph.D. Thesis, Univ. of Glasgow (1975).